# 7

# MODEL FOR THE SEINE-NORMANDY BASIN, FRANCE

**Yves Emsellem** and **Jean-Pierre Bordet**

*ARLAB*
*Valbonne, France*

In 1969, the Secrétariat Permanent pour l'Etude des Problèmes de l'Eau, which was the Department coordinating the Agencies, with the support of the Délégation Générale à la Recherche Scientifique et Technique, launched a methodological research in order to design a comprehensive water modeling policy.[1] The first tentative application concerned the Basin of Adour Garonne Agency. Subsequently, as a pilot study for Europe, the European Communities Commission supported a policy to analyze the water—quality and quantity—for the whole country (Fig. 7-1).[2] Then, the Ministry in charge of the environment and of the quality of life developed a methodology for a prospective analysis of the environment of the whole nation, taking into account air, water and soil pollutants.[3]

The first tools concerned a global approach for large territories. In 1971, the Agency of the Seine–Normandy Basin elaborated a global sketch for its policy, called POPOLE, and was consequently ready for a further detailed analysis.[4] The coordination of the available methods allowed a serious reconsideration of each part of the comprehensive model, and the present chapter is centered around the Seine–Normandy model—called POTAME—which is the most important achievement of these studies.

The objective was to work out and utilize a prospective water resources management device to govern the choice of investments, taking into account population distribution, economic factors, environment and the imbrication of natural resources. Also brought to light were the implications of the choice of strategies for resource development as well as for flood prevention guarantees, water supply security, water resource distribution and quality objectives.

## 7-1 BASIC CHOICES

The design of a comprehensive model integrating such aspects as water resources, draw off, conveyance and distribution of water, production and disposal of pollution, sewage plants, design and implementation of reservoir dams and water-

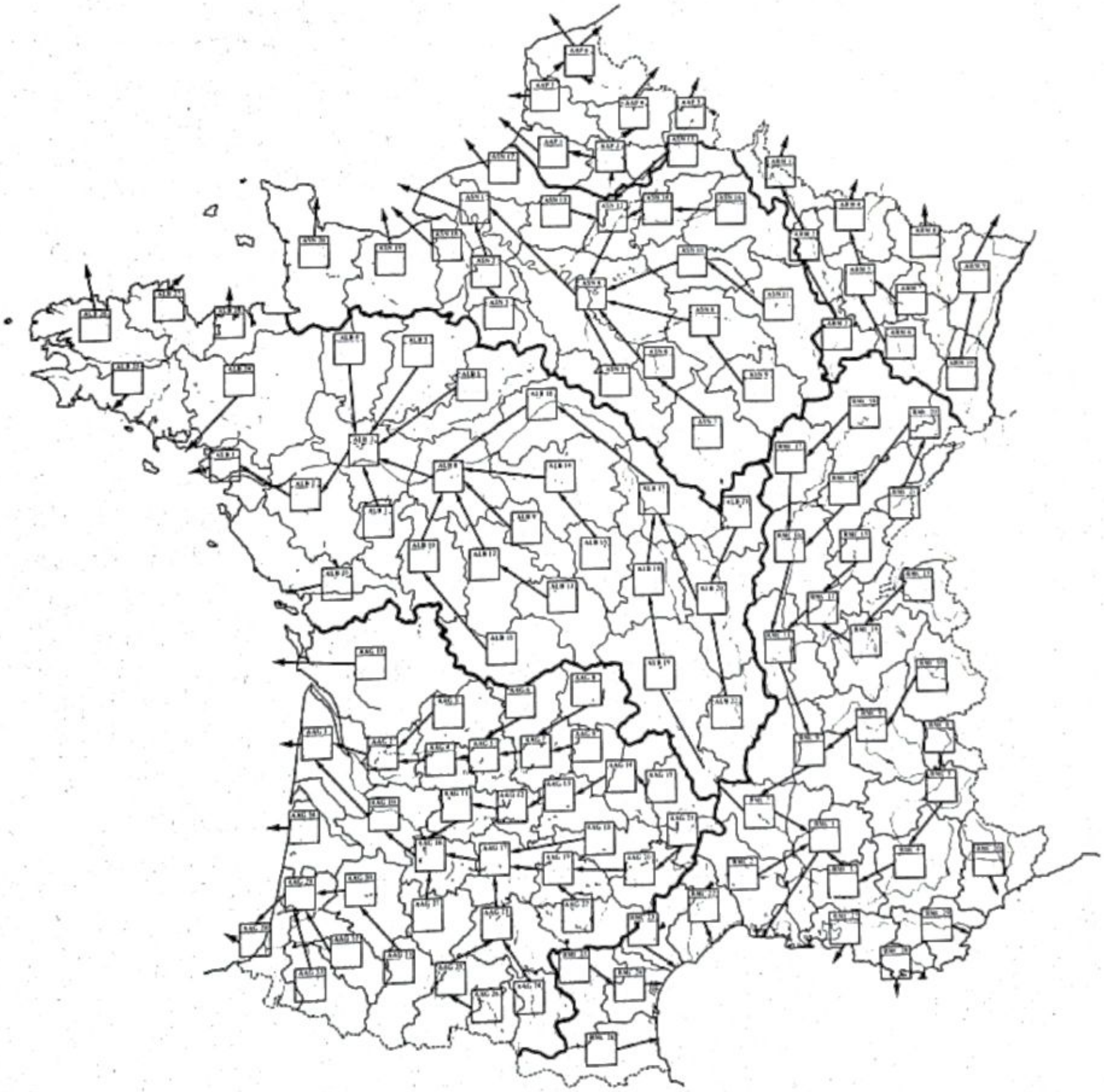

FIGURE 7-1
Water planning demand and supply.

treatment stations, obviously requires that both a general framework and the different basic elements be clearly defined.

The Seine-Normandy basin, including five sub-basins, constitutes the working scale. The basic territorial unit must be consistent not only with the hydrological subdivision of the basin, but also with the administrative subdivisions of France, in order for the economic and demographical data to be utilized.

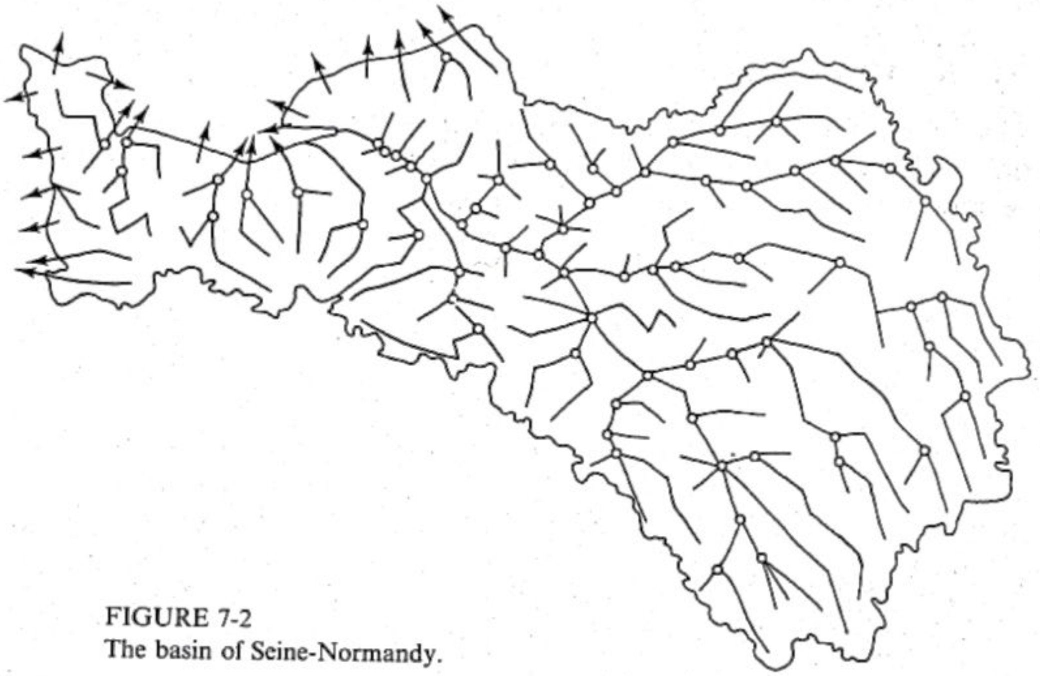

FIGURE 7-2
The basin of Seine-Normandy.

This basic unit, called a "cell," is generally composed of two or three "cantons" or townships, possibly with a few neighboring villages added or removed. In this way a subdivision of 316 cells is obtained for the whole of the basin. These cells can be grouped into different larger units: *départment*, program region, or sub-basin.*

Consequently seven elementary water uses are considered:

| | |
|---|---|
| irrigation | industrial uses: |
| livestock | cooling heat |
| domestic uses | cleaning manufacturing |

The term "water requirements" designates on the one hand water drawing requirements and, on the other hand, pollutant production requirements as well as disposal after use and partial consumption of water, containing acceptable concentrations of various pollutants according to the kind of user.

---

* France is composed of approximately 22 regions, 95 *départements*, 400 *arrondissements* or districts, 3,600 "cantons" or townships, and 36,000 "communes." It is also divided into 6 hydrological basins.

The pollutants considered for the national environmental studies were the following:[3]

*Air*

CO
SO 2
nitrogen oxydes
hydrocarbons
dusts
lead
radiation

*Water*

nitrates
nitrites
phosphates
oxydizable carbonaceous matter
oxydizable nitrogenous matter
suspended matter
hydrocarbons
radiation
temperature
toxics
insecticides

*Soil*

urban solid wastes

Dissolved oxygen was, of course, considered for water. As far as the Seine-Normandy model is concerned, the following parameters and their relations have been specially studied:

dissolved oxygen
phosphates
ammonium
nitrates
BOD
hydrocarbons

Moreover, for each basic cell, the populations of large towns, small towns, and rural areas have been distinguished since water requirements, investments and pollution differ in structure according to these populations.

In order to clearly individualize the diversity of water requirements and pollution problems, the following economic activities have been considered, based on National Accountancy sectors:

agriculture
agricultural and food industries
solid mineral fuels
gas and electricity
petroleum
construction materials
glass
steel
non-ferrous metals
transformation
mechanical construction
electrical construction
automobiles
shipyards and aeronotics
chemistry
textiles
clothing
leather goods
wood
paper and cardboard
publishing
buildings and public works
transportation
telecommunications
housing
utilities

For each of these branches, as well as for business, households, and administrations, the Input–Output Tables (I/O T) have been evaluated in the traditional manner for each dateline, every year or five years from 1970 to the year 2000.

For detailed calculations several industrial branches have been divided into sub-branches in which water disposal and water requirements differ; for example, for electricity the subdivisions are:

- hydraulic
- thermal:
  - coal
  - fuel
- nuclear:
  - PWR
  - BWR

## 7-2 PRELIMINARY DEMOGRAPHIC ECONOMIC MODEL

The evaluation and projection of industrial production and population in each cell require the use of a demographic and economic model called "SPIRE." This model, described in other publications, has undergone some adaptations. As a reminder, we might recall that this model produces a population projection based on regional census data as well as on different hypotheses concerning fertility, birth-rate, death-rate and migrations. Each program region is in this way furnished with a population evaluation according to sex and age brackets, and the whole of these evaluations comprises the entire nation.

These results are computed for the whole of all the regions in France which include the investigated basin. From these results, the parameters concerning the territorial units or cells, which are the geographical frame of the data processing, have been deduced. For this purpose a demographic model is used, for processing the evaluation of age pyramids per cell. The consistency between the results in the cells and the information dealing with the concerned region is checked afterward.

This ensures coherence on both national and regional levels, since the sum of the population of the different basins is, of course, equal to the total population of France.

In the comprehensive model the following three types of community have been distinguished: large towns (population over 30,000), small towns, and rural areas. By the use of territorial development and land reclamation scenarios, estimations of population distribution on the cell level, according to community types, can be ascertained in the same way as for populations. Thus for each basin cell, for the past, present and the future, we can divide the total population into large towns, small towns, and rural areas, for each cell and each year, and for each evolution scenario of the country and its regions.

As to industrial production projections, which will be taken as a basis for evaluation of pollution emission and water requirements, the methods utilized are the same as for the comprehensive model.

Let us review those methods briefly. Using the results of the National

Accountancy from 1959 to 1968, i.e., essentially the Gross National Product, Final Demand, Input–Output Tables, Productivity by Sector, we can calculate the total domestic production for the whole of France in constant francs (basis: 1970). For these calculations we employ a traditional Leontieff model with hypotheses concerning final demand and technological evolution. We can deduce effectively employed population figures and separate them according to program region, using data from the 1968 census with a check on the census of 1976.

A calibration process then modifies productivity by branch and rate of activity according to age and region, so as to ensure consistency between the working population and jobs which are indispensable for production. In this way the number of people employed in each sector and each region is obtained.

Moving on to the basin scale, we use the results of the census on the "canton" and "commune" levels to calculate attraction coefficients according to sector and cell. These "Florence coefficients" make it possible to distribute the offer of jobs in a given region among the different cells. Using average production figures obtained from national statistics, these jobs are transformed into production, expressed in millions of 1970 French francs. Thus for each cell and each year an evaluation of total production and of production according to sector is obtained.

Hence finally, as will be seen, it is possible to define the future development of the population and of economic activity, using past and present data as well as this set of models.

In this way, we also determine the evolution of water requirements. Sets of environmental development objectives and protection strategies are determined, and a group of such objectives and strategies is called a "scenario." The results therefore show a basic coherency between population, economy and technology on the one hand, and country, region and cells on the other.

## 7-3 WATER REQUIREMENTS AND POLLUTANT PRODUCTION

### 7-3.1 General Structure of the System

Drawing water is a requirement, disposing of it after use is a necessity, and producing pollution in small or large amounts is part of the technical process of water use. At the outset we distinguished seven uses of water in the basin, three general (agricultural, livestock and domestic) and four industrial (washing, cooling, heating and manufacturing). Each of these uses consumes a proportion of water and, at the time of disposal, contains pollutants, depending on the various techniques and users involved.

### 7-3.2 Calculation of Requirements

**Domestic** Water requirements are estimated first by utilizing coefficients for each inhabitant according to community type. Here we are, of course, concerned with high-quality water (possibly having been pre-treated after being drawn). In order to account for the needs of livestock, which are far from negligible in some

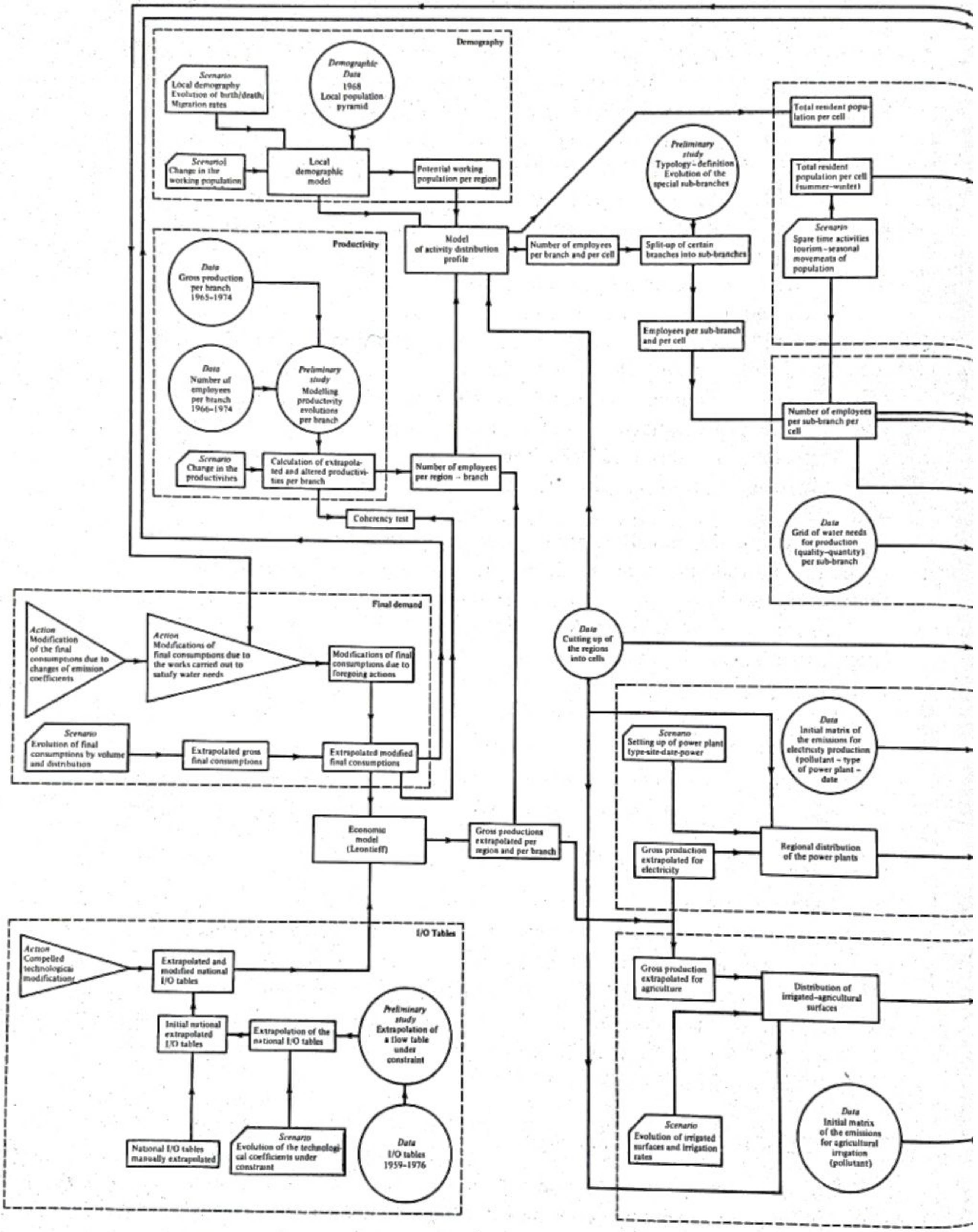

FIGURE 7-3
Long-term evolution of water pollution in France, 1985–2000.

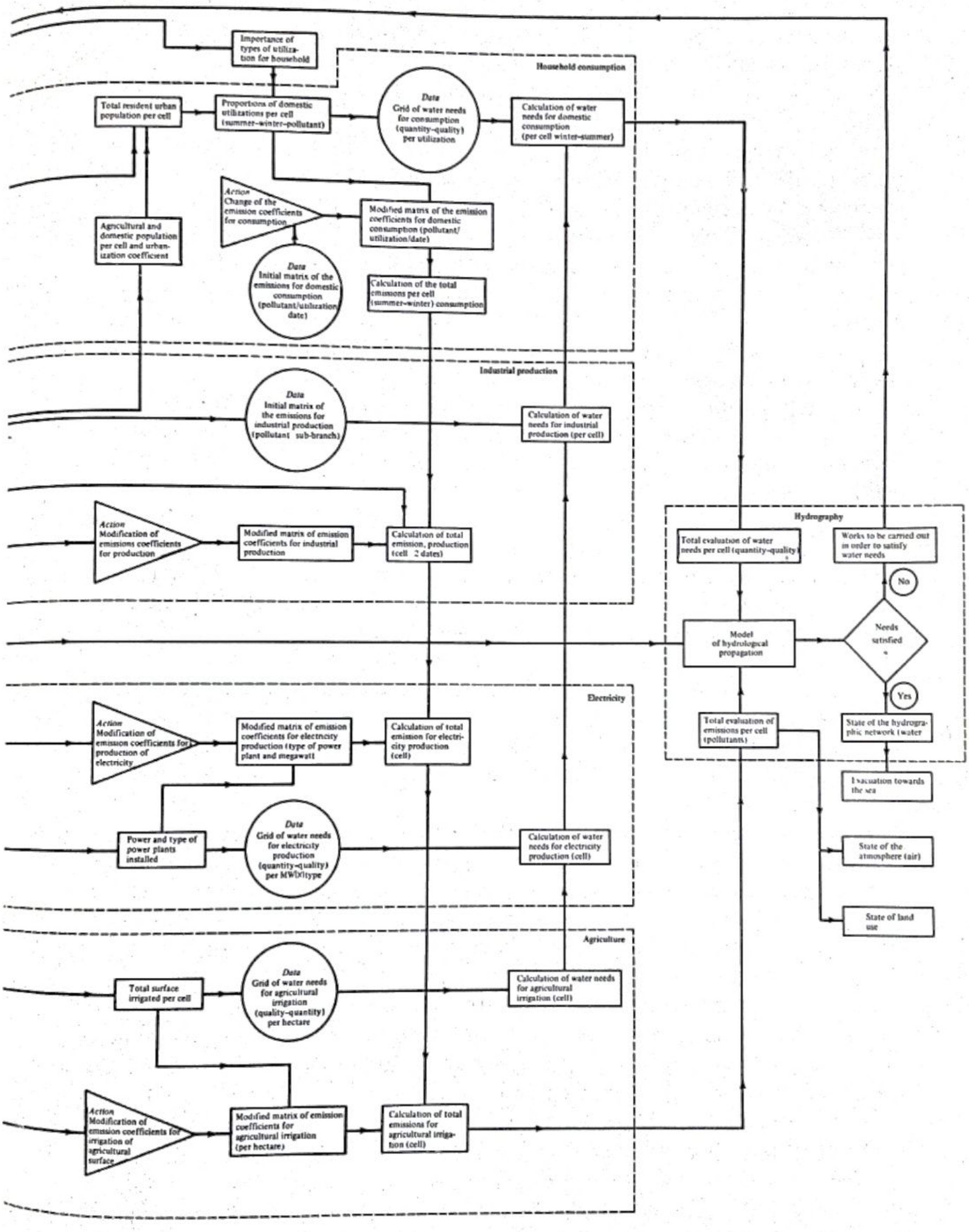
Importance of types of utilization for household
Household consumption
Total resident urban population per cell
Proportions of domestic utilizations per cell (summer-winter-pollutant)
Data
Grid of water needs for consumption (quantity-quality) per utilization
Calculation of water needs for domestic consumption (per cell winter-summer)
Action
Change of the emission coefficients for consumption
Modified matrix of the emission coefficients for domestic consumption (pollutant/utilization/date)
Agricultural and domestic population per cell and urbanization coefficient
Data
Initial matrix of the emissions for domestic consumption (pollutant/utilization date)
Calculation of the total emissions per cell (summer-winter) consumption
Industrial production
Data
Initial matrix of the emissions for industrial production (pollutant sub-branch)
Calculation of water needs for industrial production (per cell)
Action
Modification of emissions coefficients for production
Modified matrix of emission coefficients for industrial production
Calculation of total emission, production (cell 2 dates)
Hydrography
Total evaluation of water needs per cell (quantity-quality)
Works to be carried out in order to satisfy water needs
No
Model of hydrological propagation
Needs satisfied
Yes
Total evaluation of emissions per cell (pollutants)
State of the hydrographic network (water
Evacuation towards the sea
State of the atmosphere (air)
State of land use
Electricity
Action
Modification of emission coefficients for production of electricity
Modified matrix of emission coefficients for electricity production (type of power plant and megawatt
Calculation of total emission for electricity production (cell)
Power and type of power plants installed
Data
Grid of water needs for electricity production (quantity-quality) per MWh/type
Calculation of water needs for electricity production (cell)
Agriculture
Total surface irrigated per cell
Data
Grid of water needs for agricultural irrigation (quality-quantity) per hectare
Calculation of water needs for agricultural irrigation (cell)
Action
Modification of emission coefficients for irrigation of agricultural surface
Modified matrix of emission coefficients for agricultural irrigation (per hectare)
Calculation of total emissions for agricultural irrigation (cell)

areas, the results of the general agricultural census of 1971 have been utilized, and the development of livestock has been linked to the production of the Agricultural sector per hectare of usable agricultural surface.

The amounts used are as follows: in large towns, 220 liters per inhabitant per day (growth rate 1.75 percent per year); small towns, 110 liters per inhabitant per day (2 percent growth rate); rural areas, 90 liters per inhabitant per day (2.25 percent growth rate); livestock, 60 liters per cattle equivalent (one head of cattle or two head of swine) per day (1.75 percent growth). These coefficients are then adapted where necessary to local statistics. But it must be observed that this distinction of different domestic uses makes it possible to adapt the results of the model to local peculiarities known through statistical data provided in particular by the Basin Agencies.

Of course the annual growth rates are among the parameters which define a scenario and are therefore modifiable.

The population varies from season to season according to the number of tourists. A "spare-time scenario" is therefore introduced to represent seasonal population movement between towns, coastline, mountains and countryside, within regions as well as across frontiers.

**Agricultural requirements** Water requirements here are for irrigation, and amounts were measured in the general agricultural census of 1971, distinguishing between underground or surface origins of the water involved. This census provides results by cell for 1971, and different irrigation development plans (furrow, sprinkler, drip) cause water requirements to vary with time.

The basic element here is the irrigated hectare and the type of crop. When a rural area is stabilized, the needs for drawing water are considered to be constant. This is justified for a northern region like Seine–Normandy, but must be modified for other areas further to the south.

**Power plant requirements** The basis for calculating these requirements is the type of station and the number of megawatts supplied for different datelines, according to the scheduled power plants decided on at national level. At present, as all power plants in the region are fuel-operated, the set coefficient per megawatt supplied (70 percent load factor) is 40 liters per second per megawatt.

**Industry** Two types of industrial water use are distinguished: *heat–manufacture*, requiring high quality water and *washing–cooling*, for which water of a lower quality may suffice. A grid of requirements according to sector and use has been compiled, based on years for which production and consumption are known.

A first hypothesis for recycling industrial water for washing, scrubbing and cooling has been expressed by a decrease of 2 percent per annum in requirements for this use, and this decrease can be parametered in the scenarios.

Using production figures by branch, it is therefore possible to evaluate industrial requirements for each cell. At present, branch by branch, requirements were evaluated on the one hand by a grid obtained through statistical analysis based on the actual bureau data as well as on the supplementary data. The indicator for each branch is a million French francs of production. The results are water-drawing requirements for washing–cooling and boilers–manufacturing, the total being drawn when no recycling is necessary or affected.

On the other hand, actual surveys made it possible to check these data and to specify the respective shares for washing–cooling, boilers–manufacturing, as well as eventual recycling and reuse. The amount of water drawn for each type of activity is known through the billing files of the Agency.

The general table of quality requirement for each use is shown in Table 7-1.

Table 7-1

| | Quality | | Pollutants | | | | | |
|---|---|---|---|---|---|---|---|---|
| | Good | Poor | MOC | MON | NIT | PHOS | HYDR. | Consumption |
| *Domestic* (inhabitant) | | | | | | | | |
| large towns | X | | X | X | | X | X | X |
| small towns | X | | X | X | | X | X | X |
| rural | X | | X | X | | X | X | X |
| *Agricultural* (hectare) | | | | | | | | |
| irrigated | X | X | X | X | X | X | | X |
| non irrigated | | | X | X | X | X | | |
| cattle | X | X | X | X | | X | | X |
| *Power plants* (MW) | | | | | | | | |
| fuel plants | | X | X | X | | | | X |
| nuclear plants | | X | X | X | | | | X |
| *Industry* (production by million of francs). | | | | | | | | |
| cooling–cleaning | | X | X | X | | | (X) | X |
| heating–process | X | | X | X | | | (X) | X |

### 7-3.3 Disposal Requirements

Each use of water consumes a proportion of the total amount drawn, which we call in this case "consumption." It is thus possible, by use of statistical data, to calculate the consumption of the different users and the amount of water which will disappear in each cell.

The average consumption rates applied are:

| | |
|---|---|
| Rural and agricultural domestic | 95% |
| Urban domestic (both large and small towns) | 15% |
| Industry | 6% |
| Power plants | 1% |

Moreover, the Agency billing file indicates the proportion of underground and surface water drawn (cubic meters per second) and the initial proportion of these amounts according to origin.

### 7-3.4 Calculation of Pollutant Emission

**Domestic, agriculture, energy** These same principles are applied to compute pollutant emission: sets of coefficient are used for each pollutant and each source, determined by survey and by agency data. Gross flow rates are thus deduced for each pollutant and each pollution source. Table 7-2 summarizes these elements. It is only an example and should not be considered a norm.

For energy production, heating has been transformed into $BOD_5$ equivalent and equivalent nitrogenized oxydizable matter based on the power supplied.

**Industry** For industry the process is necessarily different, since the pollution coefficient method utilized on the national level does not enable us to consider the local particularities which are fundamental on the cell level.

Here it is necessary to distinguish between industries connected to the purifying or water-softening network and those which are not so connected. For this purpose, we use connection rate data provided by the anti-pollution billing file for each cell. Total industrial production of the cell is thus divided between connected and unconnected industries.

To calculate the corresponding gross pollution we again utilize the billing file, which indicates for each "commune" the amount of pollution produced, purified and eliminated, expressed in either oxydizable matter or suspended matter.

The hypothesis used to trace the evolution of this pollution is as follows: in each cell the amount of pollution produced evolves according to industrial production. Moreover, food agriculture industries include a certain proportion of phosphates. Calculations have led to an average coefficient of 300 kg/d for an annual production equivalent to 1 million 1970 French francs. The average values for the other pollutants are: 1,000 kg/d of $NH_4$ per annual million 1970 francs for the paper industry, or 2,000 kg/d of $NH_4$ per million 1970 francs for some chemical production. As far as special industries such as coal thermal plants are concerned, the equivalent of 1 kg/(d MW) for smoke washing is estimated. A nitrate concentration of about 15 mg/l has been estimated for water coming from some underground aquifers. This concentration was determined by specific surveys and analyses.

Table 7-2 POLLUTION PRODUCTION COEFFICIENTS ACCORDING TO POLLUTANT AND SOURCE

| Pollutant (mg/l)<br>(Source) | $BOD_5$ | $NH_4^+$ | $NO_3^-$ | $PO_4^{---}$ | Hydroc. |
|---|---|---|---|---|---|
| Agriculture (ha) | 35 | * | 20* | 5.35* | * |
| Domestic rural (hab) | 46 | 6.25 | — | 1.1 | 0.07 |
| Small towns (hab) | 59 | 8.00 | — | 1.50 | 0.07 |
| Large towns (hab) | 72 | 9.75 | — | 2.35 | 0.07 |
| Power plant equivalent (MW) | 27.2 | (†) | — | — | — |

* These coefficients vary according to program region and evolve along with the corresponding technological coefficients (e.g., chemical purchases by Agriculture).

† For coal power plant, washing of smoke is considered a source of $NH_4^+$ emission.

## 7-4 WATER RESOURCES AND FLOW BALANCE

The basic territorial cells are linked together by a series of directional arrows describing the hydrological network, subdivisions having been made in such a way as to obtain a simple graph while respecting administrative boundaries.

For each cell, the flow is determined as follows:

Flow rate downstream from the cell = sum of flow rates coming from upstream
+ local resources
+ underground water pumping
+ water brought in by derivations or canals
− water removed by derivations or canals
+ destocking of local dams
+ flow coming from collection of waste waters from other cells
− net consumption of water
− collected water discharged into another cell.

The unit is one cubic meter per second.

First of all, local resources correspond to the flow drained locally by the hydrographical network, all of the underground and surface resources, alluvial and shallow.

The assessment is thus the resultant of a group of phenomena from a preceding period. It is in fact determined from a critically severe period that is, a low level at a time when rain is non-existent (in theory). For example, the autumn of 1971, decennial in nature, has often been taken as a reference period, along with other critical periods such as the low water levels of 1949 or 1976.

The choice of a reference period was a delicate matter, as two options were present for simulating more or less severe hydrological situations.

*1* Utilizing classified flow rates of the same frequency, for instance 80 percent, 90 percent or 95 percent flow rate.
*2* Utilizing real situations.

For various reasons the second option was chosen.

**Reasons of logic** Choosing classified flow rates of the same frequency to represent the hydrological network leads to a situation in which the frequency has no connection with the reference frequency: if, for instance, each reach is assigned a decennial flow rate, the resultant situation is not decennial. In other words, the decennial low water level situation for a group of measurement stations is not itself decennial.

**Reasons of coherency** The upstream to downstream balance only makes sense if the flow rates considered are synchronous. This is very important for calculating

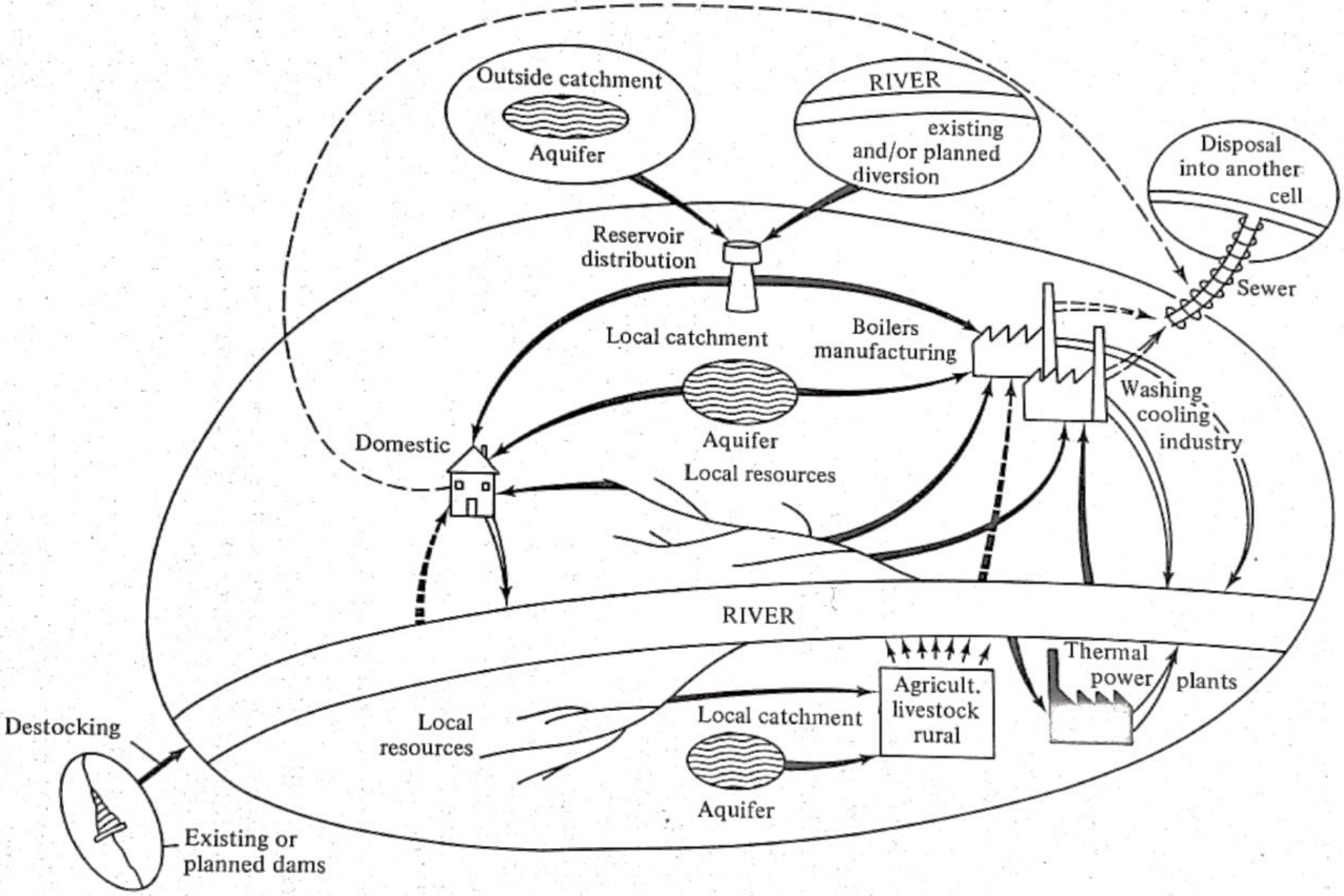

FIGURE 7-4
Diagram of water drawn in a given cell.

local resources which can be checked according to the regionalized specific flow rate, using optimal mapping techniques such as "kriging."

**Reasons of homogeneity** Not all hydrological stations have been in use for the same amount of time, and the classified flow rates coming from these different stations are therefore not comparable. Furthermore, certain old records now have only an historical significance.

Finally, the gradual setting up of dams requires calculations in order for the flow rates prior and subsequent to dam construction to be comparable.

In order to avoid these problems, the hydrological reference situations are therefore real situations. Another verification is also carried out by estimating specific flow rates according to sub-basin. As all calculations are done by computer, this verification is facilitated by the automatic outline of cells, their surfaces and lengths.

Moving downstream along the branched chain network, we can reconstruct the flow rates leaving each cell and compare these results with the measurements carried out in gauging stations. For example, local resources are calculated to calibrate a flow rate corresponding closely to the low water level of September–October 1971.

By modifying these local resources, we can simulate another low water level situation.

Water underground aquifer pumpings can vary from their 1970 value to a higher limit, depending on the region and deriving from the local hydrogeological studies. Current pumpings are considered to be actually available resources, as the 1935 law* to this effect has been extended to every area of France in which the problem of over-utilization of water aquifers has occurred.

By destocking local dams, we mean that which is destocked and not what the dam is capable of destocking in absolute terms. Moreover, public safety is guaranteed here by simulating, for the present or the future, multiple objective dams, a part of which is intended to prevent flooding, supply irrigation or water, or produce energy.

In the same way, the requirement–resources assessment will be made for successive datelines, modifying the following elements according to need:

Water drawn from aquifers, by increasing the amount to local requirements
Derivation, by creating new ones if necessary
Destocking, by building new dams
Transfers between cells
Purifying capacities for water quality

The purifying capacity supplied in each cell is indeed part of the description of water resources, as well as distribution networks, characterized here by known connection rates.

In the same way, the description of resources is completed by yield in the

---

* This law submits the drilling of important water wells to an administrative license.

purification of carbonaceous and nitrogenous organic matter, in nitrates and phosphates for primary and secondary treatment units.

Simulation of self-purification completes the flow assessment for quantity and quality.

## 7-5 BALANCE OF NEEDS AND RESOURCES

### 7-5.1 Allocation Strategy

The means at our disposal to ensure agreement between requirements and resources are composed of the five following elements:

analysis of the present distribution
modification of this distribution
construction or destocking of upstream dam-reservoirs
evolution of the tapping of underground layers
utilization of derivations and canals

The initial distribution of amounts of water drawn is known through the billing files. To satisfy additional future requirements, a resource allocation strategy must be chosen, depending in some cases on the region involved. In order to have a wide variety of possibilities, these strategies are detailed and parametered. Let us take a practical example of one of these strategies:

Water is initially allocated according to parametered strategies like those shown in Table 7-3 which describes the water supply scheme of a cell.

Table 7-3

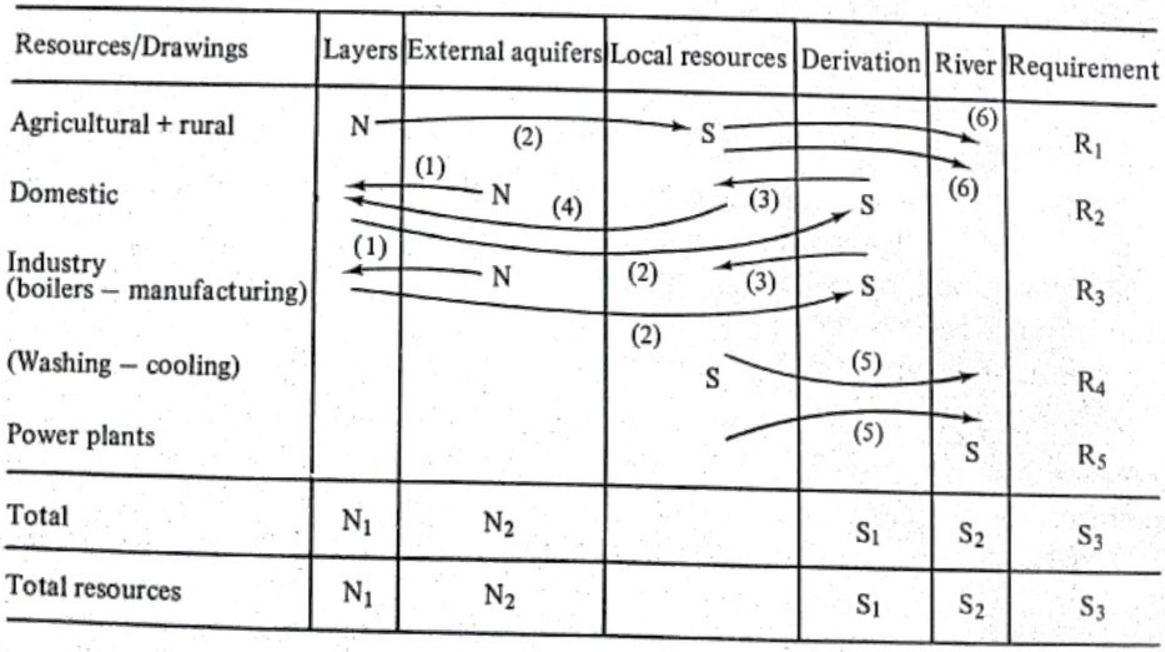

| Resources/Drawings | Layers | External aquifers | Local resources | Derivation | River | Requirement |
|---|---|---|---|---|---|---|
| Agricultural + rural | N | (2) | S | | (6) | $R_1$ |
| Domestic | | (1) N (4) | (3) | S | (6) | $R_2$ |
| Industry<br>(boilers – manufacturing) | (1) | N | (2) (3) | S | | $R_3$ |
| (Washing – cooling) | | | (2) S | (5) | | $R_4$ |
| Power plants | | | | (5) | S | $R_5$ |
| Total | $N_1$ | $N_2$ | | $S_1$ | $S_2$ | $S_3$ |
| Total resources | $N_1$ | $N_2$ | | $S_1$ | $S_2$ | $S_3$ |

To satisfy requirements by drawing on resources for this example, the above process is in seven steps:

*1* Assessment of amounts drawn from aquifers outside the cell by the general water supply network, when existing—unsatisfied surplus carried over into local layers.
*2* Assessment of amounts drawn from local layers—surplus carried over into derivation and local resources.
*3* Assessment of amounts drawn from derivations—surplus carried over into local resources.
*4* Assessment of amounts drawn from local resources—domestic surplus carried over into local aquifers if possible.
*5* Assessment of amounts drawn from local resources—industrial surplus carried over into river.
*6* Final assessment of amounts drawn from local resources—Surplus carried over into river.
*7* Assessments of amounts drawn from rivers—calculation of deficit and required destocking.

Of course, the logic of the strategy is parametered.

### 7-5.2 Setting up Destocking and Derivations

For certain low water level conditions, or subsequent to high population or economic growth, some deficits may occur in a few sensitive zones. To make up such deficits, dams must be set up or destocked upstream from the zones showing a deficit. A list of reservoir-dams already constructed is available, as well as a certain number of possible sites. These sites are characterized by an available destocking flow rate to support low water levels.

The procedure adopted to simulate construction and utilization of reservoir-dams makes it possible to avoid using a global linear programming optimization method, which is both cumbersome and expensive. One need only use the branched chain character of the hydrological network and the fact that water flows downstream.

Each cell is credited with the sum of available local upstream destockings. Then, the deficit of the cell is compared with its destocking credit to determine the amount of required upstream destocking. The deficits and credits of downstream cells are then reduced by this amount, continuing on down the network.

The position of new dams must then be determined. To carry out this positioning, we start with the hypothesis that all the dams have been constructed and deduct the corresponding flow rates; all those which are superfluous are then eliminated, starting upstream, by comparing the destocking capacity of each dam with the least difference between required downstream flow rate and maximum available downstream flow rate. A special algorithm insures that dams are not overlapping, and the very minimum of construction—or investment—is carried out.

Only one ambiguity remains when several upstream tributaries allow for the construction of dams of equivalent capacity. In this case, the decided dateline calendars for dams are referred to, bringing flood prevention into play.

The procedure is similar for derivations, which add some complexity to the logic of the program, due to the fact that they introduce short circuits into the branched chain. They are introduced as real derivations and potential derivations with the corresponding flow rates.

### 7-5.3 Underground Aquifers

It is tempting, considering the quality of the underground aquifer models, to wire a model of these aquifers under the surface network. In fact, the large number of available studies and the large size of the cells (about twenty square kilometers) makes it possible to evaluate the maximum resources available in aquifers per cell. This simplifies the job by imposing a control of relations between underground aquifers and the surface network. This leaves us with a complete hydrological balance and a distribution of amounts of water drawn throughout the basin.

We must also be concerned with the quality of the water in the rivers of the basin. This is done simultaneously, as the quality and quantity of the water cannot be disassociated; they are only separated for purposes of clarity in this chapter.

## 7-6 DISPOSAL CALCULATIONS

Not all the pollution produced is eliminated directly into the river. The number of purifying or water-softening plants in service, as well as infiltration measures, are very important in the basin and must therefore be taken into account.

First of all, the amounts treated and infiltrated must be estimated for 1971, the year during which the pollution inventory has been carried out. In order to do this, the results of this inventory and certain additional measurement campaigns are used to deduce the self-purification coefficients.

Before studying the phenomena occurring in the river, it is necessary to simulate the action of treatment plants.

The available data are estimations of treatment capacities, load coefficients and plant yields from 1971 to about 1980. The processes to be simulated are rather different, depending on whether the disposal is connected to a purification network or not. Three types of prior treatment are distinguished:

For unconnected users: infiltration and softening
For connected industries: pretreatment with sewer disposal

These amounts are evaluated as a percentage of the quantities produced. At the pollutant level, infiltration obviously concerns all pollutants, but on the other hand, for pre-treatment and treatment, simulation of the treatment plant is necessary. The diagram is shown in Fig. 7-5.

Simulation of a classical plant, secondary treatment, gives a theoretical yield of 80 percent for $BOD_5$, 40 percent for $NH_4^+$, 0 percent for $NO_3^-$, 30 percent for $PO_4^{---}$ and 80 percent for hydrocarbons.

These equations are only applied to that part of the waste which goes through the plant; we can thus estimate the real wastes of connected and unconnected industry.

For domestic waste, the part which is unconnected is disposed of directly into the river. For the connected part, the plant simulation is the same.

The fact that the purifying network may end up at a plant located outside the cell must also be taken into account. This is especially true for the Paris area and for some syndicates of communities. Disposal will be positioned within the cell where it takes place.

Concerning disposal of calories, which modify the self-purifying coefficients, a simplification became apparent. In effect, according to the hydrological flow of the different streams of water, fast or slow, large or small, turbulent or quiet, hot or cold, analysis shows that, at least for the Seine–Normandy basin, it is possible to transform temperature increases into BOD disposal, using simple formulae and charts. This method was therefore chosen.

## 7-7 SELF-PURIFICATION

### 7-7.1 Model Used

For each pollutant considered, the depreciation model is very simple and can be represented by the following formulae, in which the indexes (0) indicate initial loads, (*d*) the distances in kilometers, and $\alpha$, $\beta$, $\gamma$, $\delta$ locally determined coefficients.

| | Local disposal | Diffuse disposal |
|---|---|---|
| $BOD_5$ | $L = L_0 \cdot e^{-\alpha d}$ | $L = \frac{L_0}{\alpha l} \cdot (1 - e^{-\alpha \cdot d})$ |
| $NH_4^+$ | $A = A_{\partial} \cdot \frac{4}{3 + e^{\beta d}}$ | $A = \frac{4 \cdot A_0}{3 \cdot \beta} \log_e \left( \frac{4 \cdot e^{\beta d}}{3 + e^{\beta d}} \right)$ |
| $NO_3^-$ | $N = N_{\partial} \cdot \delta$ | — |
| $PO_4^{---}$ | $P = P_0 \cdot e^{-\gamma \cdot d}$ | $P = \frac{P_0}{\gamma \cdot l} \cdot (1 - e^{-\gamma \cdot d})$ |

These formulae come from observation of the Streeter–Phelps equations for self-purification of BOD, and from observation of the logistic forms already noted by Velz for nitrogenized organic matter (Fig. 7-6).

Hydrocarbons are considered to be conservative. The disposal pattern is as follows (Fig. 7.7):

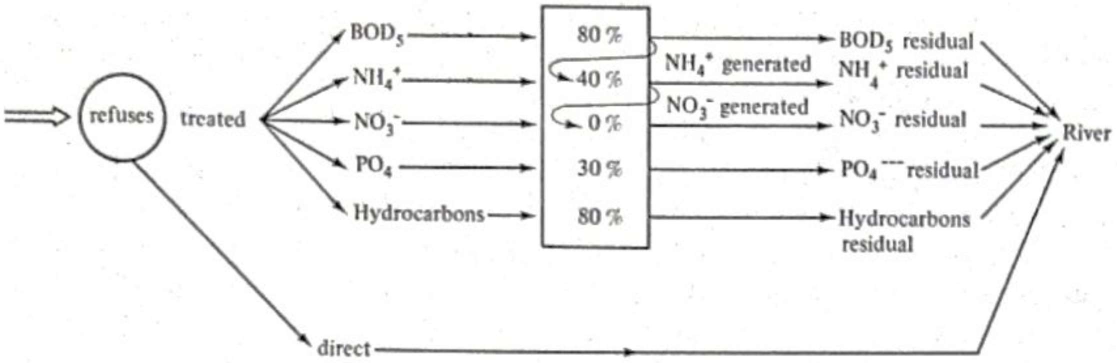

FIGURE 7-5
Flow diagram of wastes, their treatments and disposals in a river.

Agricultural and rural: diffuse disposal along the whole length of the cell ($l$).
Domestic and industrial: local disposal in the middle of the cell ($l/2$).
Large towns: disposal positioned at distance $l_v$ from the cell exit.
Thermal power plants: disposal positioned at distance $l_c$ from the cell exit.

The degradation of organic matter liberates a quantity of $NH_4^+$ as it reduces BOD. On nitrification, this gives $NO_3^-$. This process has been simulated for river purification as was done for plant purification.

Knowing the different waste matters, we deduce from these equations flows of pollutants leaving the cell, and using the reconstructed flow rates, we deduce concentrations at the cell exit.

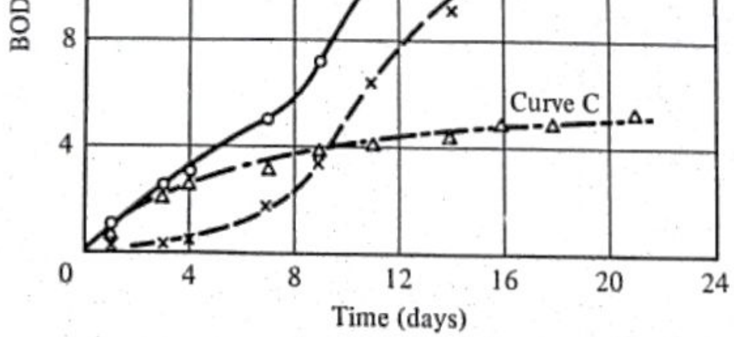

FIGURE 7-6
Degradation of organic matter. (According to Cl. J. Velz. Curve A: BOD total; curve B: nitrogenized compounds; curve C: carbonaceous compounds.)

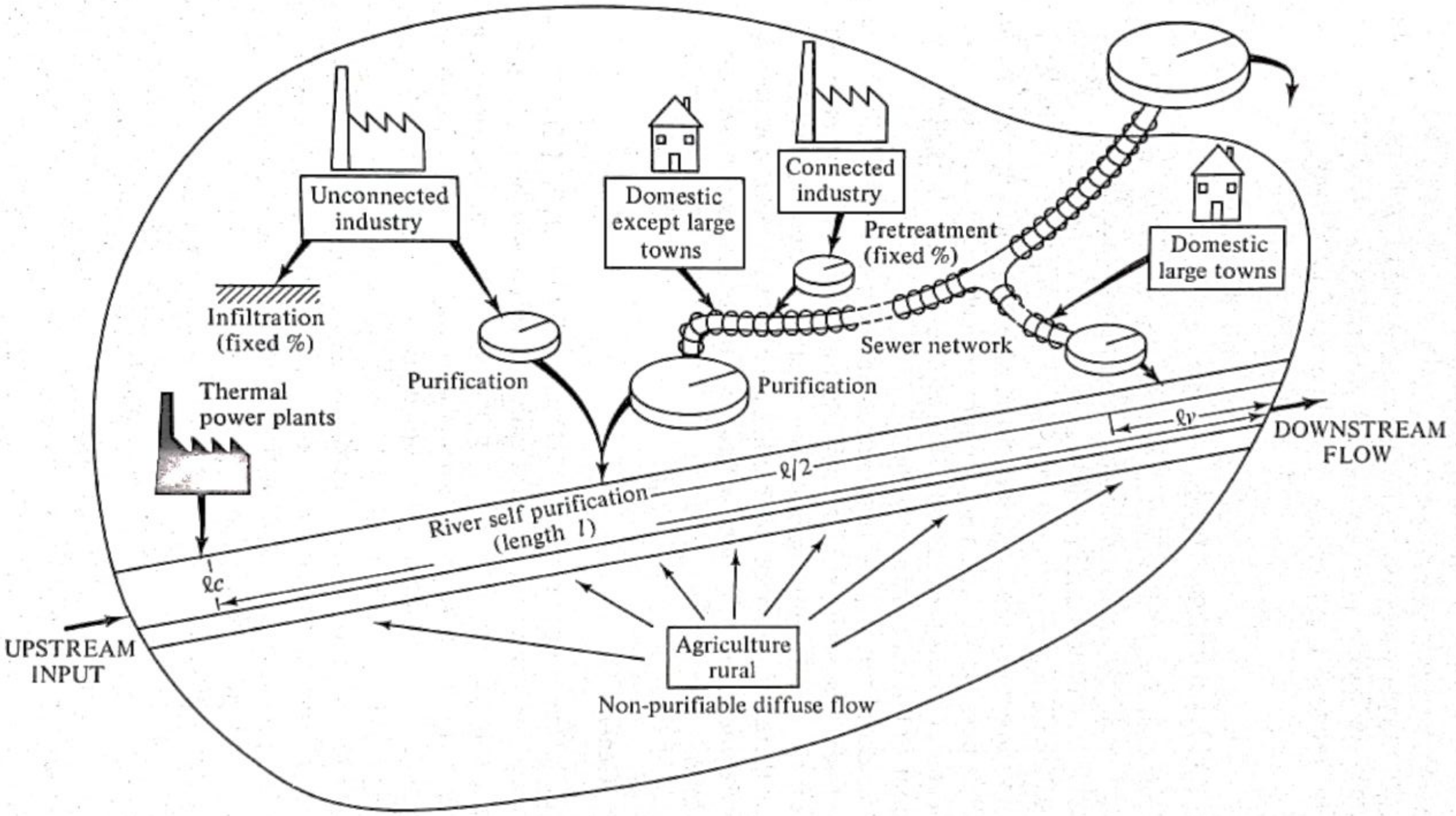

FIGURE 7-7
Diagram of pullutant flows in a cell.

The most important parameter remains dissolved oxygen. But, considering the size of the cells and the disposal diagram adopted, it is difficult to use the classical Streeter–Phelps model for reoxygenation by showing the different sag curves. It was therefore considered preferable to make a balance of the oxygen in each cell.

Both the flow of oxygen entering the cell and the flow brought through local resources are known. Purification of $BOD_5$ and $NH_4^+$ requires consumption of a certain amount of oxygen which may be evaluated using the formulae given above.

### 7-7.2 Calibration of the Model

The coefficients $\alpha$, $\beta$, $\gamma$, $\delta$ and $\omega$ must be determined for each cell. In order to make this calibration, it is necessary to estimate as accurately as possible the real wastes as well as the concentrations at the cell exists on the date considered. This date will once again be September 1971, for which the results of the national pollution inventory are available. Successive numerical approximation methods make it possible to calculate unknown coefficients and to reconstruct the purification process for each cell. The calibration was checked on the data of the National Pollution Survey of 1976.

The coefficients considered are characteristic of each cell; they account for local conditions, such as the actual location of disposal points, small dams, and inaccuracies concerning disposal, they are therefore considered to be constant as long as there are no important modifications of wastes or of water use in the cell. They are not self-purification coefficients, but specific depreciation coefficients for each cell.

### 7-7.3 General Diagram

The pollutants considered are $BOD_5$, $NH_4^+$, $NO_3^-$, $PO_4^{---}$ and hydrocarbons. The concentration of dissolved oxygen will be evaluated in order to determine the quality of the water and the future purification strategy. Each pollutant is submitted to transformations which are analytically expressed by "self-purification" models. No ambiguity is to be feared for $BOD_5$, and we utilize the first Streeter–Phelps equation.

As for other pollutants, no simple expressions are found in the literature which are appropriate to our comprehensive model. It was therefore necessary to develop expressions that would make it possible to obtain results compatible with the data and with known elements.

Before going on to a study of self-purification, a comprehensive analysis of pollutants and of their relations with river types and disposal centers was made, on the basis of data gathered during the national pollution inventory of 1971. This analysis, made by Benzecri Correspondences Factorial Analysis methods, led to an initial classification of the basin waters. The parameters measured were the following:

Biological oxygen demand (BOD); chemical demand (COD); self-consumption of oxygen (AUTOC 02); oxydizability (OXYDB); lotic index (LI); lentic index (CI); suspended matters (SM) sodium (Na); sulphates ($SO_4$); conductivity (COND); dissolved oxygen ($O_2$); substances extractable by chloroform (SEC); orthophosphates (ORTH); foam; PH, Calcium ($Ca^{++}$); $CO_3H^-$; Pb; Cr; Cu; Cd; saturation index (IND SAT); $NH_4$, $NO_2$; $K^+$; $Cl^-$; $NO_3$; decantable matter (DECMAT); $MG^{++}$, detergents (DETAN); transparency; colour; flow rate; hydrocarbons (HYDRC); iron; fluoride; Mn; Zn.

All these parameters constitute, in one point, a vector and the correspondence factorial analysis makes it possible to classify these different vectors and to analyze relationship parameters. The result is synthesized, as shown in Fig. 7-8 by projection of the vector cluster on the first two inertia axes of the diagrams.

We are now going to describe in detail the models used and their utilization. The result we are seeking is obviously composed of the concentrations of the different pollutants as they leave each cell.

### 7-7.4 Detailed Self-purification Diagram

Two categories of pollutants must be distinguished for these models. First the $BOD^5$–oxygen–$NH_4^+$–$NO_3^-$ group, in which there is interrelation, and then $PO_4^{---}$ and hydrocarbons, considered to be independent. The transformation diagram used is the following:

A load of oxydizable matter $C_0$ (or organic matter) is eliminated into the river by a water-softening plant located at a certain distance from the cell exit.

The oxydizable matter (MO), constituting a parameter used by the Basin Agencies, is evaluated by use of the formula

$$\mathrm{MO} = \frac{2}{3}\,\mathrm{BOD}^5 + \frac{1}{3}\,\mathrm{COD}$$

and is expressed in kilograms of oxygen. This oxydizable matter is the characteristic parameter of purification costs and purification plant capacity, whence its practical and statistical importance.

Certain studies make it possible to use the ratio

$$\mathrm{BOD}_5 \simeq 0.8\ \mathrm{MO}$$

to go from oxydizable matter to a given amount of $BOD_5$.

It is known furthermore that ultimate biological oxygen demand is related to $BOD_5$ by the ratio:

$$\mathrm{BOD}_{20} = (0.03T + 0.87)\,\mathrm{BOD}_5$$

in which $T$ is water temperature in degrees Celsius.

The biodegradation of carbonaceous organic matter constitutes a preliminary auto-purification process. Dissolved oxygen thus transforms this carbo-

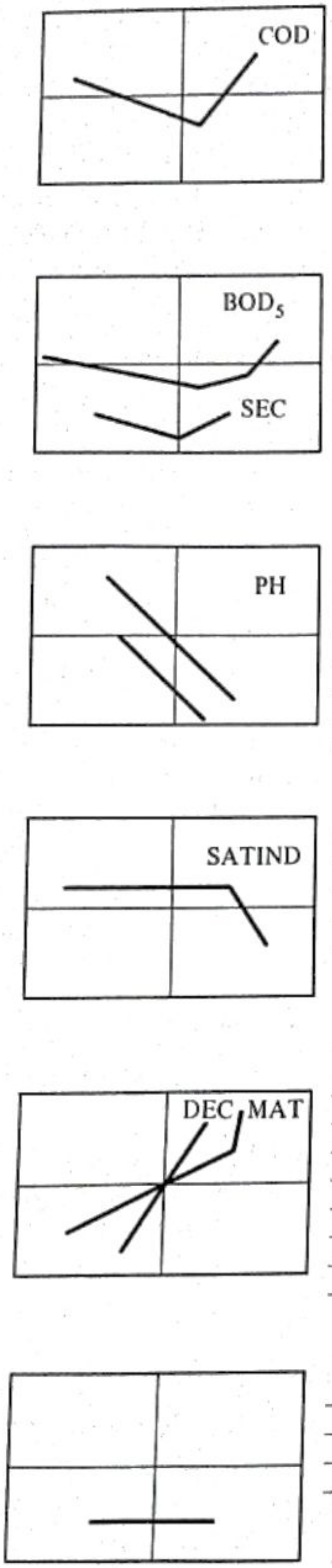

- COD
- AUTOC $O_2$
- OXYDB
- CI-LI
- SM

Related to quality of water and sensitive to flow rates

- $BOD_5$
- $Na_+$ – COND
- $SO_4$ – $O_2$ DIS
- SEC
- ORTH ($PO_4^{---}$)
- FOAM

Related to the quality, not to the flow rates

- PH
- $Ca^{+++}$
- $CO_3H^-$
- Pb
- Cr
- Cu
- Cd

Cluster for mean quality water

- SAT IND
- $NH_4^+$
- $NO_2$
- K+
- Cl–

Related to water quality and to discrimination among high quality water and probably PH

- FLOW 3–4–5
- $NO_3$
- DEC MAT
- $Mg^{++}$
- DETAN
- TRANSPARENCY
- COLOUR
- HYDRC

Almost only flow influenced

- Fe
- F
- Mn
- Zn

Related to water quality for slightly to highly polluted water

FIGURE 7-8
General diagrams of different pollutants.

naceous organic matter (MOC) and liberates nitrogenized organic matter represented by the pollutant $NH_4^+$. When we measure the quantity of oxygen consumed by this transformation, we can use the following model, derived from Streeter and Phelps:

$$L = L_0(1 - e^{-k_1 t})$$

in which $L_0$ is the initial load in MOC, $k_1$ is a self-purification coefficient and $t$ is the time. We can also formulate

$$L = L_0(1 - e^{k_1(d/v)})$$

in which $d$ is the distance covered during a time ($t$) at a velocity ($v$).

As we do not know the details of the flow speed at all points of a river, we use the formula

$$L = L_0(1 - e^{-\alpha d})$$

in which $\alpha$ is a depreciation coefficient which incorporates the flow speed.

The residual load, at the end of a distance ($d$) is obtained by:

$$L = L_0\, e^{-\alpha d}$$

which makes it possible to calculate $BOD_5$ concentration, provided that $L_0$ is expressed in terms of $BOD_5$.

Continuous transformation into $NH_4^+$ can be represented by the disposal equivalent to the production of $NH_4^+$ at the same place as the initial load $L_0$. The graph derived from the Velz diagram (Fig. 7.6) makes it possible to evaluate the equivalent quantity of $NH_4^+$.

The oxygen consumed during the first part of the biodegradation process is represented by curve C. Curve B indicates the amount of oxygen consumed by the second part of the self-purification process.

The $NH_4^+$ formed by the degradation of carbonaceous compounds is transformed into $NO_3^-$ nitrates, and the amount of oxygen consumed makes it possible to evaluate the equivalent $NH_4^+$ load eliminated at the origin. By utilizing an elimination of 8 g/d per inhabitant equivalent, we can determine the ratio between oxygen consumed by the degradation of carbonaceous compounds and oxygen consumed by degradation of nitrogenized compounds. This ratio is evaluated at 0.35.

Furthermore, a degradation of 1 mg of $NH_4^+$ requires 3.56 mg of oxygen. The equivalent load of $NH_4^+$ ($A_0$) is thus obtained by the ratio

$$A_0 = \frac{0.35}{3.56}(L_0 - L)$$

The $NH_4^+$ degradation process consumes oxygen and forms nitrates represented by the ion $NO_3^-$. The ratio between the $NO_3^-$ (No) load produced and the amount of degraded $NH_4$ ($A_0 - A$) is as follows:

$$N_0 = \frac{62}{18}(A_0 - A)$$

On the whole these elements can be summarized as follows:

$C_0(\mathrm{MO})$

$\downarrow$

$L_0(\mathrm{BOD}_5) = 0.8\ C_0$

$\downarrow$

$L_0(\mathrm{BOD}_{20}) = (0.03T + 0.87)L_0(\mathrm{BOD}_5)$

$\downarrow$

Self-purification.

$L = L_0\, e^{-\alpha d} \rightarrow$ consumed oxygen

$\Delta \mathrm{O}1 = L_0(1 - e^{-\alpha d})$

$\downarrow$

$\mathrm{NH_4}^+$ equivalent load

$$A_0 = \frac{0.35}{3.56} L_0(1 - e^{-\alpha d})$$

$\downarrow$

Self-purification

$\downarrow$

$A = A_0 f(d)$

$\downarrow$

$\mathrm{NO_3}^-$ equivalent load

$$N_0 = \frac{62}{18}(A_0 - A)$$

This all occurs as if the load $L_0$ of $\mathrm{BOD}_5$ and a load $A_0$ of $\mathrm{NH_4}^+$ had been eliminated at the same time and in the same place.

If $A_0$ is expressed in oxygen necessary for its degradation, the ratio between the two loads is 0.35.

The total oxygen consumption for the whole of the self-purification process is equal to:

$$\Delta \mathrm{O}1 + \Delta \mathrm{O}2$$

where

$$\Delta \mathrm{O}1 = L_0(1 - e^{-\alpha d})$$

$$\Delta \mathrm{O}2 = (A_0 - A) \times 3.56$$

It is ascertained that curve B can in no case be represented by an expression of the following type:

$$L = L_0\, e^{-\alpha d}$$

We must therefore find a model to represent the biodegradation of nitrogenized compounds or nitrification.

### 7-7.5 Nitrification Model

The shape of the curve leads us to use a logistic type model

$$y = \frac{a}{1 + be^{-kt}}$$

The asymptote of the representative curve is composed of the straight line $y = a$ when $t \to \infty$.

It is known, on the other hand, that the inflexion point reached at the end of the time period $t_0$ is such that $y(t_0) = a/2$

so
$$be^{-kt_0} = 1$$
and
$$e^{kt_0} = b$$
whence
$$A = A_0 \cdot \frac{1 + e^{kt_0}}{e^{kt} + e^{kt_0}}$$

The oxygen consumed by this oxidation is

$$\Delta O_2 = 3.56(A_0 - A)$$

Using curve B, if these measures can be generalized, we have

$$A_0 \simeq 12/3.56 \text{ mg NH}_4{}^+$$

for
$$A(t_0 = 9 \text{ days}) \simeq 4/3.56 \text{ mg NH}_4{}^+$$

whence

$$e^{kt_0} \simeq 3$$

which can be described, using the distance $d_0$ corresponding to the time $t_0$ at flow speed $V$

$$e^{k\frac{d_0}{v}} = 3 = e^{\beta d_0}$$

Here again, the depreciation coefficient $\beta$ incorporates the flow speed.

The model used will therefore be

$$A = A_0 \frac{4}{3 + e^{\beta d}}$$

### 7-7.6 Model of Phosphate Purification

As we have no detailed information for phosphates, we will use a model similar to that of $BOD_5$, i.e., for a given load $P_0$

$$P = P_0\, e^{-\gamma d}$$

### 7-7.7 Other Pollutants

Other pollutants ($NO_3^-$ and hydrocarbons) are considered to be conservative—a pessimistic diagram. For $NO_3$ we use a multiplicative model: $N = N_0 \cdot \delta$ where $\delta$ is computed with the value of the actual concentration in the river.

## 7-8 POLLUTION BALANCE—PURIFICATION STRATEGY

For all those years for which purification figures are known, the concentration of pollutants leaving each cell can be very easily calculated using disposal estimations and depreciation coefficients. We thus deduce a water quality which is comparable to requisite constraints; these are called "quality objectives."

The requisite quality is a scenario variable which is set at different datelines. The means of attaining this minimal quality essentially consist, first of all, in using existing water softening plants as well as possible, and then building new ones. Additional flows may reduce concentrations by a dilution effect. In order to determine the utilization or installation of water treatment plants, it is necessary to develop a strategy which is parametered by juggling with the different technical priorities and which may evolve as time goes by.

The amount of $BOD_5$ to be purified is thus considered as an unknown, and this purification is simulated through a water-treatment plant. Highest concentrations are allowed and required purification rates for $BOD_5$, $NH_4^+$, $NO_3^-$ and $PO_4^{---}$ are deduced. It is then quite easy to design the plant corresponding to these criteria. The simulation model can also be used alone. Purification rates and connection rates are then imposed and the resulting pollution state is calculated.

We must point out here that dilution by means of dams is not considered to be one of the ways of attaining quality objectives. Indeed, diluting pollution only carries over into the ocean those problems which have not been solved on land.

### 7-8.1 Simulation Equations for Purification and Self-purification

**Simulation of purification plants** In order to evaluate the net disposals in the river, it is necessary to simulate the work of the purification plants already set up and also to take into account the work of the plants to be built.

The following graph gives the process which has been chosen. Note that it is not a true purification plant, but a fictitious one assembling all the equipment set up in each cell (Fig. 7.9).

Part of the gross pollutant flow does not go through the plant and is therefore directly rejected. Part of the flow is processed in a biological plant (secondary). The remainder is processed through a physico-chemical plant (tertiary). Parameters $\theta$ and $\theta'$ are representative of the yield of the various phases of the process.

We know the load rate and the real yield of the plants already set up in 1975. It is therefore possible to simulate their real work and deduce the

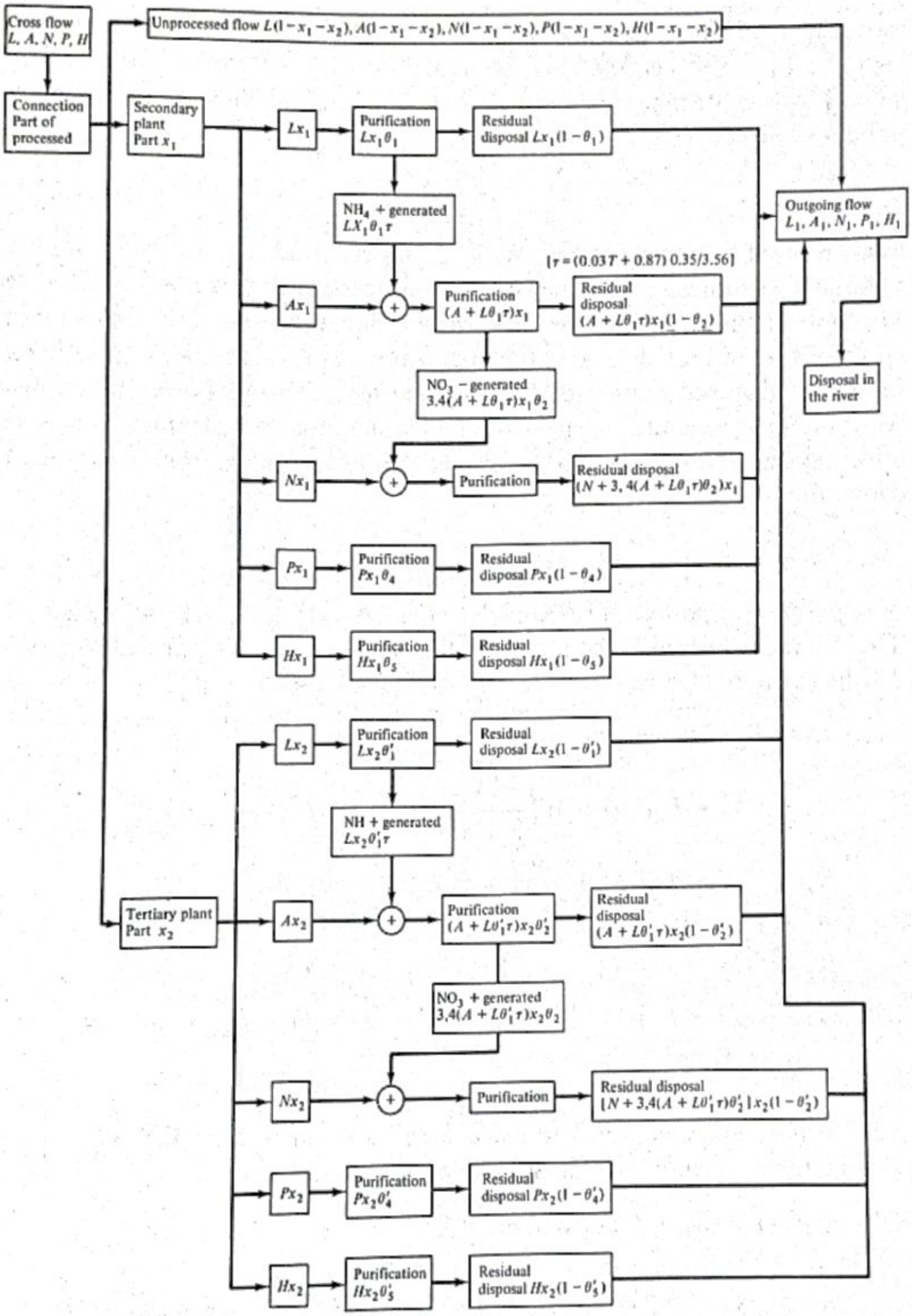
Cross flow $L, A, N, P, H$
Unprocessed flow $L(1-x_1-x_2), A(1-x_1-x_2), N(1-x_1-x_2), P(1-x_1-x_2), H(1-x_1-x_2)$
Connection Part of processed
Secondary plant Part $x_1$
$Lx_1$
Purification $Lx_1\theta_1$
Residual disposal $Lx_1(1-\theta_1)$
Outgoing flow $L_1, A_1, N_1, P_1, H_1$
$NH_4$ + generated $LX_1\theta_1\tau$
$[\tau = (0.03T + 0.87)\, 0.35/3.56]$
$Ax_1$
+
Purification $(A + L\theta_1\tau)x_1$
Residual disposal $(A + L\theta_1\tau)x_1(1-\theta_2)$
Disposal in the river
$NO_3$ − generated $3.4(A + L\theta_1\tau)x_1\theta_2$
$Nx_1$
+
Purification
Residual disposal $(N + 3,4(A + L\theta_1\tau)\theta_2)x_1$
$Px_1$
Purification $Px_1\theta_4$
Residual disposal $Px_1(1-\theta_4)$
$Hx_1$
Purification $Hx_1\theta_5$
Residual disposal $Hx_1(1-\theta_5)$
$Lx_2$
Purification $Lx_2\theta'_1$
Residual disposal $Lx_2(1-\theta'_1)$
NH + generated $Lx_2\theta'_1\tau$
Tertiary plant Part $x_2$
$Ax_2$
+
Purification $(A + L\theta'_1\tau)x_2\theta'_2$
Residual disposal $(A + L\theta'_1\tau)x_2(1-\theta'_2)$
$NO_3$ + generated $3,4(A + L\theta'_1\tau)x_2\theta_2$
$Nx_2$
+
Purification
Residual disposal $[N + 3,4(A + L\theta'_1\tau)\theta'_2]x_2(1-\theta'_2)$
$Px_2$
Purification $Px_2\theta'_4$
Residual disposal $Px_2(1-\theta'_4)$
$Hx_2$
Purification $Hx_2\theta'_5$
Residual disposal $Hx_2(1-\theta'_5)$

FIGURE 7-9

assessments of their net disposal. We should add that, as far as particular areas are concerned, it is necessary to simulate purification by infiltration (farm sewage, lagoon waste storage, disposal wells) which eliminates a great deal of the pollutant flow.

**Simulation of self-purification** With the simple models described elsewhere, it is possible to simulate the self-purification process in the river of the flow rejected. We have distinguished diffuse disposal and local disposal and the diagrammatic spots of the various disposals (upstream flow, rural disposal, domestic disposal, industrial disposal connected or unconnected, thermal power plant disposal). All these processes are given in the following equations, from which is set up a linear system which has to be solved in order to comply with the quality constraints assigned.

*Non-purified disposals: upstream flow* ($L_E$, $A_E$, $N_E$, $P_E$, $H_E$ *in kg/d*)
The distance covered is the length of the cell, *l*. After self-purification, we obtain downstream of the cell:

$$L_{\bar{E}} = L_E\, e^{-\alpha l} = L_E \alpha_E$$

$$A_{\bar{E}} = [A_E + L_E(1 - \alpha_E)\tau] \frac{4}{3 + e^{\beta e}} = [A_E + L_E(1 - \alpha_E)\tau] \beta_E$$

$$N_{\bar{E}} = \{N_E + 3.4[A_E + L_E(1 - \alpha_E)\tau](1 - \beta_E)\}\, \delta_E$$

$$P_{\bar{E}} = P_E\, e^{-\gamma l} = P_E \gamma_E$$

$$H_{\bar{E}} = H_E$$

$$\mathrm{O}_E = L_E(1 - \alpha_E) + 3.56[A_E + L_E(1 - \alpha_E)\tau](1 - \beta_E) \text{ (consumed oxygen)}$$

*Non-purified disposals: Diffuse agricultural and rural flow* ($L_A$, $A_A$, $N_A$, $P_A$, $H_A$)
The distance covered is the length of the cell, *l*.

$$L_{\bar{A}} = L_A(1 - e^{-\alpha l})/\alpha l = L_A \alpha_E$$

$$A_{\bar{A}} = [A_A + L_A(1 - \alpha_A)\tau] \cdot \frac{4}{3\beta l} \log \frac{4\, e^{\beta l}}{3 + e^{\beta l}}$$

$$= [A_A + L_A(1 - \alpha_A)\tau] \beta_A$$

$$N_{\bar{A}} = \{N_A + 3.4[A_A + L_A(1 - \alpha_A)\tau](1 - \beta_A)\}\, \delta_A$$

$$P_{\bar{A}} = P_A(1 - e^{-\gamma l})/\gamma l = P_A \gamma_A$$

$$H_{\bar{A}} = H_A$$

$$\mathrm{O}_A = L_A(1 - \alpha_A) + 3.56[A_A + L_A(1 - \alpha_A)\tau](1 - \beta_A)$$

*Non-purified disposals: Equivalent disposals of thermal power plants* ($L_c$, $A_c$, 0, 0, 0)
The distance covered is the distance between the plant and the exit from the cell, $l_c$.

$$
\begin{aligned}
L_{\bar{c}} &= L_c\, e^{-\alpha l_c} = L_c \alpha_c \\
A_{\bar{c}} &= [A_c + L_c(1-\alpha_c)\tau]\,\frac{4}{3+e^{\beta l_c}} = [A_c + L_c(1-\alpha_c)\tau]\beta_c \\
N_{\bar{c}} &= 3.4[A_c + L_c(1-\alpha_c)\tau](1-\beta_c)\,\delta_c \\
P_{\bar{c}} &= 0 \\
H_{\bar{c}} &= 0 \\
\mathrm{O}_c &= L_c(1-\alpha_c) + 3.56[A_c + L_c(1-\alpha_c)\tau](1-\beta_c)
\end{aligned}
$$

*Purified disposals: Industrial unconnected* ($\mathrm{L_I}$, $\mathrm{A_I}$, $\mathrm{N_I}$, $\mathrm{P_I}$, $\mathrm{H_I}$)
The distance covered is fixed at $l/2$. The part ($y_1$) of the disposals is processed through a secondary plant (yield $\theta_1$, $\theta_2$, $\theta_3$, $\theta_4$, $\theta_5$), part ($y_2$) through a tertiary plant ($\theta'_1$, $\theta'_2$, $\theta'_3$, $\theta'_4$, $\theta'_5$). Part $(1 - y_1 - y_2)$ is not purified.

If ($L'_I$, $A'_I$, $N'_I$, $P'_I$, $H'_I$) are the disposals at the exit of the plant, we have, as previously,

$$
\begin{aligned}
L'_{\bar{I}} &= L'_I\, e^{-\alpha l/2} = L'_I \alpha_I \\
A'_{\bar{I}} &= [A'_I + L'_I(1-\alpha_I)\tau]\cdot\frac{4}{3+e^{\beta l/2}} = [A'_I + L'_I(1-\alpha_I)\tau]\beta_I \\
N'_{\bar{I}} &= \{N'_I + 3.4[A'_I + L'_I(1-\alpha_I)\tau](1-\beta_I)\}\,\delta_I \\
P'_{\bar{I}} &= P'_I\, e^{-\gamma l/2} = P'_I \gamma_I \\
H'_{\bar{I}} &= H'_I \\
\mathrm{O}_I &= L'_I(1-\alpha_I) + 3.56[A'_I + L'_I(1-\alpha_I)\tau](1-\beta_I)
\end{aligned}
$$

Now

$$
\begin{aligned}
L'_I &= L_I(1-y_1-y_2) + L_I y_1(1-\theta_1) + L_I y_2(1-\theta'_1) \\
A'_I &= A_I(1-y_1-y_2) + (A_I + L_I\theta_1\tau)y_1(1-\theta_2) \\
&\quad + (A_I + L_I\theta'_1\tau)y_2(1-\theta'_2) \\
N'_I &= N_I(1-y_1-y_2) + [N_I + 3.4(A_I + L_I\theta_1\tau)\theta_2]y_1(1-\theta_3) \\
&\quad + [N_I + 3.4(A_I + L_I\theta'_1\tau)\theta'_2]y_2(1-\theta'_3) \\
P'_I &= P_I(1-y_1-y_2) + P_I y_1(1-\theta_4) + P_I y_2(1-\theta'_4) \\
H'_I &= H_I(1-y-y_2) + H_I y_1(1-\theta_5) + H_I y_2(1-\theta'_5)
\end{aligned}
$$

which gives, by separating the terms corresponding to the unprocessed disposals and the processed ones:

$$\boxed{L_I' = L_I\alpha_I - L_I y_1 \theta_1 \alpha_I - L_I y_2 \theta_1' \alpha_I}$$

$$\boxed{\begin{aligned} A_I' = {} & A_I + L_I(1 - \alpha_I)\tau)\beta_I - y_1[A_I\theta_2 - L_I\tau\theta_1(\alpha_I - \theta_2]\beta_I \\ & - y_2[A_I\theta_2' - L_I\tau\theta_1'(\alpha_I - \theta_2']\beta_I \end{aligned}}$$

$$\boxed{\begin{aligned} N_I' = {} & (N_I + 3.4(A_I + L_I(1 - \alpha_I)\tau)(1 - \beta_I)\,\delta_I \\ & - y_1\{N_I\theta_3 - 3.4A_I\theta_2(\beta_I - \theta_3) \\ & - 3.4L_I\theta_1\tau\,[\theta_2(1 - \theta_3) + (1 - \beta_I)(\alpha_I - \theta_2)]\}\,\delta_I \\ & - y_2\{N_I\theta_3' - 3.4A_I\theta_2'(\beta_I - \theta_3') \\ & - 3.4L_I\theta_1'\tau\,[\theta_2'(1 - \theta_3') + (1 - \beta_I)(\alpha_I - \theta_2')]\}\,\delta_I \end{aligned}}$$

$$\boxed{P_I' = P_I\gamma_I - P_I y_1 \theta_4 \gamma_I - P_I y_2 \theta_4' \gamma_I}$$

$$\boxed{H_I' = H_I - H_I y_1 \theta_5 - H_I y_2 \theta_5'}$$

$$\boxed{\begin{aligned} \mathrm{O}_I = {} & L_I(1 - \alpha_I) + 3.56[A_I + L_I\tau(1 - \alpha_I)](1 - \beta_I) \\ & - 3.56y_1[A_I\theta_2 + L_I\tau\theta_1(\theta_2 - \alpha_I)](1 - \beta_I) \\ & - 3.56y_2[A_I\theta_2' + L_I\tau\theta_1'(\theta_2' - \alpha_I)](1 - \beta_I) \end{aligned}}$$

*Domestic and connected industrial* ($\mathrm{L_U}$, $\mathrm{A_U}$, $\mathrm{N_U}$, $\mathrm{P_U}$, $\mathrm{H_U}$)
With no large town in the cell, the distance to cover is again given as $l/2$. In the opposite case, we assume that urban disposals and those from connected industries occur at the same place as large town disposals, i.e., a distance $l_v$ from the exit of the cell. Note $(x_1)$ as the part of the disposal processed through a secondary plant, $(x_2)$ as the part processed through a tertiary plant, and $(1 - x_1 - x_2)$ as the unprocessed part of the disposal.

We get the same quantities as for the unconnected industries with $x$ instead of $y$, the index $U$ or $V$ instead of $I$, and the yield $(\sigma_1, \sigma_2, \sigma_3, \sigma_4, \sigma_5, \sigma_1', \sigma_2', \sigma_3', \sigma_4', \sigma_5')$ instead of $(\theta_1, \theta_2, \theta_3, \theta_4, \theta_5, \theta_1', \theta_2', \theta_3', \theta_4', \theta_5')$.

*Global assessment*

From the previous equations we can deduce the downstream flow ($L_s$, $A_s$, $N_s$, $P_s$, $H_s$) resulting from the disposals and purifications. This flow (changed into concentrations) will have to be compared to the concentrations limit given by the constraint "quality objective."

*Global assessment: $BOD_5$*

$$L_S = L_{\bar{E}} + L_{\bar{A}} + L_{\bar{C}} + L_{\bar{I}} + L_{\bar{U}}$$

With $L_0 = L_E\alpha_E + L_A\alpha_A + L_C\alpha_C + L_I\alpha_I + L_U\alpha_U$ we obtain

$$\boxed{L_S = L_0 - L_I y_1 \theta_1 \alpha_I - L_I y_2 \theta'_1 \alpha_I - L_U x_1 \sigma_1 \alpha_U - L_U x_2 \sigma'_1 \alpha_U}$$

If $C_L$ is the concentration limit and $Q_s$ the downstream flow, we have

$$\boxed{\begin{aligned} & L_I\theta_1\alpha_I y_1 + L_I\theta'_1\alpha_I y_2 + L_U\sigma_1\alpha_U x_1 \\ & \qquad + L_U\sigma'_1\alpha_U x_2 \geq L_0 - C_L Q_S \end{aligned}}$$

*Global assessment: $NH_4{}^+$*

$$A_S = A_{\bar{E}} + A_{\bar{A}} + A_{\bar{C}} + A_{\bar{I}} + A_{\bar{U}}$$

With

$$\begin{aligned} A_0 = {} & A_E\beta_E + A_A\beta_A + A_C\beta_C + A_I\beta_I + A_U\beta_U \\ & + \tau[L_E(1-\alpha_E)\beta_E + L_A(1-\alpha_A)\beta_A \\ & + L_C(1-\alpha_C)\beta_C + L_I(1-\alpha_I)\beta_I \\ & + L_U(1-\alpha_U)\beta_U] \end{aligned}$$

we obtain

$$\begin{aligned} A_S = A_0 & - y_1[A_I\theta_2 - L_I\tau\theta_1(\alpha_I - \theta_2)]\beta_I \\ & - y_2[A_I\theta'_2 - L_I\tau\theta'_1(\alpha_I - \theta'_2)]\beta_I \\ & - x_1[A_U\sigma_2 - L_U\tau\sigma_1(\alpha_U - \sigma_2)]\beta_U \\ & - x_2[A_U\sigma'_2 - L_U\tau\sigma'_1(\alpha_U - \sigma'_2)]\beta_U \end{aligned}$$

which implies, with the concentration limit $C_A$ and the downstream flow $Q_s$ the constraint: $A_s \leq C_A Q_s$

$$\boxed{\begin{aligned} & [A_I\theta_2 - L_I\tau\theta_1(\alpha_I - \theta_2)]\beta_I y_1 \\ & + [A_I\theta'_2 - L_I\tau\theta'_1(\alpha_I - \theta'_2)]\beta_I y_2 \\ & + [A_U\sigma_2 + L_U\tau\sigma_1(\alpha_U - \sigma_2)]\beta_U x_1 \\ & + [A_U\sigma'_2 - L_U\tau\sigma'_1(\alpha_U - \sigma'_2)]\beta_U \cdot x_2 \geq A_0 - C_A Q_S \end{aligned}}$$

*Global assessment:* $NO_3^-$

$$\delta_A = \delta_E = \delta_C = \delta_S = \delta_U = \delta$$

$$N_S = N_E + N_{\bar{A}} + N_C + N_{\bar{I}} + N_{\bar{U}}$$

With
$$\begin{aligned} N_0 = \{ & N_E + N_A + N_C + N_I + N_U \\ & + 3.4[A_E(1-\beta_E) + A_A(1-\beta_A) + A_C(1-\beta_C) + A_I(1-\beta_I) \\ & + A_U(1-\beta_U)] + 3.4\tau[L_E(1-\alpha_E)(1-\beta_E) + L_A(1-\alpha_A)(1-\beta_A) \\ & + L_C(1-\alpha_C)(1-\beta_C) + L_I(1-\alpha_I)(1-\beta_I) + L_U(1-\alpha_U)(1-\beta_U)]\} \end{aligned}$$

we get the constraint $N_S \leq C_v Q_s$, i.e.,

$$\boxed{\begin{aligned} & [N_I\theta_3 - 3.4A_I\theta_2(\beta_I - \theta_3) - 3.4L_I\theta_1\tau \\ & \quad \times (\theta_2(1-\theta_3) + (1-\beta_I)(\alpha_I - \theta_2))]\,\delta y_1 \\ & + [N_I\theta_3' - 3.4A_I\theta_2'(\beta_I - \theta_3') - 3.4L_I\theta_1'\tau \\ & \quad \times (\theta_2'(1-\theta_3') + (1-\beta_I)(\alpha_I - \theta_2'))]\,\delta y_2 \\ & + [N_U\sigma_3 - 3.4A_U\sigma_2(\beta_U - \sigma_3) - 3.4L_U\sigma_1\tau \\ & \quad \times (\sigma_2(1-\sigma_3) + (1-\beta_U)(\alpha_U - \sigma_2))]\,\delta x_1 \\ & + [N_U\sigma_3' - 3.4A_U\sigma_2'(\beta_U - \sigma_3') - 3.4L_U\sigma_1'\tau \\ & \quad \times (\sigma_2'(1-\sigma_3') + (1-\beta_U)(\alpha_U - \sigma_2'))]\,\delta x_2 \geq N_0 - C_N Q_S \end{aligned}}$$

*Global assessment:* $PO_4^{---}$

$$P_S = P_E + P_{\bar{A}} + P_C + P_{\bar{I}} + P_{\bar{U}}$$

With
$$P_0 = P_E\gamma_E + P_A\gamma_A + P_C\gamma_C + P_I\gamma_I + P_U\gamma_U$$

we obtain the constraint $P_S \leq C_p Q_S$ *i.e.*,

$$\boxed{\begin{aligned} & P_I\theta_4\gamma_I y_1 + P_I\theta_4'\gamma_I y_2 + P_U\sigma_4\gamma_U x_1 \\ & + P_U\sigma_4'\gamma_U \cdot x_2 \geq P_0 - C_p Q_S \end{aligned}}$$

*Global assessment: Hydrocarbons*

$$\begin{aligned} H_S &= H_E + H_{\bar{A}} + H_C + H_{\bar{I}} + H_{\bar{U}} \\ &= H_E + H_A + H_C + H_I + H_U - H_I y_1\theta_5 \\ &\quad - H_I y_2\theta_5' - H_U x_1\sigma_5 - H_U x_2\sigma_5' \end{aligned}$$

We use no constraint for this pollutant.

*Global assessment: Oxygen*

The total consumed oxygen can be read

$$
\begin{aligned}
\mathrm{O}_T = {} & L_E(1-\alpha_E) + L_A(1-\alpha_A) + L_C(1-\alpha_C) \\
& + \mathrm{L}_I(1-\alpha_I) + L_U(1-\alpha_U) \\
& + 3.56[(A_E + L_E\tau(1-\alpha_E))](1-\beta_E) \\
& + (A_A + L_A\tau(1-\alpha_A))(1-\beta_A) \\
& + (A_C + L_C\tau(1-\alpha_C))(1-\beta_C) \\
& + (A_I + L_I\tau(1-\alpha_I))(1-\beta_I) + (A_U + L_U\tau(1-\alpha_U))(1-\beta_U) \\
& - 3.56y_1[A_I\theta_2 + L_I\tau\theta_1(\theta_2-\alpha_I)](1-\beta_I) \\
& - 3.56y_2[A_I\theta_2' + L_I\tau\theta_1'(\theta_2'-\alpha_I)](1-\beta_I) \\
& - 3.56x_1[A_U\sigma_2 + L_U\tau\sigma_1(\sigma_2-\alpha_U)](1-\beta_U) \\
& - 3.56x_2[A_U\sigma_2' + L_U\tau\sigma_1'(\sigma_2'-\alpha_U)](1-\beta_U)
\end{aligned}
$$

which can also be read:

$$\mathrm{O}_T = \mathrm{O}_0 - \mathrm{O}_1 y_1 - \mathrm{O}_2 y_2 - \mathrm{O}_3 x_1 - \mathrm{O}_4 x_2$$

If we balance the oxygen in the cell, we have

Downstream oxygen = Upstream oxygen + input of local resources (at saturation level) − consumption ($\mathrm{O}_t$) + reoxygenation

We assumed that reoxygenation was proportional to the consumption with a coefficient $\omega(<1)$; hence

$$\mathrm{O}_s = \mathrm{O}_e + \Delta\mathrm{O} + \mathrm{O}_T(\omega - 1)$$

and the constraint "quality objective" implies that $\mathrm{O}_s \geq C_0 Q_s$ whence the constraint on $\mathrm{O}_T$ is:

$$\mathrm{O}_T < \frac{C_0 Q_s - \mathrm{O}_e - \Delta\mathrm{O}}{\omega - 1}$$

Thus we obtain the linear equation

$$\mathrm{O}_1 y_1 + \mathrm{O}_2 y_2 + \mathrm{O}_3 x_1 + \mathrm{O}_4 x_2 > \mathrm{O}_0 - (C_0 Q_s - \mathrm{O}_e - \Delta\mathrm{O})/\omega - 1$$

### 7-8.2 Equipment Programme

The constraints of the objective of quality, described above, allow the problem to be solved to be presented in the form of a linear system of inequality. We can write this system in the following form

$$\begin{aligned}
L_1 y_1 + L_2 y_2 + L_3 x_1 + L_4 x_2 &\geq L_0 - C_L Q_S \\
A_1 y_1 + A_2 y_2 + A_3 x_1 + A_4 x_2 &\geq A_0 - C_A Q_S \\
N_1 y_1 + N_2 y_2 + N_3 x_1 + N_4 x_2 &\geq N_0 - C_N Q_S \\
P_1 y_1 + P_2 y_2 + P_3 x_1 + P_4 x_2 &\geq P_0 - C_p Q_S \\
\mathrm{O}_1 y_1 + \mathrm{O}_2 y_2 + \mathrm{O}_3 x_1 + \mathrm{O}_4 x_2 &\geq \mathrm{O}_0 - (C_0 Q_S - \mathrm{O}_C - \Delta \mathrm{O})/\omega - 1 \qquad T \\
y_1 + y_2 &\leq 1 \\
x_1 + x_2 &\leq 1 \\
x_1, x_2, y_1, y_2 &\geq 0
\end{aligned}$$

We can find one solution to this system, without any other condition, but it is simpler to transform the equation system (I) into a small linear program, by choosing one linear function of $(y_1, y_2, x_1, x_2)$ to minimize.

$$(\mathrm{II}) = (\mathrm{I}) + \min(C_1 y_1 + C_2 y_2 + C_3 x_1 + C_4 x_2)$$

If we choose, for example, to express the cost of installation of a tertiary plant as about five times more than a secondary plant, we get:

$$C_1 = C_3 = 1 \text{ and } C_2 = C_4 = 5$$

The solution of the system when it exists enables one to go back to quantities to be purified for each pollutant. What remains to be found out is the way to purify these quantities.

In the case where no solution exists, we suppose that all the disposals are processed by tertiary purification ($y_2 = x_2 = 1$) and we suggest other ways of complying with this objective of quality. In the model used, we retained three of these:

*1* Supplementary purification in the upstream cells, in order to limit the incoming flow. We show the surplus concentration entering the cells.
*2* If the possibility of an upstream withdrawal exists, we show the dilution necessary in respect of quality constraints.
*3* Finally, we can try to reduce the pollutants by special technologies and reduce the quantities $L_I$, $A_I$, $N_I$, $P_I$, $H_I$, $L_u$, $A_u$, $N_u$, $P_u$, and $H_u$.

The flow chart in Fig. 7.10 shows the calculating procedures set up.

### 7-8.3 Application

The preceding methods have been applied, for example, in the Oise-Aisne sub-basin of the Seine-Normandy basin, in a first step, and then generalized all over the basin.

The map (Fig. 7-11) shows the quantities from which the $\mathrm{BOD}_5$ has to be removed to comply with the objectives of quality 1985 for this sub-basin (kilograms per day).

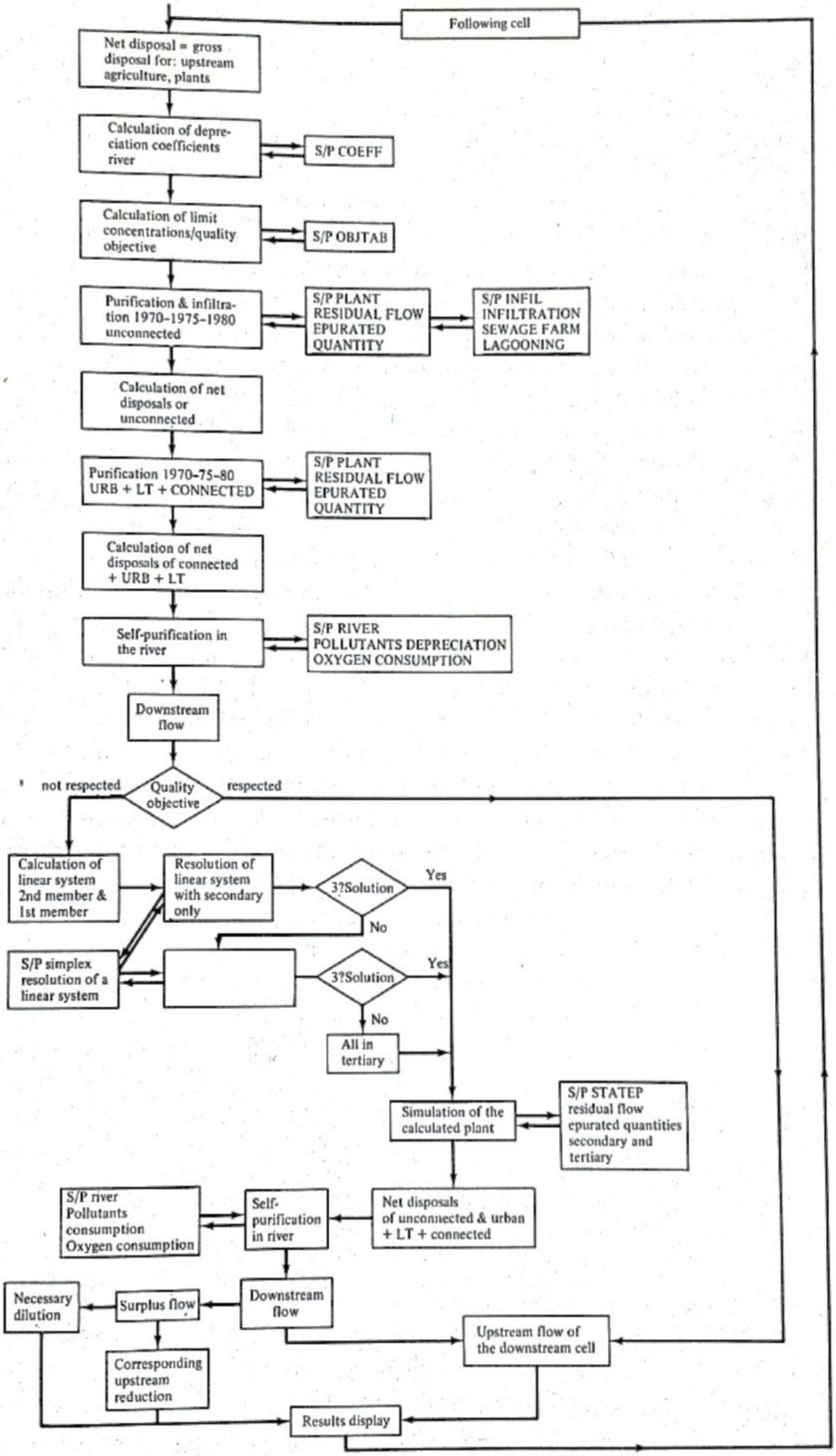
Following cell
Net disposal = gross disposal for: upstream agriculture, plants
Calculation of depreciation coefficients river
S/P COEFF
Calculation of limit concentrations/quality objective
S/P OBJTAB
Purification & infiltration 1970–1975–1980 unconnected
S/P PLANT RESIDUAL FLOW EPURATED QUANTITY
S/P INFIL INFILTRATION SEWAGE FARM LAGOONING
Calculation of net disposals or unconnected
Purification 1970–75–80 URB + LT + CONNECTED
S/P PLANT RESIDUAL FLOW EPURATED QUANTITY
Calculation of net disposals of connected + URB + LT
Self-purification in the river
S/P RIVER POLLUTANTS DEPRECIATION OXYGEN CONSUMPTION
Downstream flow
not respected
Quality objective
respected
Calculation of linear system 2nd member & 1st member
Resolution of linear system with secondary only
3?Solution
Yes
No
S/P simplex resolution of a linear system
3?Solution
Yes
No
All in tertiary
Simulation of the calculated plant
S/P STATEP residual flow epurated quantities secondary and tertiary
S/P river Pollutants consumption Oxygen consumption
Self-purification in river
Net disposals of unconnected & urban + LT + connected
Necessary dilution
Surplus flow
Downstream flow
Upstream flow of the downstream cell
Corresponding upstream reduction
Results display

FIGURE 7-10

## 7-9 PROJECTIONS

The first part of this report consisted in developing simulation diagrams and determining the necessary constants to make the model operable and capable of reconstructing a known situation. Starting from the year 1971, calculations are made for 1974, and the evolution of rivers is compared with known figures.

The development of water-treatment plants and dams in service is known until around 1980. So for these years it is not necessary to utilize the strategies of water-treatment plant installation and reservoir-dam construction.

For 1980, however, the model is utilized in projection. Such projections require different entries derived from economic, demographic, technological and environmental scenarios established elsewhere. Let us give some details.

Projection of quantity and quality of drawn water as well as of polluting waste requires a good previous knowledge of the demographical situation—number of residents, type of community, implantation—as well as of industrial, agricultural and energy installations. The difficulty encountered in carrying out definite forecasts led to designing the projection model as a simulation model of coherent scenarios. The management of the simulation parameters thus makes it possible to utilize the most widely differing scenarios with periodic up-dating.

As the extrapolation methods are based on recent tendencies and mandatory submission to imposed constraints, the design and use of such methods are only meaningful under the hypothesis of a certain stability of human and economic structures in the environment, especially the absence of conflicts or crises which could modify or destroy human and economic potential.

SPIRE, on the other hand, does not assume a tendential evolution.

Considering the impossibility of creating an economic model, or a complete demographical model for one region only, and in order to ensure coherency and compatibility with the rest of France, it is preferable to extract projections

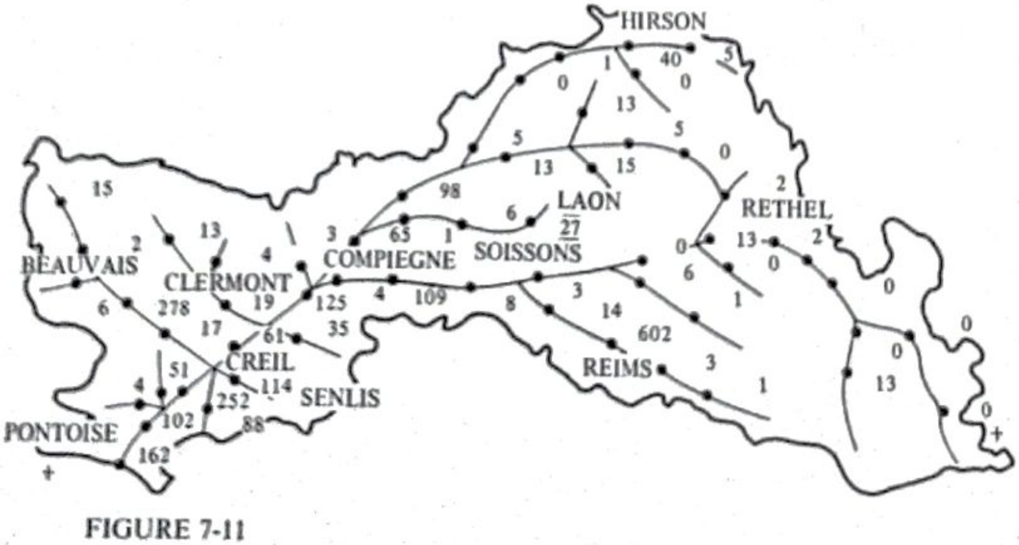

FIGURE 7-11
Map indicating quantities from which $BOD_5$ has to be removed for water quality compliance.

concerning the Seine–Normandy basin only from the results of a model for the whole of France.

This has the advantage of avoiding extrapolations of wealth and of local population which, as experience has shown, lead to attributing to the region a share of increase higher than that which other regions would postulate in their own calculations.

### 7-9.1 General Outline of the Economic Model

**Presentation** This is a Leontieff model based on the use of the input–output tables of the National Accounts. The goal of this model is to calculate the active population actually employed in each economic sector and each of the zones considered.

The almost total absence of data concerning production, productivity, consumption, inter-regional exchange and so on, on the regional level, implies the construction of a national model for which the results are then regionalized. All calculations are made in constant 1970 French francs and do not therefore require financial calculations.

**Economic data** We have at our disposal (from the INSEE, or National Institute for Statistics and Economic Studies) Input–Output Tables in constant 1962 or 1970 French francs for the years 1959 to 1974. In these tables are found

($X_i$) Total production by industrial sector
($Y_i$) Final demand, divided into:
  Household, Administrative and Financial Institution consumption
  Investment in Capital Equipment for households, administrations, financial Institutions and companies
  Exports, stock variations
($A_{ij}$) Volumes of goods exchanges between sectors
($V_j$) Added values by sector
($M_j$) Margins for each sector
($IM_j$) Imports and fees and taxes by sector
($P_j$) Production of each sector at domestic cost

Using these elements, it is possible to move on to technological coefficients, and linear formalism can be adopted to calculate the total gross production for each sector starting from the final demand per sector.

**Employment** At each census figures are available for the number of employed people, in each branch and in territorial unit.

On the other hand, the figures available annually, which are linked to demography, concern active people employed in each economic sector. The model can therefore be checked by moving from industrial branch to economic sector.

**Pseudo-productivity** Starting from the previous elements, we calculate for each year the ratio of production at domestic cost by branch to jobs in the corresponding sector. This is thus a global apparent productivity which measures production per job in each branch in constant 1970 French francs. This coefficient usually evolves quite regularly and, after extrapolation, makes it possible to move on from production per branch to the corresponding jobs quite easily.

### 7-9.2 Design of the Model

**Evolution of the TES** (Input–Output Tables). The first difficulty lies in extrapolating the TES. This extrapolation respects those tendencies observed in preeeding years, but must also be able to undergo forecasted or simulated technological modifications.

Using the TES of the National Accounts, begin by calculating the "technological coefficients," dividing interbranch exchange volumes by domestic cost production of these branches.

On examining these elements from 1959 to 1974, we ascertain that these sums (or weights) in lines, columns and totals, evolve with the passage of time. The T.E.S. extrapolation is thus carried out in two steps, either letting the table evolve tendentially or imposing evolution constraints on its margins, with or without constraint by a linear extrapolation for one year. The first step consists in making the margins and then the inside of the table evolve. Then, the second step ensures the accountable balance of the table. In order to achieve such a balance, each line of the table has to be proportionally corrected so that the sum of its elements are equal to the value resulting from the extrapolated margins. This correction has to be made also for the columns and again for the lines and so on until stabilization of the table is achieved. This method (RAS method), used many times during the model, efficiently insures the consistency of the results which will be used as data at the following step. This means that the induced effects of a given development, e.g., chemistry, on transport or energy are taken into consideration. The economic development under study is thus possible and coherent.

In this way a TES is obtained each year with weights in lines and columns and with margin coefficients extrapolated in the same way.

**Leontieff model** Knowing the technological matrix $A^{t+1}$ on the date $t + 1$, in order to calculate gross production by branch, it is necessary to know final demand, imports, and margins by branch. This is a classical Leontieff model, which provides gross production for each branch.

Using the transfer coefficient composed of the apparent pseudo-productivities, we obtain for each division employment figures per economic sector for the whole of France.

**Final demand** The development of economic scenarios is thus described by the hypotheses concerning final demand, that is: types of consumption in households and administrations; investment in capital for households, companies and administrations; structure of imports and exports; and various results such as business. Starting with these elements, and to give a concrete example, the relations between energy and environment can be analyzed, taking effects induced on utilities and population into account.

**Results of the economic model** The results are presented for any year desired, on a listing page. They include the following elements:

Date
Names of branches
Extrapolated and adjusted technological coefficient tables
Weight of the columns for the table (the complement to 1 is the added value coefficient)
(on line is the second part of the table)
Weights of the lines for the table
Total production in millions of 1970 French francs per branch
Final demand in millions of 1970 French francs per branch
Number of jobs per corresponding sector
Pseudo-productivity extrapolated for each branch (modifiable to ensure coherency between employment and active population)
Added value per branch in millions of 1970 French francs

The demographical model used has several objectives. The first is to have at our disposal demographical scenarios which are coherent with the economic development model. Especially for this purpose, the regional situations vacant in the economy are checked against situations wanted by the active population in each age bracket. The next objective is to have the population evolve in time according to birth rate and life expectancy for the different age brackets. Next, to check the effect of alternating, definitive or touristic migration on water demand and pollutant production. The model also enables us to identify the different communities—large towns, small towns, rural areas—so that they are coherent with the economy.

These objectives being specified, the procedure is a classical one, as such models are henceforth usual and common.

In order to carry out the latter studies, fifteen years of Input–Output Tables and the censuses from 1962 to 1968 were used to calculate:

Technical coefficients and their evolution (one franc for a given branch requires so many centimes from another branch)
Final consumption per branch according to growth scenarios
Regionalization of exchanges based on territorial development plans
Apparent productivity figures (in francs/job/branch), with their evolution and distribution
Job per sector and per region

Potential active population by region in time
Population and its regionalization in time

The period from 1959 to 1975 was used as a point of reference. The 1975 census was used as a check. The period analyzed goes from 1970 to the year 2000.

## 7-10 THE SCENARIOS

### 7-10.1 Forecasting and the Scenario

Forecasting is very difficult—especially as far as the future is concerned, as the old Chinese proverb goes. The difficulty of describing the future accurately led us to adopt the procedure followed by the SESAME team, using scenarios and trajectories.

First of all the future is not described by a single point, but is delimited by a series of possible situations—scenarios which are not mere extrapolations of the past. Extrapolation, in fact, explains nothing. In order to be able to act on each individual factor, each scenario is checked in terms of coherency: this at least ensures that the situations taken as references are possible, even if they do not predict the future. Moreover, the sensitivity of development decisions to the variation of natural and socio-economic phenomena can be estimated according to a logical whole.

This coherency is also ensured all along the way leading to the alternate situations. On these trajectories, numerous mechanisms can come into play in an operational way, with the trajectories remaining logical with respect to each other: energy policy, birth-rate evolution, structure of household consumption, technological evolution.

In a word, we delimit a hypothetical tendential future, the likelihood of which can be checked by possible situations, and coherent trajectories leading to this future are then sought.

### 7-10.2 Options

The scenarios are organized into systems coming into play at different levels of the problem.

First of all, environmental protection and water policy are part of territorial development. Territorial development is described according to a certain number of options and means, and environmental and water policy is translated into a certain number of actions.

Such options and actions act upon a system, described in terms of:

Population
Migration and birth and death rate
Evolution of the active population
Employment
Growth rates of macroeconomic aggregates

Interindustrial exchanges
Regional economic exchanges
Structure and modes of household consumption
Modification of productivity
Energy consumption and types of energy
Structure of imports and exports

### 7-10.3 Checks

This initial set must be consistent in several respects. First of all, it must ensure consistency between the economy and the population. Indeed, a development objective is translated in terms of final consumption and in terms of production, using technical coefficients provided by the Input–Output Tables for the latter. But this production must itself be carried out with the help of the active population and is expressed, owing to productivity, in terms of jobs available.

Now the population evolution, in total mass and in distribution, is based on the evolution of birth-rate, death-rate and migration. Furthermore, each age group has an activity rate which makes it possible to reconstruct the active population. On this level, then, an all-inclusive control of job supply and demand can be ensured, the difference between the two showing the amplitude of social tensions or the need to reduce the rhythm of growth or to increase productivity.

The first all-inclusive control cannot be considered as perfect, for it must be completed by a regional control of job supply and demand. And so the production, consumption and productivity figures must be regionalized. This regionalization makes it possible at the same time to check the coherence of the territorial development diagrams.

There are therefore five possible checks or controls. The first, between population and economic growth; the second, between territorial development and regional activity; the third, on the level of potential social tensions; the fourth, between the regional salary indexes and productivities; the fifth, on the national accounts level.

Furthermore, numerous verifications are possible by comparison with the results of studies based on economic or financial projections: growth of total productivity, of active employed population, of added value, of added value by branch, or employment by sector, of energy consumption, of regionalized demography and employment.

It is obvious that at this point in the report it must not be overlooked that a large computer—in this case a CDC 7600—was needed for the tens of thousands of data and results involved.

### 7-10.4 Scenarios and Strategies

A set of consistent scenarios was thus built up considering alternatives related to the following aspects:

| | |
|---|---|
| Territorial development: | voluntarist<br>tendential |
| Growth of macroeconomic aggregates, productions, final demands | |
| Household consumption: | tendential<br>non-tendential |

Energy consumption
Production technology
Import-export structure
Birth rate and migrations.

These scenarios are completed by:

Environmental protection objectives
Flood prevention safety goals
Water supply security goals

Strategies are then tested on:

Types of construction to be built
Choice of priorities in construction
Distribution of resources
Permissible frequency of risks
Investment mass which can be envisaged
Distribution of financial charges.

One may legitimately wonder whether the development of such an arsenal was really necessary. Three main reasons can be cited in favour of this basic work.

First of all, the induced effects of any economic or demographical action, or of carrying out an environmental policy, are far from negligible, due to interaction between branches of the economy on the one hand, and between job supply and demand on the other hand.

For instance, it suffices to say that a purely agricultural region needs chemistry—fertilizers—energy, transports, utilities, markets: in other words urban areas. In the present example we have not even distinguished breeding, forests, crops, irrigation, and transformations through agricultural industries.

Furthermore, as extrapolation techniques do not ensure internal consistency in development, they lead each "actor" in the scheme to assign himself the main part of future development: the sum of independent regional population predictions, which refer to a figure of 60 million inhabitants for France in the year 2000, gives a total between 72 and 76 million people, for whom, in addition to the general inaccuracy, nobody could know the means of survival, production and investment, quite apart from unemployment rates. Consistency between scenarios must therefore be ensured.

Finally, a certain accuracy or subtlety of the tools used is necessary to describe both the economic and the hydrological network.

When all is said and done, it must be admitted that recent upheavals in the energy situation and in supply structures are responsible for the apparent complexity of the system, the instructions for which are simple in the long run. Then, the chosen method consists in answering a set of questions for each scenario:

If economic and demographical evolution in a certain direction is desired, protecting natural resources in a certain way, ensuring satisfaction of water requirements and protecting the population against floods, then

*1* Are any impossibilities encountered? Which ones? How can they be reduced?
*2* What investments and what operational expenses must be programmed?
*3* What rules are necessary?

Instead of trying to predict the future, it is therefore encircled with situations and possible evolutions, and we compare strategy files, for the assessments of

**Table 7-4 DISPLAY PARAMETERS**

| Order No | Unit | Meaning |
|---|---|---|
| 1 | — | Number of the cell |
| 2 | 1,000 inhab. | Total population |
| 3 | MF 1970 | Total production |
| 4 | 10 × kg/d | Gross $BOD_5$ |
| 5 | 10 × kg/d | Gross $NH_4^+$ |
| 6 | 10 × kg/d | Gross $PO_4$ |
| 7 | 10 × kg/d | Capacity of domestic treatment plant |
| 8 | 10 × kg/d | Capacity of industrial treatment plant |
| 9 | 10 × kg/d | $BOD_5$ domestic purification |
| 10 | 10 × kg/d | $NH_4^+$ domestic purification |
| 11 | 10 × kg/d | $PO_4$ domestic purification |
| 12 | 10 × kg/d | $BOD_5$ industrial purification |
| 13 | 10 × kg/d | $NH_4^+$ industrial purification |
| 14 | 10 × kg/d | $PO_4$ industrial purification |
| 15 | % | Rate of secondary purification |
| 16 | % | Rate of tertiary purification |
| 17 | inhab. eq. | Secondary purification |
| 18 | inhab. eq. | Tertiary purification |
| 19 | — | Quality objectives |
| 20 | — | Quality |
| 21 | — | Limiting parameter |
| 22 | $m^3/s$ | Layer resources |
| 23 | $m^3/s$ | Local resources |
| 24 | $m^3/s$ | Water drawn from layers |
| 25 | $m^3/s$ | Water drawn from local resources |
| 26 | $m^3/s$ | Water drawn from rivers |
| 27 | $m^3/s$ | Agricultural needs |
| 28 | $m^3/s$ | Domestic needs |
| 29 | $m^3/s$ | Industrial needs |
| 30 | $m^3/s$ | Consumption |
| 31 | $m^3/s$ | Gross flow rate |
| 32 | $m^3/s$ | Deficit |
| 33 | $m^3/s$ | Constant flow rate |
| 34 | mg/l | $BOD_5$ surplus |
| 35 | mg/l | $NH_4^+$ surplus |
| 36 | mg/l | Dissolved oxygen deficit |

water resources and requirements, in quantity and quality, is expressed in investments, operational costs, and in the harmonious development of the economy and the population itself.

## CONCLUSION

The model is operative and used through interactive programs. A first file of calibration or decisions parameters is described in Tables 7-4 to 7-5.

The experience shows which are the sensitive parameters for each scenario and strategy, and which parameters prevent aims being reached. The maps of these parameters are obtained on the display with a hardcopy.

Moreover, a basic constraint of a conversational model is that it should require only short computation times: each complete economic and demographic scenario requires about 5 minutes of VAX 11-780 and the analysis of one set of strategy devoted to reach one option—composed of a set of aims of water supply and of quality objectives—requires less than 10 seconds of CPU. This enables it to be used even during a meeting of the Governing Board of the Agency, through a graphic terminal.

## ACKNOWLEDGMENT

It is obvious that the global analysis was only possible by reason of the efforts

Table 7-5 LIST OF ANNUAL MODIFIABLE INDIVIDUAL VARIABLES

| Order No | Code | Unit | Meaning (for each cell) |
|---|---|---|---|
| 1 | IOB | — | Quality objective (7 levels, 6 pollutants) |
| 2 | SIR | hectares | Irrigated surface |
| 3 | SIN | $m^3/s$ | Water drawn from layers for irrigating |
| 4 | SIR | $m^3/s$ | Superficial water drawing |
| 5 | RES(I, 1) | $m^3/s$ | Layer resources |
| 6 | RES(I, 2) | $m^3/s$ | Outer water-catchment resources |
| 7 | RES(I, 3) | $m^3/s$ | Local resources |
| 8 | RES(I, 4) | $m^3/s$ | Deviation resources |
| 9 | CBAR | $m^3/s$ | Capacity of dams which can be installed |
| 10 | DES | $m^3/s$ | Effected destockings |
| 11 | CX | $m^3/s$ | Input or water drawn from canals |
| 12 | PIN | MW | Electric power of installed plants |
| 13 | T0R | % | Connecting rate of industry |
| 14 | PIF | % | Infiltration percentage of flows of the infiltrated unconnected |
| 15 | PEP | % | Average capacity rate of the plants |
| 16 | PPR | % | Average output of the plants |
| 17 | CEP(I, 1) | kg Mo/j | Purification capacity for unconnected (except infiltration) |
| 18 | CEP(I, 2) | Inhab. Eq. | Purification capacity for connected + urban + large town |
| 19 | VAN | $m^3/s$ | Minimum admissible flow rate |

made by several multidisciplinary teams. It is a pleasure to acknowledge the major contributions of Pierre-Frédéric Ténière-Buchot, André Lesouef, Daniel Caille and Albert André, Rémi Barré, Jacques Theys, Alain Drach and Philippe Mirenovicz, Alain Dreyfus, Jean-Marie Espinasse, Philippe Hubert and Patrice Ramain, and to dedicate the result to the memory of Arthur Melzer.

## REFERENCES

1. Paramètres numériques et non numériques de la gestion des ressources en eau (SPEPE-DGRST).
2. Analyse à l'échelle de la France des ressources en eau et de leur qualité ainsi que analyse des besoins futurs et des problèmes d'approvisionnement à moyen et long terme (CCE—ARLAB).
3. Incidence de différentes hypothèses de développement socio-économique et d'aménagement du territoire sur l'état de l'environnement à moyen et long terme (SOPRA/ARLAB).
4. PROGRAMME SUR ORDINATEUR, "Politique de la pollution des eaux PO.POL.E.," (P.F. Ténière Buchot), in Futuribles.

**Table 7-6** THE MAIN ECONOMIC AND DEMOGRAPHIC PARAMETERS OF THE SPIRE MODEL

---

UNMODIFIABLE DATA

**For the whole of France**
Ages pyramid—men and women per area (1968 or 1975)
Working rate—men and women per area (1968 or 1975)
Employment per branch (CN) and per area (1968 or 1975)
Death rate—men and women (1968 and 2000)
Reproduction rate per age (1968 or 1975)
Distribution of the population: large town–small town–rural (1968 or 1975)
Input/Output Table (28 or 36 branches) (1968, 1975) or (1970, 1977)
Productivity per branch (1968–1975)
Matrix of the local migrations (1968 or 1975)

**For the studied area**
Ages pyramid—men and women per cell (1968 or 1975)
Employment per branch (CN) and per cell (1968 or 1975)
Distribution of the population: large town–small town–rural per cell (1968–1975)

SCENARIO CONSTRAINTS

Constraint on the TES technological coefficients
Constraint on the TES sums—axis and/or column
Constraint on the productivity per branch
Constraint on the input and output per area (migration)
Constraint on the reproduction rate (lower amount of births)
Constraint on the establishment or disappearance of jobs per area

SCENARIO

Consumption vector (28 or 36 branches) (1980–1985–1995)

**Table 7-7** POTAME MODEL (AFBSN-ARLAB). LIST OF MODIFIABLE GENERAL PARAMETERS

| Order No | Code | Initial value | Meaning |
|---|---|---|---|
| 1 | TC(1) | 0.95 | Consumption rate agriculture–rural |
| 2 | TC(2) | 0.15 | Consumption rate domestic |
| 3 | TC(3) | 0.06 | Consumption rate industry–boiler–manufacturing |
| 4 | TC(4) | 0.06 | Consumption rate industry–washing–cooling |
| 5 | TC(5) | 0.01 | Consumption rate power plants |
| 6 | T5 | −0.02 | Annual growth rate of needs industry–washing–cooling |
| 7 | TETA(1, 1) | 0.80 | $BOD_5$ yield—secondary plant |
| 8 | TETA(2, 1) | 0.40 | $NH_4^+$ yield—secondary plant |
| 9 | TETA(3, 1) | 0.00 | $NO_3^-$ yield—secondary plant |
| 10 | TETA(4, 1) | 0.30 | $PO_4^{---}$ yield—secondary plant |
| 11 | TETA(5, 1) | 0.80 | Hydrocarbons yield—secondary plant |
| 12 | TETA(1, 2) | 0.95 | $BOD_5$ yield—tertiary plant |
| 13 | TETA(2, 2) | 0.80 | $NH_4^+$ yield—tertiary plant |
| 14 | TETA(3, 2) | 0.80 | $NO_3^-$ yield—tertiary plant |
| 15 | TETA(4, 2) | 0.80 | $PO_4^{---}$ yield—tertiary plant |
| 16 | TETA(5, 2) | 0.95 | Hydrocarbons yield—tertiary plant |
| 17 | TBES(1, 1) | 3,050.00 | Water need boiler–manufacturing I.A.A. |
| 18 | TBES(2, 1) | 1,270.00 | Water need boiler–manufacturing C.M.S. |
| 19 | TBES(3, 1) | 1,170.00 | Water need boiler–manufacturing Oil |
| 20 | TBES(4, 1) | 380.00 | Water need boiler–manufacturing Const. Mat. |
| 21 | TBES(5, 1) | 0.00 | Water need boiler–manufacturing Glass |
| 22 | TBES(6, 1) | 0.00 | Water need boiler–manufacturing Iron and steel |
| 23 | TBES(7, 1) | 500.00 | Water need boiler–manufacturing pr. transformation |
| 24 | TBES(8, 1) | 900.00 | Water need boiler–manufacturing Mechanical construction |
| 25 | TBES(9, 1) | 400.00 | Water need boiler–manufacturing Electric construction |
| 26 | TBES(10, 1) | 350.00 | Water need boiler–manufacturing Cars |
| 27 | TBES(11, 1) | 0.00 | Water need boiler–manufacturing Naval-Aero |
| 28 | TBES(12, 1) | 4,320.00 | Water need boiler–manufacturing Chemistry |
| 29 | TBES(13, 1) | 4,550.00 | Water need boiler–manufacturing Textile |
| 30 | TBES(14, 1) | 3,970.00 | Water need boiler–manufacturing Leathers |
| 31 | TBES(15, 1) | 450.00 | Water need boiler–manufacturing Wood |
| 32 | TBES(16, 1) | 18,260.00 | Water need boiler–manufacturing Paper–Cardboard |
| 33 | TBES(17, 1) | 9,400.00 | Water need boiler–manufacturing Various Industries |
| 34 | TBES(18, 1) | 500.00 | Water need boiler–manufacturing Services and other |
| 35 | TBES(1, 2) | 3,660.00 | Water need washing–cooling I.A.A. |
| 36 | TBES(2, 2) | 8,225.00 | Water need washing–cooling C.M.S. |

| | | | |
|---|---|---|---|
| 37 | TBES(3, 2) | 10,910.00 | Water need washing–cooling Oil |
| 38 | TBES(4, 2) | 1,490.00 | Water need washing–cooling Const. Mat. |
| 39 | TBES(5, 2) | 9,380.00 | Water need washing–cooling Glass |
| 40 | TBES(6, 2) | 46,130.00 | Water need washing–cooling Iron and steel |
| 41 | TBES(7, 2) | 1,520.00 | Water need washing–cooling Pr. Transformations |
| 42 | TBES(8, 2) | 2,400.00 | Water need washing–cooling Mechanical constructions |
| 43 | TBES(9, 2) | 450.00 | Water need washing–cooling Electric constructions |
| 44 | TBES(10, 2) | 3,180.00 | Water need washing–cooling Cars |
| 45 | TBES(11, 2) | 3,500.00 | Water need washing–cooling Naval-Aero |
| 46 | TBES(12, 2) | 14,140.00 | Water need washing–cooling Chemistry |
| 47 | TBES(13, 2) | 6,500.00 | Water need washing–cooling Textile |
| 48 | TBES(14, 2) | 3,410.00 | Water need washing–cooling Leathers |
| 49 | TBES(15, 2) | 1,350.00 | Water need washing–cooling Wood |
| 50 | TBES(16, 2) | 32,400.00 | Water need washing–cooling Paper–Cardboard |
| 51 | TBES(17, 2) | 0.00 | Water need washing–cooling Various industries |
| 52 | TBES(18, 2) | 500.00 | Water need washing–cooling Services and other |
| 53 | EM(1, 1) | 46.00 | Emission coefficient (g/d) rural pop.—$BOD_5$ |
| 54 | EM(1, 2) | 8.00 | Emission coefficient (g/d) rural pop.—$NH_4^+$ |
| 55 | EM(1, 3) | 0.00 | Emission coefficient (g/d) rural pop.—$NO_3^-$ |
| 56 | EM(1, 4) | 1.00 | Emission coefficient (g/d) rural pop.—$PO_4^{---}$ |
| 57 | EM(1, 5) | 0.07 | Emission coefficient (g/d) rural pop.—Hydrocarbons |
| 58 | EM(2, 1) | 72.00 | Emission coefficient (g/d) large towns pop.—$BOD_5$ |
| 59 | EM(2, 2) | 8.00 | Emission coefficient (g/d) large towns pop.—$NH_4^+$ |
| 60 | EM(2, 3) | 0.00 | Emission coefficient (g/d) large towns pop.—$NO_3^-$ |
| 61 | EM(2, 4) | 2.30 | Emission coefficient (g/d) large towns pop.—$PO_4^{---}$ |
| 62 | EM(2, 5) | 0.07 | Emission coefficient (g/d) large towns pop.—Hydro. |
| 63 | EM(3, 1) | 60.00 | Emission coefficient (g/d) urban pop.—$BOD_5$ |
| 64 | EM(3, 2) | 8.00 | Emission coefficient (g/d) urban pop.—$NH_4^+$ |
| 65 | EM(3, 3) | 0.00 | Emission coefficient (g/d) urban pop.—$NO_3^-$ |
| 66 | EM(3, 4) | 1.50 | Emission coefficient (g/d) urban pop.—$PO_4^{---}$ |
| 67 | EM(3, 5) | 0.07 | Emission coefficient (g/d) urban pop.—Hydrocarbons |
| 68 | TAB(1, 1) | 50.00 | Limit concentration (mg/l)—$BOD_5$ level 1 |
| 69 | TAB(1, 2) | 25.00 | Limit concentration (mg/l)—$BOD_5$ level 2(3) |
| 70 | TAB(1, 3) | 10.00 | Limit concentration (mg/l)—$BOD_5$ level 3(2) |
| 71 | TAB(1, 4) | 7.00 | Limit concentration (mg/l)—$BOD_5$ level 4 |
| 72 | TAB(1, 5) | 5.00 | Limit concentration (mg/l)—$BOD_5$ level 5(1B) |
| 73 | TAB(1, 6) | 4.00 | Limit concentration (mg/l)—$BOD_5$ level 6 |
| 74 | TAB(1, 7) | 3.00 | Limit concentration (mg/l)—$BOD_5$ level 7(1A) |
| 75 | TAB(2, 1) | 16.00 | Limit concentration (mg/l)—$NH_4^+$ level 1 |

| Order No | Code | Initial value | Meaning |
|---|---|---|---|
| 76 | TAB(2, 2) | 8.00 | Limit concentration (mg/l)—$NH_4^+$ level 2(3) |
| 77 | TAB(2, 3) | 2.00 | Limit concentration (mg/l)—$NH_4^+$ level 3(2) |
| 78 | TAB(2, 4) | 1.00 | Limit concentration (mg/l)—$NH_4^+$ level 4 |
| 79 | TAB(2, 5) | 0.50 | Limit concentration (mg/l)—$NH_4^+$ level 5(1B) |
| 80 | TAB(2, 6) | 0.30 | Limit concentration (mg/l)—$NH_4^+$ level 6 |
| 81 | TAB(2, 7) | 0.10 | Limit concentration (mg/l)—$NH_4^+$ level 7(1A) |
| 82 | TAB(3, 1) | 200.00 | Limit concentration (mg/l)—$NO_3^-$ level 1 |
| 83 | TAB(3, 2) | 100.00 | Limit concentration (mg/l)—$NO_3^-$ level 2(3) |
| 84 | TAB(3, 3) | 44.00 | Limit concentration (mg/l)—$NO_3^-$ level 3(2) |
| 85 | TAB(3, 4) | 44.00 | Limit concentration (mg/l)—$NO_3^-$ level 4 |
| 86 | TAB(3, 5) | 44.00 | Limit concentration (mg/l)—$NO_3^-$ level 5(1B) |
| 87 | TAB(3, 6) | 44.00 | Limit concentration (mg/l)—$NO_3^-$ level 6 |
| 88 | TAB(3, 7) | 44.00 | Limit concentration (mg/l)—$NO_3^-$ level 7(1A) |
| 89 | TAB(4, 1) | 5.00 | Limit concentration (mg/l)—$PO_4^{---}$ level 1 |
| 90 | TAB(4, 2) | 3.00 | Limit concentration (mg/l)—$PO_4^{---}$ level 2(3) |
| 91 | TAB(4, 3) | 2.00 | Limit concentration (mg/l)—$PO_4^{---}$ level 3(2) |
| 92 | TAB(4, 4) | 1.50 | Limit concentration (mg/l)—$PO_4^{---}$ level 4 |
| 93 | TAB(4, 5) | 1.00 | Limit concentration (mg/l)—$PO_4^{---}$ level 5(1B) |
| 94 | TAB(4, 6) | 0.70 | Limit concentration (mg/l)—$PO_4^{---}$ level 6 |
| 95 | TAB(4, 7) | 0.50 | Limit concentration (mg/l)—$PO_4^{---}$ level 7(1A) |
| 96 | TAB(5, 1) | 0.50 | Limit concentration (mg/l)—Hydro. level 1 |
| 97 | TAB(5, 2) | 0.20 | Limit concentration (mg/l)—Hydro. level 2(3) |
| 98 | TAB(5, 3) | 0.10 | Limit concentration (mg/l)—Hydro. level 3(2) |
| 99 | TAB(5, 4) | 0.05 | Limit concentration (mg/l)—Hydro. level 4 |
| 100 | TAB(5, 5) | 0.02 | Limit concentration (mg/l)—Hydro. level 5(1B) |
| 101 | TAB(5, 6) | 0.01 | Limit concentration (mg/l)—Hydro. level 6 |
| 102 | TAB(5, 7) | 0.005 | Limit concentration (mg/l)—Hydro. level 7(1A) |
| 103 | TAB(6, 1) | 1.00 | Limit concentration (mg/l)—Dis. oxy. level 1 |
| 104 | TAB(6, 2) | 2.00 | Limit concentration (mg/l)—Dis. oxy. level 2(3) |
| 105 | TAB(6, 3) | 3.00 | Limit concentration (mg/l)—Dis. oxy. level 3(2) |
| 106 | TAB(6, 4) | 4.00 | Limit concentration (mg/l)—Dis. oxy. level 4 |
| 107 | TAB(6, 5) | 5.00 | Limit concentration (mg/l)—Dis. oxy. level 5(1B) |
| 108 | TAB(6, 6) | 6.00 | Limit concentration (mg/l)—Dis. oxy. level 6 |
| 109 | TAB(6, 7) | 7.00 | Limit concentration (mg/l)—Dis. oxy. level 7(1A) |
| 110 | FGV | 0.220 ($m^3/s$) | Daily need/inhabitant large town |
| 111 | T4 | 0.0175 | FGV annual growth rate |

| | | | |
|---|---|---|---|
| 112 | FUR | 0.110 ($m^3/s$) | Daily need/inhabitant urban |
| 113 | T3 | 0.0200 | FUR annual growth rate |
| 114 | FRU | 0.0900 ($m^3/s$) | Daily need/inhabitant rural |
| 115 | T1 | 0.0255 | FRU annual growth rate |
| 116 | FBE | 0.0600 ($m^3/s$) | Daily need/(eq. bovines) |
| 117 | T2 | 0.0175 | FBE annual growth rate |
| 118 | MODBO5 | 0.80 | Conversion coefficient MO → $BOD_5$ |
| 119 | DBNH | p.35 | Passage coefficient $BDO_{20} \rightarrow NH_4^+$ |
| 120 | AMOX | 3.56 | Passage coefficient $NH_4^+ \rightarrow$ Oxygen |
| 121 | AMNI | 3.40 | Passage coefficient $NH_4^+ \rightarrow NO_3^-$ |
| 122 | PS | 1.00 | Weight of secondary purification |
| 123 | PT | 5.00 | Weight of tertiary purification |
| 124 | TEP | 1.00 | Reduction coefficient of industrial emissions |
| 125 | TCEL | 0.70 | Load rate of thermal power plants |
| 126 | TQEL | 0.0275 | Thermic equivalent $BOD_5$ thermal power plants |
| 127 | TELC | 0.0400 | Water need—thermal power plants |
| 128 | TQCH | 1.00 | Emission $NH_4^+$ (kg/MW) thermal power plants (smokes washing) |
| 129 | EA1 | 35.00 | Emission $BOD_5$ Agriculture |
| 130 | EA2 | 20.00 | Emission $NO_3^-$ Agriculture |
| 131 | EA3 | 5.50 | Emission $PO_4^{---}$ Agriculture |
| 132 | EQIA | 1.20 | Emission phosphates by the I.A.A. (kg/MF70) |
| 133 | EQCH | 8.00 | Emission $NH_4^+$ for chemistry (kg/MF70) |
| 134 | EQPC | 25.00 | Emission $NH_4^+$ for paper-cardboard (kg/MF70) |
| 135 | EQNI | 15.00 | Amount of nitrate in layers water (mg/l) |
| 136 | C(1, 1) | 1.0000 | Chemistry purchase coefficient for agriculture 1970 |
| 137 | C(2, 1) | 1.1400 | Chemistry purchase coefficient for agriculture 1975 |
| 138 | C(3, 1) | 1.2800 | Chemistry purchase coefficient for agriculture 1980 |
| 139 | C(4, 1) | 1.8933 | Chemistry purchase coefficient for agriculture 1985 |
| 140 | C(5, 1) | 2.5069 | Chemistry purchase coefficient for agriculture 1990 |
| 141 | C(6, 1) | 3.1200 | Chemistry purchase coefficient for agriculture 1995 |
| 142 | C(7, 1) | 3.7333 | Chemistry purchase coefficient for agriculture 2000 |
| 143 | C(1, 2) | 1.0000 | Fuel purchase coefficient for domestic purposes 1970 |
| 144 | C(2, 2) | 1.1952 | Fuel purchase coefficient for domestic purposes 1975 |
| 145 | C(3, 2) | 1.2769 | Fuel purchase coefficient for domestic purposes 1980 |
| 146 | C(4, 2) | 1.3828 | Fuel purchase coefficient for domestic purposes 1985 |
| 147 | C(5, 2) | 1.4917 | Fuel purchase coefficient for domestic purposes 1990 |
| 148 | C(6, 2) | 1.5825 | Fuel purchase coefficient for domestic purposes 1995 |
| 149 | C(7, 2) | 1.6762 | Fuel purchase coefficient for domestic purposes 2000 |

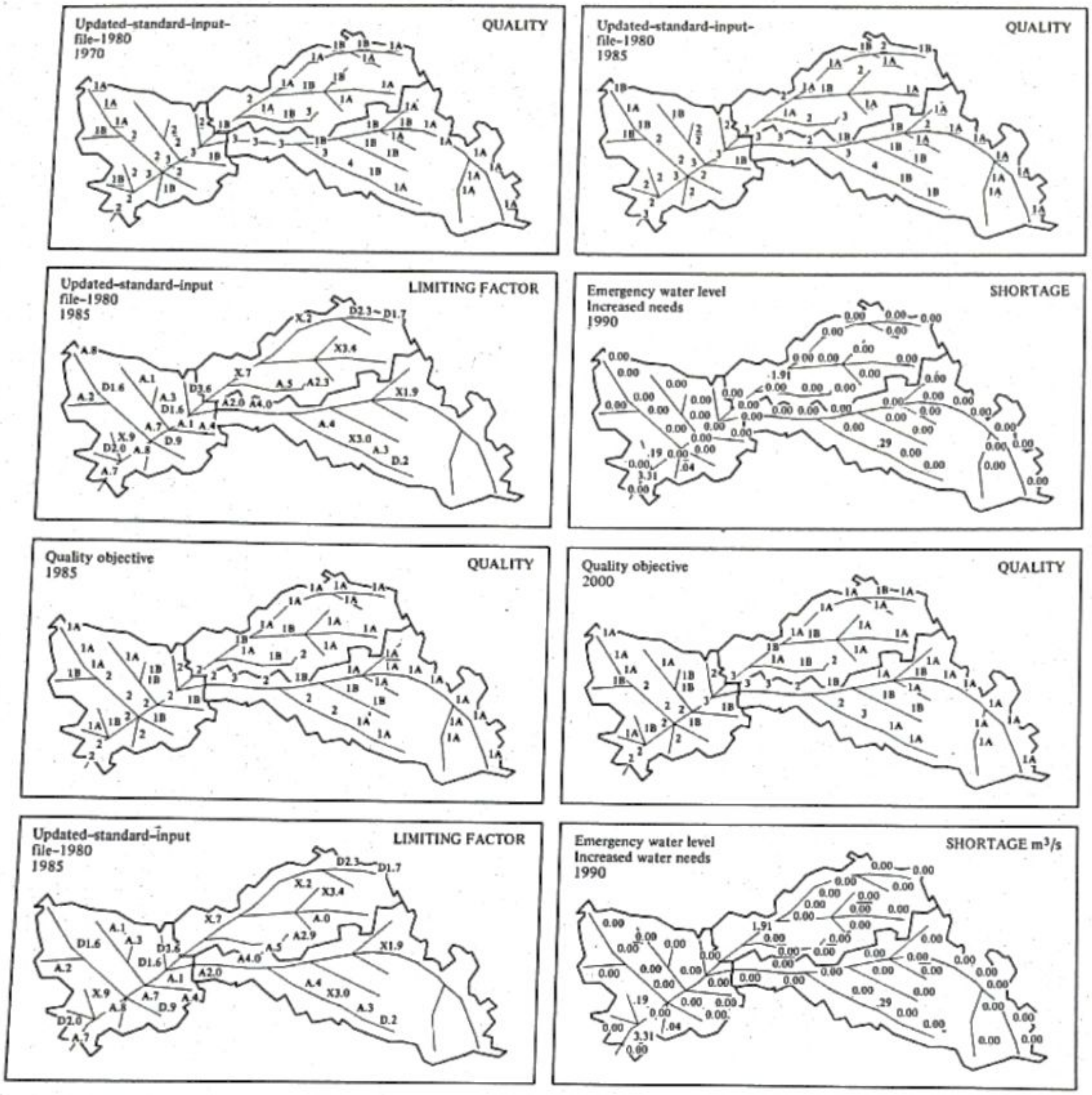

Updated-standard-input-file-1980 1970 QUALITY

Updated-standard-input-file-1980 1985 QUALITY

Updated-standard-input file-1980 1985 LIMITING FACTOR

Emergency water level Increased needs 1990 SHORTAGE

Quality objective 1985 QUALITY

Quality objective 2000 QUALITY

Updated-standard-input file-1980 1985 LIMITING FACTOR

Emergency water level Increased water needs 1990 SHORTAGE $m^3/s$

FIGURE 7-12
Examples of hardcopies of output display.

# 8

# MODELS FOR STRATIFIED IMPOUNDMENTS

**Gerald T. Orlob**

*Department of Civil Engineering*
*University of California*
*Davis, CA*

## 8-1 INTRODUCTION

In this chapter we trace the development of mathematical modeling of surface water impoundments, from the first simple thermal energy budget models through models designed to simulate the complex water quality–ecologic relationships of such water bodies. Emphasis is placed on simulation models, capable of describing the temporal behavior of the water body, including the transport and distribution of fluid masses and their physical, chemical, and biological attributes. Discussion is directed primarily to one-dimensional models of highly stratified systems and the pragmatic devices used by the modeler in representing the functional behavior of the prototype. Specific examples are presented to exemplify the state-of-the-art and highlight both capabilities and limitations of this class of model. Some future directions for research and development are identified.

Mathematical modeling of surface water impoundments in the United States developed in the mid 1960s when pollution control efforts were directed toward solution of problems of nutrient enrichment of natural and artificial impoundments. In addressing questions of nutrient enrichment, the principal focus was initially on such notorious examples of advanced deterioration of water quality as Lake Erie, but this was attended by a rising concern for the protection of other smaller lakes and reservoirs that were beginning to show the first signs of accelerating eutrophication. The general uncertainty concerning the effectiveness of specific control measures, such as flow regulation, phosphorous removal or denitrification, for example, was due in part to a lack of understanding of the complex response mechanisms of the impoundment—hydrodynamic, hydrologic, water quality, and ecologic. This called for additional field work to describe quantitatively the behavior of impounded waters and the development of an analytical capability, i.e., a model, to predict the changes that could be expected from particular strategies for management of lakes and reservoirs.

Faced with the need, but also with a general lack of knowledge of the quantitative behavior of natural and man-made impoundments, the Engineering Laboratory of the Tennessee Valley Authority was among the first in the United States to recognize the importance of comprehensive field investigation of actual operating reservoirs. Throughout most of 1966, for example, TVA carried out an intensive study of its Fontana Reservoir, including hydrologic, hydrographic, meteorologic and water quality characterization of the impoundment. The data derived from this study was to serve subsequently as the base for the development of a complete quantitative description of the energy budget for impoundments.[1] At the same time it provided stimulus to the development of some of the first mathematical models for simulation of the thermal energy distribution in natural and man-made impoundments.[2]

These early efforts to formulate explicit mathematical models concentrated primarily on exchanges of thermal energy through the air–water interface, penetration of shortwave energy into the water column, and advective transport into the water column of heat associated with the natural inflow and the regulated outflow. Modelers sought to represent the annual thermal cycle of deep impoundments, those that exhibit pronounced density stratification during the summer season. Because the dominant thermal gradients in such water bodies were along the vertical axis, these early models were structured as one-dimensional in the mathematical sense, assuming homogenity of water properties over horizontal planes or throughout segments oriented horizontally. Also, since density differences tended to dominate the flow regime in such systems, the hydrodynamic behavior of the water body was not treated explicitly. Nevertheless, these models were found to give credible results in simulation of existing lakes and reservoirs that exhibited thermal stratification. They became popular for studies of operational characteristics of both existing and proposed reservoirs and are in wide use today.

Water quality modeling of impoundments developed first as a logical extension of modeling of the thermal structure of stratified water bodies [Chen and Orlob].[3,4,10] It was carried still further by aquatic biologists and engineers concerned with pollution control strategies for eutrophying lakes.[5,6,7,8,9] Recently, the state-of-the-art of modeling of eutrophic systems has advanced rapidly in characterizing the biodynamic behavior of lakes,[10] perhaps even outdistancing our present capability to describe rigorously the internal circulation of natural water bodies.

In the succeeding sections of this chapter we will review the conceptualization and formulation of the important class of impoundment models, those for deep, stratified water bodies with low inflow to volume ratios. We will deal first with thermal energy balances and the mechanisms of heat exchange through the air–water interface. Next, we will examine the formulation of the one-dimensional temperature model and an implicit technique for solution of the governing equations. Formulation of a water quality–ecologic model for a stratified impoundment is reviewed. Examples of model applications are presented to illustrate capabilities. A discussion of extensions of the modeling approach to more complex impoundment systems concludes the chapter.

## 8-2 PRACTICAL CONSIDERATIONS

### 8-2.1 Background

Among the first attempts at mathematical characterization of impoundment behavior were those by limnologists who sought to explain the annual thermal cycle and the formation of a thermocline. McEwen[11] and Hutchinson[12] estimated heat transfer coefficients using assumed temperature profiles. Ertel[13] designed a diffusional model of the thermocline formation, assuming a constant coefficient of diffusion, independent of time or depth. These efforts were not successful, however, in producing a credible representation of the entire annual cycle of thermal energy in lakes or reservoirs.

A need to simulate the annual temperature cycle of surface water impoundments developed with the pending construction, during the post World War II period, of major dams in the western United States. Raphael[14] developed a manual technique for calculation of the thermal energy budget for proposed reservoirs which he successfully applied to Oroville Reservoir on California's Feather river and to several reservoirs of the Columbia river system.[15,16] The method allowed reasonable estimation of downstream temperatures from these projects but failed to provide a description of the energy distribution within the impoundment. Burt also developed a somewhat similar procedure which he applied to Pacific Northwest reservoirs;[17-19] however, like Raphael's method it was essentially a manual procedure.

During the early 1960s, the concern of conservation groups and biologists for the survival of aquatic life in temperature-sensitive environments stimulated government agencies to sponsor investigation of improved methods for predicting the annual temperature cycle in operating reservoirs. Accordingly, it was necessary also to improve techniques for estimating heat energy exchange across the air–water interface.

In the following review of impoundment modeling we begin with the problem of quantitative determination of the heat flux through the surface of an impoundment. From this point we examine briefly the mechanisms of distributing thermal energy downward (or upward) in the water column. This will set the stage for formulation of the first simple models of the late 1960s and for their subsequent evolution to the present state-of-the-art.

### 8-2.2 Thermal Energy Budget

The total heat energy of the water column above 0°C is called the *gross heat* and is defined as

$$H_g = \frac{1}{A_0} \int_z^0 c\rho A_z \theta_z dz \qquad (8\text{-}1)$$

where $H_g$ = gross heat, calories
$\theta_z$ = temperature at depth $z$, °C
$A_0$ = surface area of impoundment, $(L^2)$
$A_z$ = area of horizontal plane at depth $z$, $(L^2)$
$c$ = specific heat (cal $F^{-1}$)
$\rho$ = density $(FT^2L^{-4}$ or $ML^{-3})$
$z$ = depth $(L)$

The gross heat, $H_g$, of the impoundment varies with influxes and effluxes of thermal energy according to the general heat budget equation.

$$\frac{\partial H_g}{\partial t} = \frac{c\rho}{A_0} \Big\{ \underbrace{Q_i\theta_i - Q_0\theta_{z'}}_{\text{Advection}} + \underbrace{q_n A_0 + q_s A_s}_{\substack{\text{Surface heat exchange} \\ \text{Air water} \quad \text{Solid-water}}} + \underbrace{\int_{z0}^{0} h' A_z dz}_{\substack{\text{Chemical-biochemical} \\ \text{reactions}}} + \underbrace{\int_{z0}^{0} \varepsilon A_z dz}_{\substack{\text{Kinetic energy} \\ \text{dissipation}}} \Big\} \qquad (8\text{-}2)$$

where $Q_i$ = inflow, $m^3\ sec^{-1}$
$Q_0$ = outflow, $m^3\ sec^{-1}$
$\theta_i$ = temperature of inflow, °C
$\theta_{z'}$ = temperature at level of outflow, °C
$q_n$ = net heat flux at air-water interface, kcal $m^{-2}\ sec^{-1}$
$q_s$ = heat flux at solid-water interface, kcal $m^{-3}\ sec^{-1}$
$h'$ = rate of heat production (utilization) by chemical-biochemical reactions, kcal $m^{-3}\ sec^{-1}$
$\varepsilon$ = rate of heat production by dissipation of kinetic energy, kcal $m^{-3}\ sec^{-1}$
$A_s$ = area of solid-water interface

and other terms are as previously defined.

Among these processes the more dominant are those of advection and heat exchange through the air–water interface. Temperature gradients between solid boundaries and the water body are usually so small that solid–water exchange may be neglected; chemical–biochemical reactions occur only rarely at significant levels; and kinetic energy dissipation is usually very small in relation to air–water exchanges and advective heat transport.

While advective exchanges of heat with the water body are very important in characterizing the gross heat budget of the impoundment they are tied closely with phenomena that can be explicitly defined, e.g., hydrology of the basin tributary to the impoundments and, in the case of operating reservoirs, the scheduling of controlled releases. These can usually be dealt with by prescribing boundary conditions in accord with prototype behavior.

### 8-2.3 Surface Heat Exchange

Heat exchanges through the air–water interface are dependent on both the internal hydromechanical behavior of the water body and the physics of its interaction with the overlying air mass. Meteorologic factors such as solar radiation, wind, humidity, pressure, and cloudiness figure prominently in the many physical processes involved. The aggregate effect of the most important of these processes is represented in the general heat flux equation

$$q_n = q_{sn} + q_{\mathrm{at}} - q_{ws} - q_e - q_h \tag{8-3}$$

where $q_n$ = net heat energy transfer across the air–water interface (cal $L^{-2}T^{-1}$)
$q_{sn}$ = net solar radiation heat flux
$q_{\mathrm{at}}$ = net atmospheric radiation heat flux
$q_{ws}$ = water surface radiation heat flux
$q_e$ = evaporation heat flux
$q_h$ = sensible heat flux

Among the early investigations to formulate explicitly the independent energy flux terms, one of the most comprehensive was that undertaken in the late 1960s by the Tennessee Valley Authority's Engineering Laboratory. This led to publication by the laboratory of the report, from which the following formulations have been derived.[1]

**Net solar radiation, $q_{sn}$** Net solar radiation is the residual at the water surface of the solar radiation received at the top of the atmosphere after reducing this flux by attenuation through the atmospheric column, by interception by clouds, and by reflection at the water surface, such that

$$q_n = q_0 f(A)(1 - R_t)(1 - 0.65\,C^2) \tag{8-4}$$

where $q_0$ = solar radiation intensity on a horizontal plane at the top of the atmosphere (cal $L^{-2}T^{-1}$)
$f(A)$ = atmospheric attenuation factor, a function of optical properties of air column, dust content, moisture, and terrestrial surface reflectance[20]
$R_t$ = reflectivity of water surface: $R \cong 0.03$
$C$ = cloudiness in parts of sky covered by clouds: $0 < C < 1.0$

Solar radiation intensity at the top of the atmosphere for a given location and time is given by

$$q_0 = \frac{I_0}{r^2} \sin \alpha \tag{8-5}$$

where $I_0$ = solar constant, equal to incident solar radiation at top of atmosphere for mean distance between the earth and the sun; (cal $L^{-2}T^{-1}$); $I_0 \cong 2.0$ cal cm$^{-2}$ min$^{-1}$
$r$ = radius vector, i.e., ratio of actual earth–sun distance to mean; $0.9833 < r < 1.0167$ and $0.9669 < r^2 < 1.0337$
$\alpha$ = solar altitude in radians, a function of latitude, sun's declination, and local hour angle of the sun; $0 < \alpha < \pi/2$

**Atmospheric radiation $q_{at}$** Atmospheric radiation is the net long wave flux from the atmospheric air mass, including clouds, after reflection from the water surface. It is a function of absolute air temperature, cloudiness and water surface reflectivity, as follows

$$q_{\mathrm{at}} = C_{\mathrm{at}}\sigma T_2^6(1 + 0.17C^2)(1 - R_a) \tag{8-6}$$

where $q_{\mathrm{at}}$ = long wave atmospheric radiation from a cloudy sky, (cal $L^{-2}T^{-1}$)
$C_{\mathrm{at}}$ = empirical coefficient; $0.906 \times 10^{-5} < C_{\mathrm{at}} < 0.999 \times 10^{-5}$; Swinbank's coefficient $= 0.938 \times 10^{-5}$
$\sigma$ = Stefan–Boltzmann Constant = 4.875.10$^{-8}$ kcal/m$^2$ hr °K$^4$
$T_2 = 273.2 + \theta_{a2}$, °K; $\theta_{az}$ = dry bulb air temperature at 2 m above the ground, °C
$C$ = cloudiness in parts of sky covered by clouds, $0 < C < 1.0$
$R_a$ = reflectivity of water surface for atmospheric radiation; $R_a \cong 0.03$

**Water surface radiation $q_{ws}$** Water surface radiation is the long wave radiation flux from the water mass emitting as a black body at specific surface temperature. It is a function of water surface emissivity and water surface temperature,

$$q_{ws} = -\varepsilon_w \alpha T_0^4 \tag{8-7}$$

where $q_{ws}$ = long wave water surface (back) radiation; (cal $L^{-2}T^{-1}$)
$\varepsilon_w$ = emissivity of the water surface, i.e., the ratio of the radiation emission of the water surface to that of a perfect black body; $\varepsilon \cong 0.96$ (dimensionless)
$T_0 = 273.2 + \theta_0$; $\theta_0$, average water surface temperature, °C
$\alpha$ = Stefan–Boltzmann Constant, $\alpha = 4.875 \cdot 10^{-8}$ kcal/m$^2$ hr °K$^4$

**Evaporation heat loss, $q_e$** Evaporative heat loss occurs as a result of the change of state of water from a liquid to a gas, water vapor, requiring sacrifice of the latent heat of vaporization.

$$q_e = -\rho_w LE \tag{8-8}$$

where $q_e$ = evaporative heat loss from the water surface, (cal $L^{-2}T^{-1}$)
$\rho_w$ = density of water, ($FT^2L^{-4}$ or $ML^{-3}$) $\rho_w = 998.2$ kg/m$^3$ at 20°C
$L$ = latent heat of vaporization (cal $M^{-1}$) $L = 597.1 - 0.57\theta_0$ cal/g
$E$ = depth of evaporated water per unit time ($LT^{-1}$)

The TVA Engineering Laboratory study provides an extensive review of various evaporation formulae, concluding that the Marciano–Harbeck formula, derived from detailed investigation of evaporation on Lake Hefner in Oklahoma, probably gives the most consistent practical results from standard weather observations.[21] This formula is

$$E = 0.00177u(e_0 - e_a) \tag{8-9}$$

where $E$ = evaporation, inches/day
$u$ = wind velocity, miles/hour
$e_0$ = saturation vapor pressure at water surface temperature, mm Hg
$e_a$ = vapor pressure of the air, mm Hg

Adjusting for observations made at specific elevations above the water surface, the equation becomes

$$E = 0.00304\, u_4(e_0 - e_2) \tag{8-10}$$

where the subscripts 2 and 4 refer to observations made at levels of 2 m and 4 m, respectively, above the water surface.

An alternative form to the Lake Hefner formulae that takes account of stability of the overlying air mass is

$$E = N \frac{p}{p_0} u(C_0 - C_a) f(\mathrm{Ri}) \tag{8-11}$$

where $E$ = height of evaporated water per unit time, m/hr
$N$ = evaporation coefficient, dimensionless
$p$ = atmospheric pressure, mb
$p_0$ = standard atmospheric pressure at sea level, 1,013 mb ($P/P_0$ may be approximated by

$$P/P_0 = (1 - 0.0226z)^{5.256}$$

with $z$ in km above mean sea level
$u$ = wind speed, m/h
$C_0 = 0.622\, e_0/P$, water vapor concentration of the saturated air at the water surface, kg vapor/kg air
$e_0$ = vapor pressure of saturated air, mb
$e_a$ = vapor pressure of air (saturation vapor pressure at dewpoint), mb
$f(\mathrm{Ri})$ = function of Richardson's Number

$$= (1 - 22\,\mathrm{Ri})^{+0.80}, \text{ for } 0 \geq \mathrm{Ri} \geq -1$$

$$= (1 + 34\,\mathrm{Ri})^{-0.80}, \text{ for } 0 \leq \mathrm{Ri} \leq 2$$

$$= 1, \text{ for } \mathrm{Ri} = 0, \text{ neutral case}$$

$$\mathrm{Ri} = \frac{g(\rho_a - \rho_0)z}{\rho_a u^2}, \text{ Richardson's Number}$$

where $g$ = acceleration of gravity ($LT^{-2}$)
$\rho_a$ = density of air (usually at $z = 2$ m) ($ML^3$)
$\rho_0$ = density of saturated air at water surface temperature ($ML^{-3}$)
$u$ = wind speed (usually at $z = 2$ m) ($LT^{-1}$)
$z$ = height above water surface ($L$)

Values of $N$ in Eq. (8-21) depend on particular conditions of meteorologic observations as follows:

For airport data:

$N = 1.89 \times 10^{-6}$ (dimensionless)
$z \cong 18$ ft

For land/lake data:

$N = 2.26 + 10^{-6}$ (dimensionless)
$z = 2$ m
$p$ and $e_a$ observed at upwind land station unaffected by lake evaporation

For lake data:

$N = 2.48 \times 10^{-6}$ (dimensionless)
$z = 2$ m

**Sensible heat loss (or gain), $q_h$** Sensible heat is transfered between air and water by conduction and transported away from (or toward) the air–water interface by convection associated with the moving air mass. It is computed by

$$q_h = -f(\text{Ri})\rho_w c_p N \frac{p}{p_0} u(\theta_0 - \theta_a) \tag{8-12}$$

where $q_n$ = forced convective sensible heat flux (cal $L^{-2}T^{-1}$)
$\theta_0$ = water surface temperature, °C
$\theta_a$ = dry bulb air temperature, °C
$c_p$ = specific heat of air at constant pressure (cal $M^{-1}$ °C$^{-1}$)

and other terms are as previously defined.

**Other heat losses** In addition to the five principal heat fluxes cited in Eq. (8-11), heat may be transferred into the water by condensation from an overlying supersaturated air mass or into or out of the system by advective transfers associated with precipitation, evaporation and/or condensation. The condensation flux is of the same general form as the combination resulting from Eqs. (8-18) and (8-21) for evaporation, except that $C_a$ and $e_0$ are interchanged and $C_a$ is required to be less than the saturation vapor concentration of the air. The heat gain by condensation is usually relatively small, hence it is often neglected in energy budget calculations or considered as a part of *net* evaporative heat loss. Heat exchanges associated with advective transport of water through the interface are usually neglected except for the most detailed studies.

### 8-2.4 Penetration of Heat into the Water Column

The radiation flux passing through the water surface is attenuated by absorption and scattering in the water column. The absorption spectrum for pure water shows an almost complete absorption of all wave lengths greater than 1.2 $\mu$m in the first few centimeters below the surface. Nearly all radiation outside the visible range (from 0.36 $\mu$m to 0.76 $\mu$m) is absorbed within the first meter or so; only visible light penetrates into the depths of the impoundment.

After initial absorption in the upper stratum, leaving only the monochromatic visible light, attenuation follows closely the relationship described by Beer's Law

$$q_{sz} = q_{sn}\, e^{-\eta z} \tag{8-13}$$

where $q_{sz}$ = solar radiation intensity at depth $z$, (cal $L^{-2}T^{-1}$)
$q_{sn}$ = net solar radiation penetrating the surface, (cal $L^{-2}T^{-1}$)
$\eta$ = bulk extinction coefficient, ($L^{-1}$)
$z$ = depth below surface, ($L$)

Application of Beer's Law usually assumes homogeneity of optical properties of the water column, i.e., $\eta$ = constant.

Experimental evidence indicates that Eq. (8-13) is not satisfactory for description of radiation attenuation in the upper stratum. As a practical matter in model development it may be sufficient simply to subtract a fixed fraction of the total incoming radiation as if it were absorbed *at* the surface and to attenuate the residual according to Beer's Law. This results in

$$q_{sz} = (1 - \beta) q_{sn}\, e^{-\eta z} \tag{8-14}$$

where $\beta$ = ratio of radiation absorbed at the surface to net incoming radiation.

Field data indicate a wide range in both $\beta$ and $\eta$ depending on the presence of suspended particles. In pure water or exceptionally clear lake water, such as that of Lake Tahoe, for example, $\beta$ may approach 0.70 while for exceptionally turbid waters the fraction of radiation *apparently* absorbed at the surface may be much less, as little as one quarter of the total. The low values of $\beta$ for turbid waters does not mean that surface absorption, per se, is less in such waters, since values of the extinction coefficient, $\eta$ would be higher. Consequently, the total absorption within the upper strata would be substantially increased. In natural impoundments in a state of advanced eutrophication extinction coefficients as high as 0.5 m$^{-1}$ might be expected. At the other extreme, in extremely clear waters of oligotrophic lakes, values as low as 0.02 m$^{-1}$ are likely. In such lakes it may be more accurate to divide the incoming radiation into components by wavelengths, each with its own characteristic extinction coefficient and $\beta$. However, experience in modeling such lakes has shown that such refinement is usually not essential for simulation of the annual temperature cycle. Equation (8-14) with appropriate values of $\beta$ and $\eta$ is satisfactory for most practical situations.

## 8-3 MODEL DEVELOPMENT

### 8-3.1 Brief Chronology

The history of mathematical modeling of surface water impoundments begins in the mid 1960s with the development of the first models for prediction of thermal energy changes of deep, stratified reservoirs. Two independent groups, one with the private consulting firm, Water Resources Engineers, Inc. (WRE) and the other identified with Massachusetts Institute of Technology (MIT) produced working models which have since been developed into practical tools for water management. From these first beginnings, to which the Engineering Laboratory of the Tennessee Valley Authority also contributed substantially with its field evaluation of reservoir temperatures and its analysis of heat exchange phenomena,[1] mathematical modeling of impoundment behavior has steadily progressed to include other water quality parameters, ecological simulation, and higher orders of phenomenological representations, physical, chemical and biological. In this section we will describe the highlights of these developments, concentrating on the major contributors to advancement of the state-of-the-art. A brief chronology of surface water model development corresponding to the succeeding discussion, is outlined in Table 8-1.

### 8-3.2 Temperature Prediction in Stratified Reservoirs

Modeling of temperature changes in stratified impoundments appears to have been stimulated initially by the California Department of Fish and Game (CDFG), which commissioned a study in 1965 to develop a predictive model.[22] At about this same time the Engineering Laboratory of TVA began its field program of investigation on Fontana Reservoir.[23] In early 1966 WRE and TVA collaborated in developing the model, the latter organization contributing the essential background for quantification of heat exchange. This combined effort culminated in a report to the CDFG in June 1967, which was revised a year later, in which the Fontana data were used as a test case.[24] Application of the resulting model has been extensive and it has been adopted in a variety of versions by many U.S. governmental agencies.

A substantially parallel effort was undertaken during the same period at MIT by Harleman and his coworkers, also in close collaboration with the TVA Laboratory. Initial emphasis was placed on laboratory experimentation,[2] but this work was extended to modeling prototype reservoirs also using the TVA data for Fontana Reservoir.[25] The MIT model, which has been well documented and tested, is presently used by TVA and other governmental agencies. It has continued to be used at MIT as a tool for research and to extend the state-of-the-art of impoundment modeling. A comparative analysis of the WRE, MIT and Cornell[26] models was performed for EPA by Parker and his coworkers using the Fontana data base.[27]

In the description of the model which follows, the notation is substantially that used in documentation for the WRE model. However, the structure of the MIT and WRE models and the principles and assumptions on which they are based are very similar. Differences lie primarily in the treatment of boundary conditions of inflow and outflow and in assumptions related to internal mixing ("effective diffusion"). Some differences in solution techniques are also noted. These are described briefly in the following.

A deep, thermally stratified impoundment is conceptualized for purposes of modeling as a one-dimensional continuum of isothermal elements, arranged as shown in Fig. 8-1. All fluxes occur along the vertical axis, through horizontal planes defining discrete control volumes such as that shown in Fig. 8-2, for which one may write the equations of mass and heat energy conservation.

**Mass conservation** For a control element of discrete thickness $\Delta z$ the mass conservation equation is

$$\frac{\partial \not{V}_j}{\partial t} = Q_j - Q_{j+1} - Q_{ij} + Q_{0j} \tag{8-15}$$

where $\not{V}_j$ = volume of $j$th control element ($L^3$)
$Q$ = vertical flow rate ($L^3T^{-1}$)
$Q_i$ = flow advected to the control volume in the horizontal plane ($L^3T^{-1}$)
$Q_0$ = flow advected from the control volume in the horizontal plane ($L^3T^{-1}$)
$z$ = depth

and all flows are functions of time.

It is noted that except for the surface element, $\partial \not{V}_j/\partial t = 0$.

**Conservation of heat** The general equation for heat energy stored in a control volume within the reservoir is

$$\frac{\partial H_j}{\partial t} = [(h_i - h_0 + h_{sz})_j - (h_{w,j} - h_{w,j+1}) + (h_{d,j} - h_{d,j+1})] \tag{8-16}$$

where $H_j$ = heat content of $j$th element, (cals)

$H_j = c\rho V_j \theta_j$

where $c$ = specific heat
$\rho$ = density
$\theta_j$ = temperature °C

**Table 8-1** BRIEF CHRONOLOGY OF DEVELOPMENT OF MATHEMATICAL MODELS OF STRATIFIED IMPOUNDMENT

| Period | Model Description | Applications | Principal researchers, developers and sponsors |
|---|---|---|---|
| 1958–1963 | BURT: deep, stratified reservoirs, energy budget, water balance, hand calculation | Snake River reservoirs | Water Research Assoc. (Burt) |
| 1961–1962 | RAPHAEL: shallow or vertically mixed reservoirs, energy budget, water balance, hand calculation | Wells, Rocky Reach, Wanapum, Priest Rapids (Columbia River) | Raphael |
| 1965–1968 | WRE: deep stratified reservoirs, temp., 1D finite difference, implicit advection–diffusion, variable geometry | Fontana, Lake Washington, Detroit, Dworshak, Libby, Hungry Horse | California Dept. of Fish and Game<br>Water Resources Engineers, Inc. (Norton, Selna, Orlob, Roesner, et al.)<br>Environmental Protection Agency (EPA) |
| 1965–1968 | MIT: stratified reservoirs, temp., 1D finite difference, explicit advection–diffusion, variable geometry | Laboratory models, Fontana Res. (TVA) | Massachusetts Inst. of Technology (Harleman, Dake, Huber, Ryan) |
| 1968–1970 | CORNELL: deep stratified lakes, temp., 1D finite difference, constant cross section, diffusion only, wind effects | Lake Cayuga | Cornell Univ. and Aerospace Lab., (Sundaram, et al.) |
| 1968–1973 | LAKECO: water quality, ecologic, implicit, 1D finite difference, mass conservation, 22 parameters | Lake Washington, Koocanusa, Tocks Island, Lincoln Lake, Tims Ford (TVA) | Office of Water Resources Research (OWRR). WRE, Inc. (Chen, Norton, King, Orlob, et al.) |
| 1968–1969 | WRE: weakly stratified reservoirs segmented (longitudinally), 1D finite difference, temp., implicit–explicit | Lake Roosevelt | EPA and WRE, Inc. (Norton, Roesner, et al.) |

| | | | |
|---|---|---|---|
| 1969–1975 | 2D-FEM: shallow lakes, circulation, finite element, implicit | Not known | Cornell Univ. (Liggett, Gallagher et al.) |
| 1971–1973 | MIT: water quality, DO–BOD, 1D, explicit, adv.–diff. variable, geom., inflow–outflow distribution | Fontana (TVA) | MIT–EPA (Harleman, Markofsky) |
| 1972–1975 | HYDROSCIENCE: water quality—ecologic, 2D finite diff., mass balance, advection–diffusion, vertically mixed, shallow lakes, 10 to 20 parameters | Western Lake Erie, Lake Ontario<br>Ontario | Great Lakes Basin Comm. and EPA<br>Manhattan College and Hydroscience, Inc. (di Toro, O'Connor, Thomann, et al.) |
| 1973–1975 | 2D-FEM: hydrodynamic-watcr quality, stratified reservoirs, finite element implicit, momentum, advection–diffusion | Lower Granite Reservoir<br>Kentucky (TVA) | WRE, Inc., Resource Management Associates, Inc. (Norton, King et al.) |
| 1972–1976 | SIMONS: 3D finite difference, stratified lakes, temperature, wind driven circulation | Lake Ontario | Canada Centre for Inland Waters (Simons) |
| 1974–1975 | BACA-ARNETT: water quality, eutrophic lakes, 1D finite element, multiple water quality parameters | Lake Washington, Lake Mendota | Battelle Memorial Inst. (Baca, Arnett) |
| 1974–1975 | LK ONTARIO: water quality—ecologic, 3D with model generated circulation, mass balance, advection–diffusion, multiple parameters | Lake Ontario | Tetra Tech–NOAA (Chen, Lorenzen, Smith) |

$h_i$ = heat advected by inflow

$$h_i = c\rho Q_i\theta_i$$

$h_0$ = heat withdrawn by outflow

$$h_0 = c\rho Q_0\theta_0$$

$h_{sz}$ = direct insolation

$$h_{sz} = \int_z^{z+\Delta z} q_{sz}a_z\,dz$$

where $q_{sz}$ = solar radiation intensity at depth $z$ (Eq. 8-14)
$a_z$ = horizontal area at depth $z$

$h_w$ = heat advected along vertical axis

$$h_{wz} = c\rho Q\theta_z$$

$h_d$ = heat diffused along vertical axis

$$h_{dz} = c\rho E_z a_z \frac{\partial\theta}{\partial z}$$

where $E_z$ = coefficient of effective diffusion.

Expressing the heat budget in terms of temperature results in

$$\frac{\partial(V_j\theta_j)}{\partial t} = \underbrace{(Q_i\theta_i - Q_0\theta_0)_j}_{\text{local advection}} + \underbrace{\left(\frac{1}{c\rho}\int_z^{z+\Delta z} q_{sz}a_z\,dz\right)_j}_{\text{solar radiation}}$$

$$\underbrace{- Q_j\theta_j + Q_{j+1}\theta_{j+1}}_{\text{vertical advection}} + \underbrace{\left(Ea\frac{\partial\theta}{\partial z}\right)_j - \left(Ea\frac{\partial\theta}{\partial z}\right)_{j+1}}_{\text{vertical diffusion}} \tag{8-17}$$

Solution of Eq. (8-17) for $\theta_j$, $j = 1, 2, 3, \ldots, n$ requires knowledge of $V_j$, $a$, $Q_i$, $Q_0$, $q_{sz}$ and $E$. $V_j(z)$ and $a(z)$ are physical characteristics which for a fixed $\Delta z$, can be obtained from area–volume–elevation curves. The other terms may be evaluated as follows.

**Local advection** In the initial version of the WRE model,[28] local inflow was assumed to enter a single element $V_j$ such that $\theta_j > \theta_i > \theta_{j-1}$. Local outflow occurred from the elements spanning the vertical dimension of the outlet(s). In a subsequent modification for the EPA, outflows were distributed uniformly over a layer estimated by Debler's criteria based on the densimetric Froude number in the zone of the outlet.[29] Sensitivity analysis indicated that distributing the outflow in a pattern of Gaussian form was not justified in view of the lack of definitive information on actual velocity patterns in the region of outlet structures.

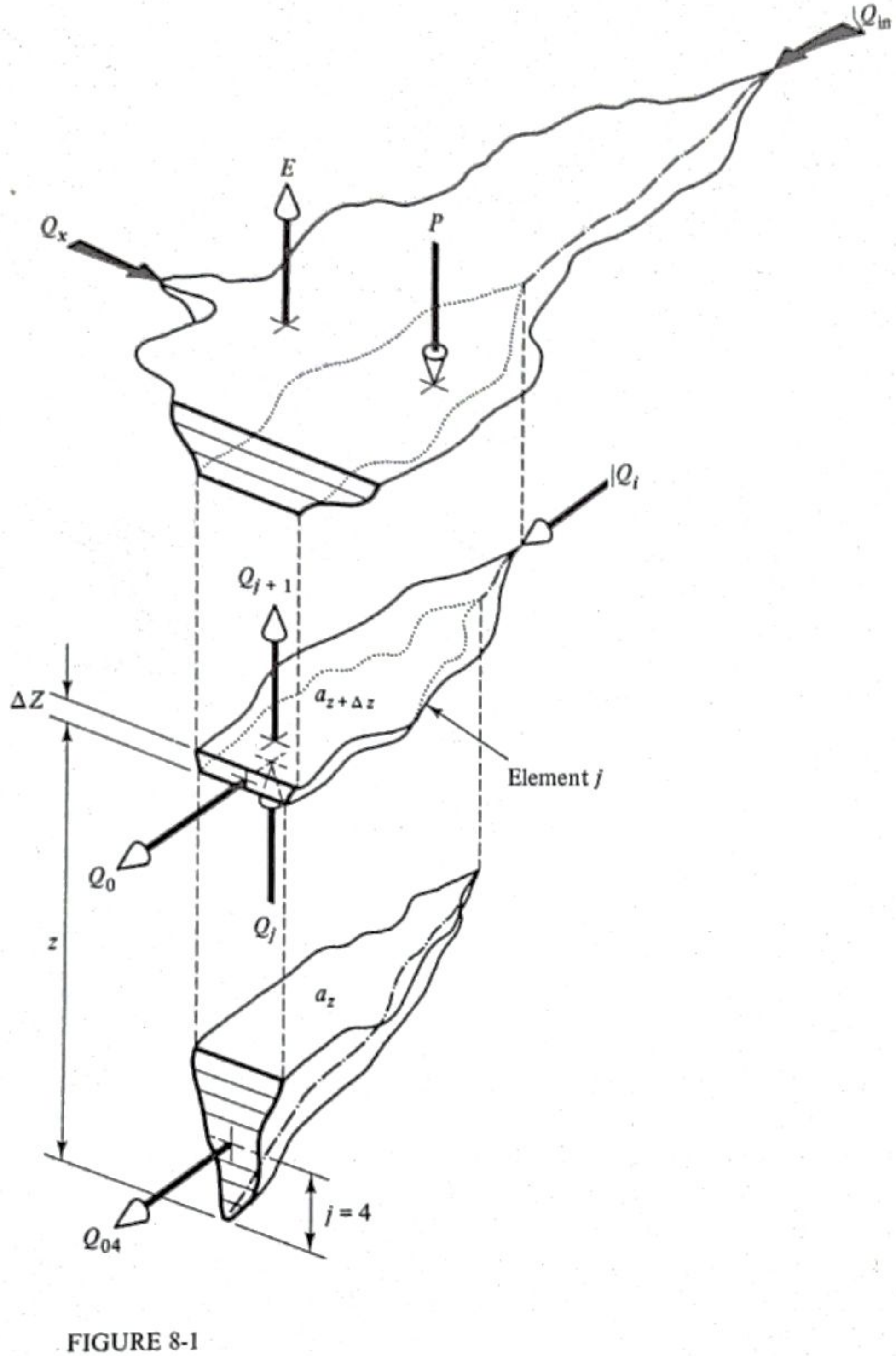

FIGURE 8-1
Conceptual representation of a reservoir (After Water Resources Engineers, Inc.[24])

The model of Huber and his coworkers[25] employs the theoretical relationship of Kao[30] to estimate the thickness of the withdrawal layer

$$\delta = 4.8\left(\frac{q^2}{g\varepsilon}\right)^{1/4} \tag{8-18}$$

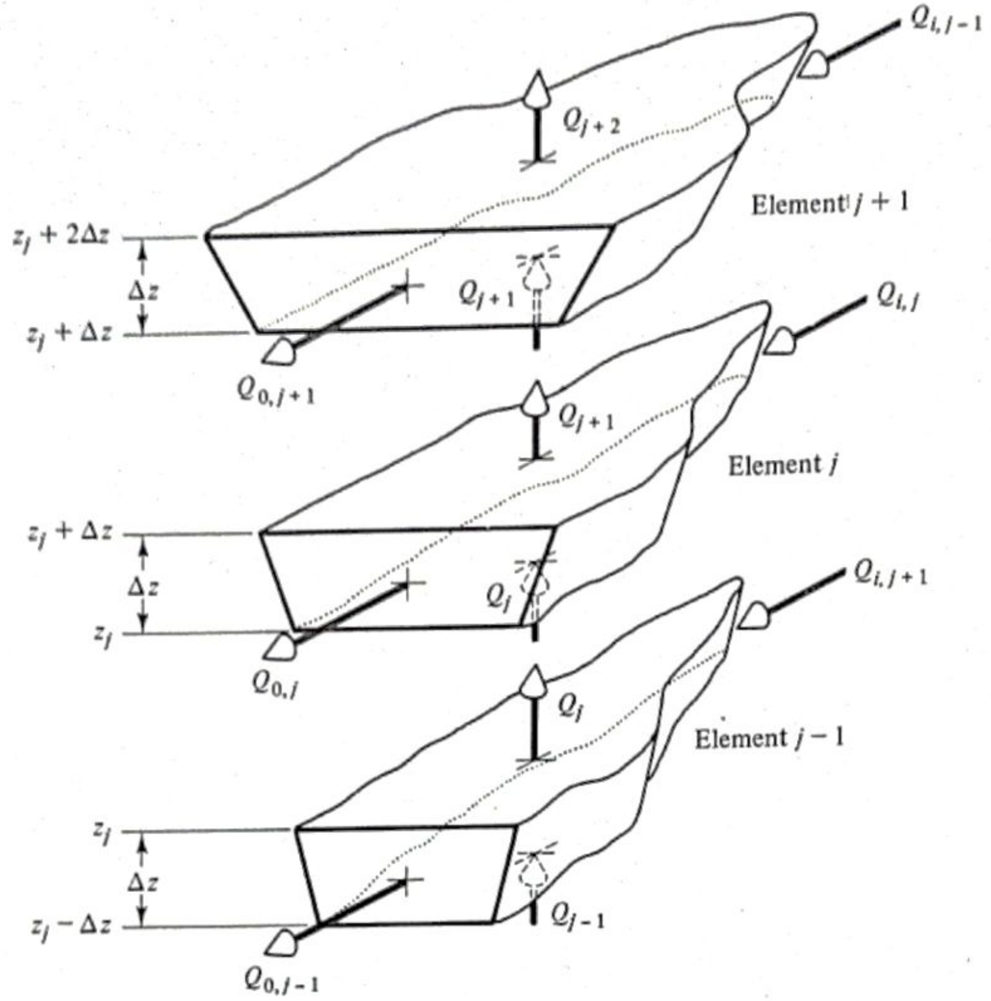

FIGURE 8-2
Water movement along three adjacent reservoir elements.

where $\delta$ = thickness of a withdrawal layer of uniform velocity approaching a line sink $(L)$
$q$ = outflow per unit width of reservoir $(L^2T^{-1})$
$g$ = acceleration of gravity $(LT^{-2})$

$$\varepsilon = \frac{1}{\rho}\frac{d\rho}{dz}, \ (L^{-1})$$

Flow is distributed in a Gaussian pattern over a layer assumed to be twice as thick as estimated by Eq. (8-18). It is noted that no field verification is available for this procedure.

Inflows are also distributed in a Gaussian pattern in the Ryan–Harleman model using a standard deviation in the velocity field that is "related to some length characteristic of the spread of the inflow velocity distribution, such as the depth of the entering stream." In this case, also, it appears that analytical work is lacking.

**Solar radiation influx** The influx of solar radiation into a control element is obtained by integration of Eq. (8-14) after multiplying by the area $a(z)$ between the limits of $z$ and $z + \Delta z$. A special case is that of the uppermost element which receives the net heat transferred across the air–water interface (Eq. (8-3)) minus that which passes through the bottom of the element (Eq. (8-14)),

$$\frac{\partial(\bar{V}_1\theta_1)}{\partial t} = \frac{1}{c\rho}[\beta q_{sn} + q_{at} + q_{ws} + q_e + q_h]a_0 + \frac{1}{c\rho}[(1-\beta)q_{sn}e^{-\eta z_1}]a_1 \quad (8\text{-}19)$$

where $\bar{V}_1$ = volume of surface element ($L^3$)
$\theta_1$ = temperature of the surface element (°C)
$a_0$ = area of reservoir surface ($L^2$)
$a_1$ = area at bottom of surface element ($L^2$)
$z_1$ = thickness of surface element ($L$)

**Effective diffusion** Aside from advective transport of heat along the vertical axis, heat is transported by molecular diffusion and also by ambient turbulence, which may be treated in an infinite fluid space as a random process analogous to molecular motion. In the laboratory, in the absence of turbulence the process is virtually one of molecular motion, but in nature the apparent mixing, whether truly random or not, results in heat transport that far exceeds that which could be expected by molecular processes alone. Moreover, the mere fact of a one-dimensional approximation of a real three-dimensional fluid mass continually in motion, suggests the need for an empirical representation of the combined processes that account for observed heat transport.

The WRE model utilized an "effective diffusion coefficient" derived by applying the advection–diffusion equation to observed temperature data. This approach was later modified to take account of the dampening effect of density stratification by making the coefficient $E_z$ a function $1/\rho\ (d\rho/dz)$. Experience with the model later revealed, however, that such refinements seem not to be justified by the results of model calibration. In practice a constant value of $E$, several orders of magnitude greater than the molecular diffusion coefficient, is usually used.

The process of model calibration usually entails some adjustment in this essentially empirical parameter to include the effects of natural processes as well as the numerics associated with solution of the model equations. Huber and his coworkers[25] note that in the laboratory the apparent numerical diffusion coefficients, calculated using the method of Bella and Dobbins,[31] are likely to be less than twice the molecular value while in the field they are "usually less than 20 times the molecular value." In later studies Harleman and Hurley experimented with diffusion coefficients up to 100 times molecular diffusion using Fontana data.[32] They observed that when heat transport is dominated by advection, as in the case of a reservoir with deep outlets, changing the vertical diffusion coefficient by a factor of 100 results in very little change in the predicted temperature profiles. On the other hand, in lakes where outflow occurs only at the surface, the predicted temperature profile is very sensitive to the magnitude of the coefficient.

**Solution technique** Solution of Eq. (8-17) is achieved by forming a finite difference set for the discretized impoundment according to the notation of Fig. 8-1. For the $j$th element the finite difference equation for temperature change in $V_j$ is

$$\begin{aligned}\dot{\theta}_j = {} & \left[\frac{1}{V_j}\left(Q + \frac{Ea}{\Delta z}\right)_j\right]\theta_{j-1} \\ & - \left[\frac{1}{V_j}\left(\frac{Ea}{\Delta z}\right)_j + \frac{1}{V_j}\left(\frac{Ea}{\Delta z}\right)_{j+1} + \frac{1}{V_j}(Q_{j+1} + Q_{0j} + \dot{V}_j)\right]\theta_j \\ & + \left[\frac{1}{V_j}\left(\frac{Ea}{\Delta z}\right)_{j+1}\right]\theta_{j+1} + \frac{1}{V_j}(Q_i\theta_i)_j + \frac{1}{V_j}\left(\frac{q_{sz}a}{c\rho}\right)_j \end{aligned} \tag{8-20}$$

Written in matrix form, Eq. (8-20) becomes

$$[I]\{\dot{\theta}\} = [S]\{\theta\} + \{P\} \tag{8-21}$$

where $[I]$ is an identity matrix, $[S]$ is a tridiagonal matrix of the bracketed $\{\ \}$ coefficients, and $\{P\}$ is a vector of the known parameters and external heat sources and sinks.

Integration of Eq. (8-20) with respect to time is accomplished by the linear acceleration method, which assumes that the change in temperature is expressed by

$$\theta_{t+\Delta t} = \theta_t + \frac{\Delta t}{2}(\dot{\theta}_t + \dot{\theta}_{t+\Delta t}) \tag{8-22}$$

or

$$\theta_{t+\Delta t} = \frac{\Delta t}{2}\dot{\theta}_{t+\Delta t} + \left(\frac{\Delta t}{2}\dot{\theta}_t + \theta_t\right) \tag{8-23}$$

in which $\theta$ and its derivative $\dot{\theta}$ are known at time $t$. Dropping the time subscripts we can state generally that

$$\theta_j = \frac{\Delta t}{2}\dot{\theta}_j + b_j \tag{8-24}$$

and in matrix form

$$\{\theta\} = \frac{\Delta t}{2}\{\dot{\theta}\} + \{b\} \tag{8-25}$$

where $\{b\}$ is a matrix of $\theta$ and its time derivative for time $t$.[32]

Equation (8-25) is then substituted in Eq. (8-31) and results in

$$[I]\{\dot{\theta}\} = [S]\{b\} + \frac{\Delta t}{2}[S]\{\dot{\theta}\} + \{P\} \tag{8-26}$$

which may be simplified to

$$[S^*]\{\dot{\theta}\} = \{P^*\} \tag{8-27}$$

where
$$[S^*] = [I] + \frac{\Delta t}{2}[S]$$

and
$$\{P^*\} = [S]\{b\} + \{P\}$$

The computational procedure steps forward in time as follows:

*1* Form $\{b\}$ from initial conditions or the most recently computed values of $\{\theta\}$ and $\{\dot{\theta}\}$.
*2* From known values of coefficients and boundary conditions, determine for the end of the time the values of $[S]$, $\{P\}$, $[S^*]$ and $\{P^*\}$.
*3* Solve for $\{\dot{\theta}\}$ from Eq. (8-27).
*4* Solve for $\{\theta\}$ from Eq. (8-25).
*5* Repeat for all succeeding time steps.

It may be noted that the steady state solution, i.e., $\dot{\theta} = 0$, is readily obtained by solution of

$$[S]\{\theta\} = -\{P\} \tag{8-28}$$

a special case of Eq. (8-21).

The implicit solution technique described above has proven to be efficient in many practical applications. It has the inherent advantages of stability in the solution and flexibility in adapting to temporal variations in boundary conditions, while preserving accuracy and economy of solution. In a study of Ross Lake on the Skagit River as a system of 73 elements ($\Delta z = 2$ m) simulation of an annual thermal cycle (365 days with $\Delta t = 0.25$ d) required approximately 140 s for execution on a Univac 1108, Exec II.

An alternative explicit solution technique has been used in the MIT model wherein the equation set is solved in spatial order ($j = 1, 2, 3, \ldots, n$) for successive times ($t = 1, 2, 3, \ldots, k$).[34] The method requires adherence to stability criteria

$$\Delta t < \frac{1}{2}\left(\frac{\Delta z}{E}\right)^2 \tag{8-29}$$

and
$$\Delta t < (\Delta z)\frac{a}{Q} \tag{8-30}$$

where $E$ is the diffusion coefficient and $Q/a$ is the vertical advection velocity. Care must be taken in the selection of $\Delta t$, especially in those cases where spatial detail is required, i.e., small $\Delta z$, or where hydrologic and operational conditions dictate large values of inflow or outflow. Elements at reservoir levels near large capacity bottom outlets often represent limiting conditions for choosing $\Delta t$ and $\Delta z$. The method usually requires somewhat less computer storage capacity than the implicit technique, however, this may be offset by increased computational effort when the $\Delta t$ required by Eqs. (8-29) or (8-30) is much smaller than necessary for description of significant temporal variations in temperature.

Experience in applying the MIT model to large reservoirs like Fontana in the TVA system indicate that it can be applied efficiently. Simulation of 306 days with a system of 50 elements using $\Delta t = 1$ d and $\Delta z = 2$ m required only 100 s for execution on an IBM 360/65.

**Demonstration of temperature simulation** Both the WRE and MIT temperature models have been widely used since they were developed to an operational level in the late 1960s. In general, the models' performances have been good for reservoirs or lakes which are strongly stratified during the summer period and which have a relatively low inflow to volume ratio, i.e., a long "residence" time. Among the impoundments simulated with the WRE model are Fontana Reservoir in the TVA system, Hungry Horse, Dworshak, Detroit, Ross and Libby Reservoirs in the Pacific Northwest, and Lake Washington in Washington State. The MIT model has been applied as well to Fontana and other reservoirs in the Tennessee Valley. Figures 8-3, 8-4 and 8-5 are illustrative of results obtained with the models in simulating prototype performance.

Figure 8-3 shows the performance of the MIT model in simulating temperature profiles in Fontana Reservoir for three representative times during the year 1966.[25,32] "A" corresponds to the period of warming of the reservoir; "B," near maximum thermal stratification; and "C," during cooling of the reservoir. In each instance, the model is in good agreement with the prototype.

Figure 8-4 shows a calibration run of the WRE model on Hungry Horse Reservoir in Montana. Computed performance (dashed lines) is compared to observed behavior (solid lines) by plotting isotherms on a field of depth versus time. Isotherms and water surface fluctuations are referenced to a fixed datum. Agreement between model and prototype is considered good.

Figure 8-5 shows results of a simulation of Libby Reservoir, also in Montana, under an operational constraint to deliver water through outlet structures as near in temperature as possible to a long term average of the natural stream.[7] The shaded area depicts the target temperature range and the three curves represent model predictions for temperatures at the reservoir surface, in the stream below the reservoir, and at the bottom. Also illustrated is the model's capability to carry the simulation through a sequence of three years with successive freeze-over, ice break-up, spring overturn, thermal stratification, and fall overturn.

## 8-4 WATER QUALITY PREDICTION IN STRATIFIED IMPOUNDMENTS

Having established a capability to represent the annual thermal cycle in stratified impoundments, the next logical advance was to extend the capability of temperature models to characterize the corresponding cycles of quality change. This was accomplished by application of the advection–diffusion equation in the same conceptual framework used for the one-dimensional temperature models (Figs. 8-1 and 8-2), adding source-sink terms for the independent processes governing the fate of quality constituents. The WRE temperature model was first adapted by Norton et al.[49] to describe the detention of conservative quality parameters in Lake Washington under alternative water management strategies. Later this modified model provided the basic framework for a comprehensive

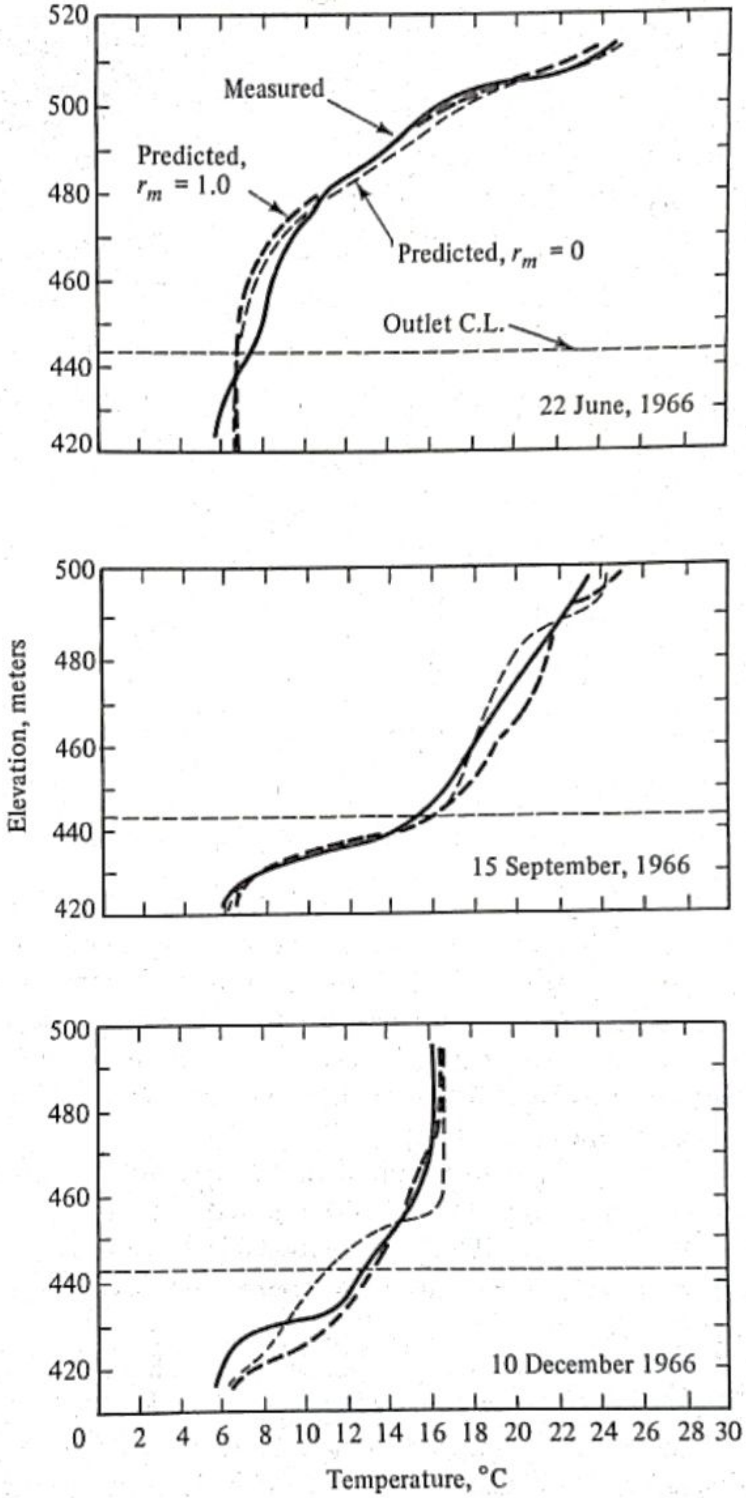

FIGURE 8-3
Predicted and measured temperature profiles, Fontana reservoir, 1966 (After Huber et al.[25]).

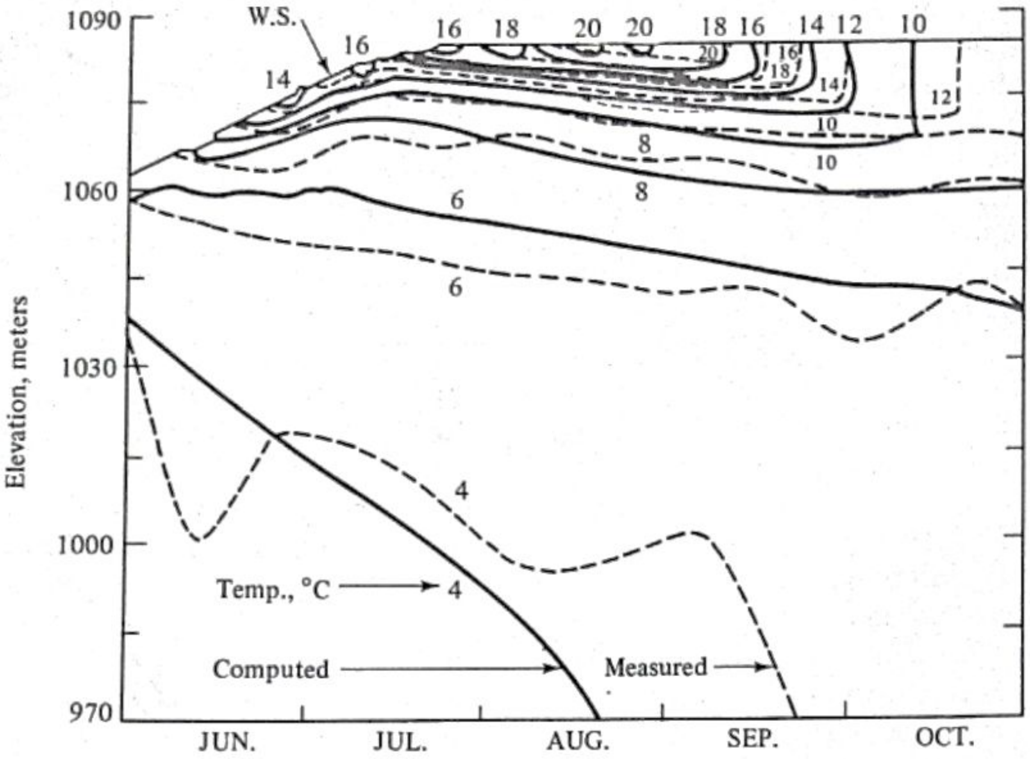

FIGURE 8-4
Simulated and observed thermal regime for Hungry Horse reservoir, 1965 (After Norton et al.[49]).

water quality–ecologic model designed to simulate temporal and spatial changes in both abiotic substances and biota in a eutrophic impoundment.[35] Following the same general approach used for the temperature model, mass conservation equations were written for each individual parameter. The equation sets were solved implicitly in a manner very similar to that outlined above for the temperature model.

The MIT temperature model was extended along similar lines in a series of development steps to deal with selected water quality parameters beginning first with the classic DO–BOD relationship.[3] Various improvements in both these models were later made by users who sought to apply them to specific problems.[7,10,36]

Currently, several water quality–ecologic models for stratified impoundments are in operational use in the United States. One of these, developed originally by WRE, has been extensively used by a number of governmental agencies. Formulation of the model is described below.

### 8-4.1 Water Quality–Ecologic Relationships

The water quality–ecologic relationships in a stratified impoundment are illustrated schematically in Fig. 8-6, a modified Odum diagram [Odum, 1971]. The diagram depicts the flow of energy in various forms through a succession of

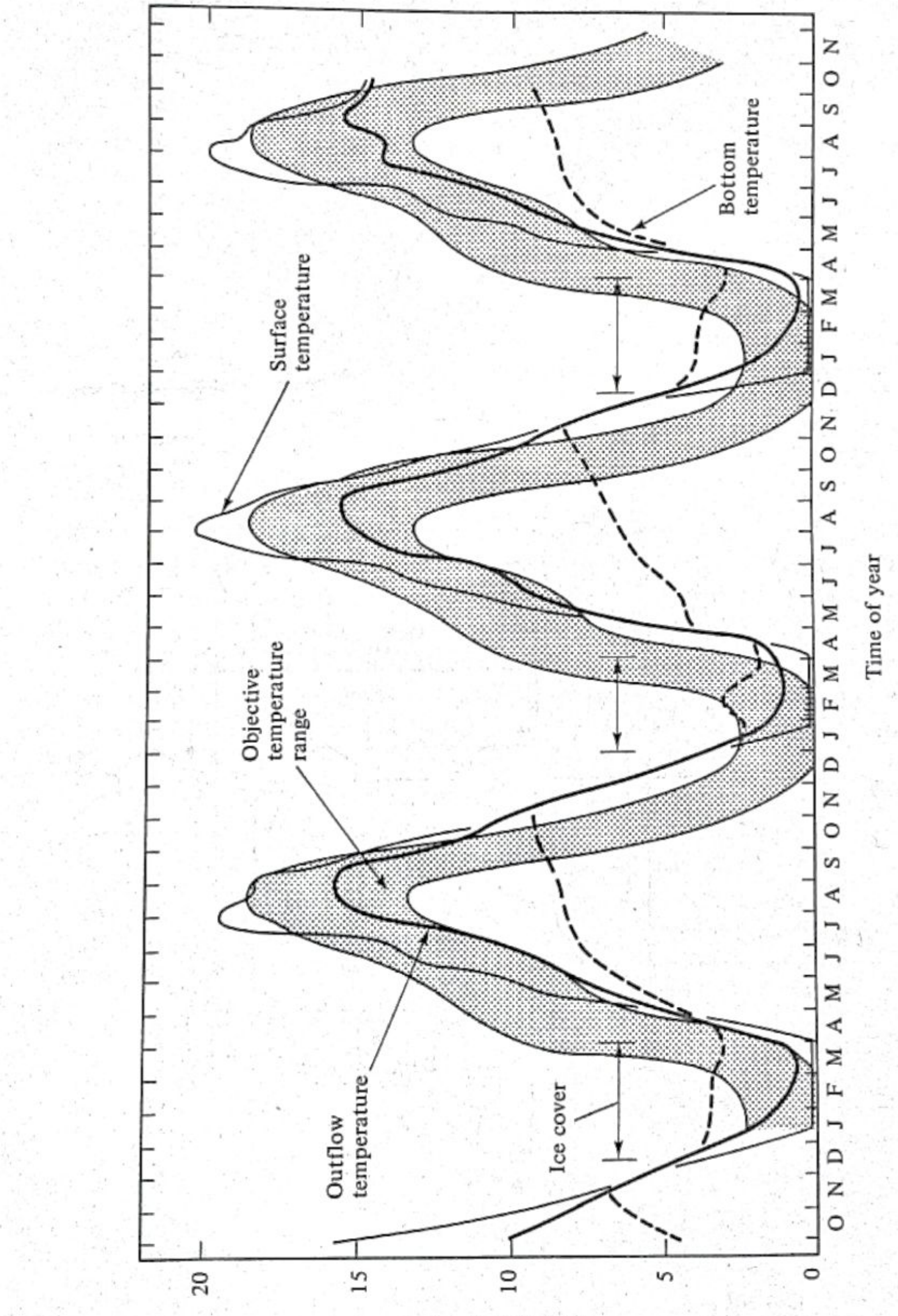

FIGURE 8-5
Simulated temperatures for three years of operation of Lake Koocanusa.

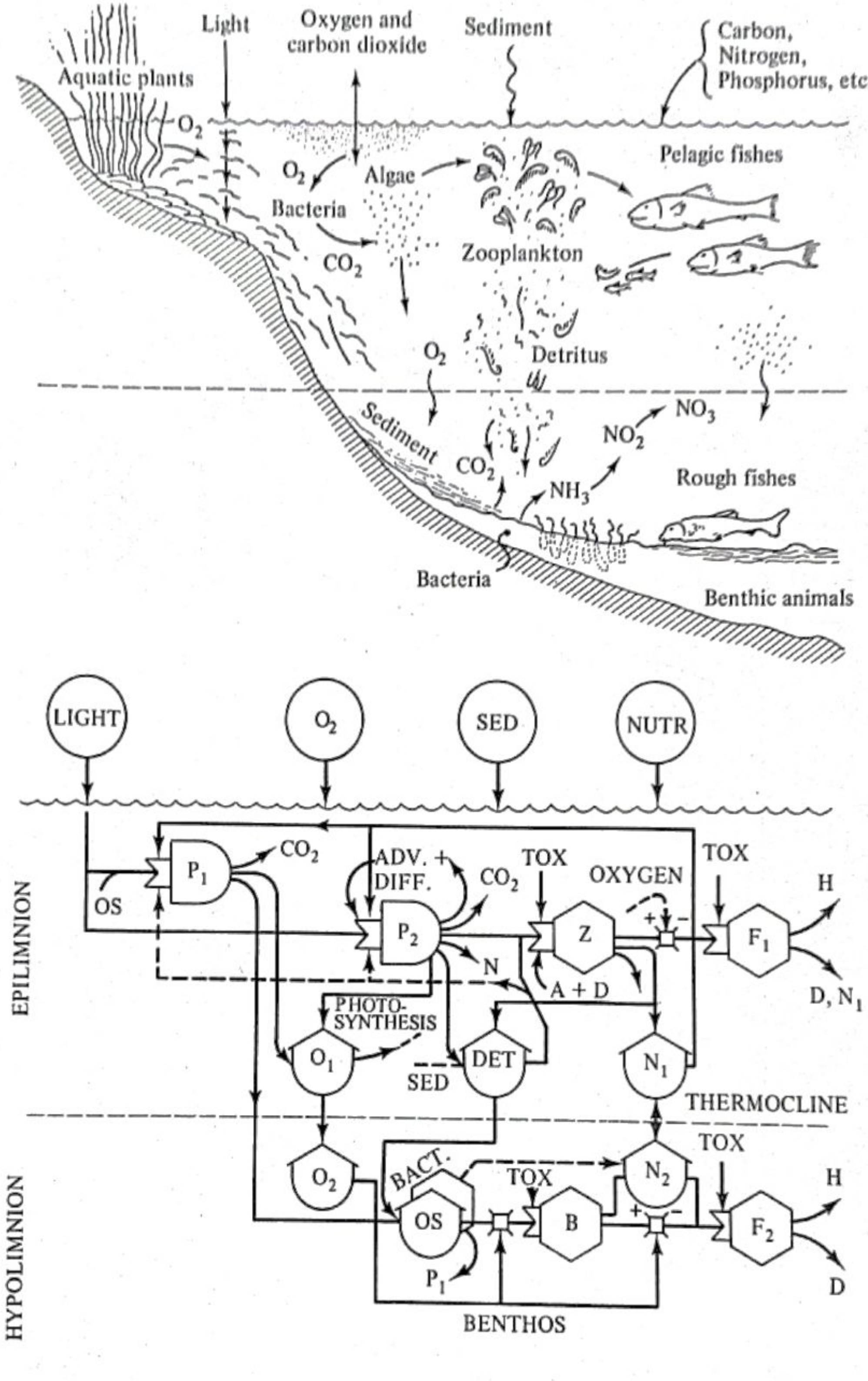

FIGURE 8-6
Ecologic relationships in a lake environment.

trophic levels within an aquatic environment characterized by quality parameters such as dissolved oxygen, carbon dioxide, primary nutrients, suspended sediment, detritus, and bottom sediments. Energy (or mass) transformations are seen as being regulated by the processes of growth, respiration, mortality, predation and decomposition, which in turn are governed by environmental quality parameters such as temperature, toxicity, and nutrients. The water quality–ecologic system depicted is highly coupled, that is, energy or mass balances for individual compartments in the system are invariably linked to several others. However, despite the apparent complexity of this system (much simplified from reality) it is possible to develop a plausible formulation for a water quality–ecologic model. This is accomplished as follows.

The general mass conservation equation for an element $j$ of a stratified impoundment is

$$\frac{\partial(V_jC_j)}{\partial t} = \underbrace{-Q_jC_j + Q_{j+1}C_{j+1}}_{\text{advection}} + \underbrace{\left(Ea\frac{\partial C}{\partial z}\right)_j - \left(Ea\frac{\partial C}{\partial z}\right)_{j+1}}_{\text{diffusion}} + \underbrace{C_j\frac{\partial V_j}{\partial t}}_{\substack{\text{volume}\\ \text{change}}} \pm \underbrace{V_j\frac{dc}{dt}}_{\substack{\text{local}\\ \text{derivative}}} \tag{8-31}$$

where $C_j$ is the concentration of any quality constituent that moves with the fluid mass and the local derivative $dc/dt$ represents all processes other than advection and diffusion that act to change the concentration in the control volume $V_j$. Equations of this form can be written for any number of quality parameters, either independent or coupled through definition of the local derivative. To illustrate, let us examine the formulation necessary to describe the balance of dissolved oxygen in a stratified impoundment, as depicted schematically in Fig. 8-6.

As an intrinsic property of water in its natural state, dissolved oxygen moves with the mass of the fluid, i.e., it is advected and diffused; it is supplied with inflow to the impoundment, by reaeration through the surface, and by photosynthetic oxygenation; and it is consumed by the processes of chemical and biochemical oxidation and by respiration of living forms. The oxygen mass balance for an element of volume $V$, considering all these processes is

$$\overline{\dot{V\mathrm{O}}} = \underset{\text{advection}}{-A} + \underset{\text{diffusion}}{D} - \underset{\substack{\text{volume}\\ \text{change}}}{\mathrm{O}\dot{V}} + \underset{\text{reaeration}}{a_sK_2(\mathrm{O}^* - \mathrm{O})} - \underset{\text{BOD}}{K_1LV} - \underset{\text{benthic demand}}{K_sa_b(\mathrm{OS})^*}$$
$$- \underset{\text{ammonia oxidation}}{\beta_1\alpha_1(\mathrm{NH_3})V} - \underset{\text{nitrite oxidation}}{\beta_2\alpha_2(\mathrm{NO_2})V} - \underset{\text{detritus oxidation}}{\beta_3\alpha_3(\mathrm{DET})V} - \underset{\substack{\text{biota}\\ \text{respiration}\\ \text{e.g., algae}}}{K_b(r_pP)V}$$
$$+ \underset{\text{photosynthesis}}{K_b(\mu_pP)\gamma V} \pm \underset{\substack{\text{external sources}\\ \text{and sinks}}}{S_0} \tag{8-32}$$

where $\mathrm{O}$ = dissolved oxygen concentration $(ML^{-3})$
$\mathrm{O}^*$ = dissolved oxygen concentration at saturation, $(ML^{-3})$
$V$ = volume $(L^3)$
$A$ = advection $(MT^{-1})$
$D$ = diffusion $(MT^{-1})$
$a$ = horizontal area at elevation element $(L^2)$
$a_s$ = surface area (uppermost element only) $(L^2)$
$K_2$ = reaeration coefficient $(LT^{-1})$
$K_1$ = biochemical oxygen demand coefficient $(T^{-1})$
$L$ = carbonaceous biochemical oxygen demand $(ML^{-3})$
$K_4$ = benthic sediment oxygen demand coefficient $(T^{-1})$
$a_b$ = bottom area associated with element $j = a_j - a_{j-1}$, $(L^2)$
$(\mathrm{OS})^*$ = organic sediment accumulation, per unit of bottom area, $(ML^{-2})$
$\mathrm{NH}_3$ = ammonia nitrogen concentration $(ML^{-3})$
$\mathrm{NO}_2$ = nitrite nitrogen concentration $(ML^{-3})$
$\mathrm{DET}$ = detritus concentration $(ML^{-3})$
$\alpha_1, \alpha_2, \alpha_3$ = stoichiometric equivalence with oxygen for ammonia, nitrite and detritus $(MM^{-1})$
$\beta_1, \beta_2, \beta_3$ = decay coefficient for ammonia, nitrite, and detritus $(T^{-1})$
$P$ = phytoplankton concentration $(ML^{-3})$
$r_p$ = respiration coefficient $(T^{-1})$
$\mu_p$ = growth coefficient $(T^{-1})$
$K_b$ = biota activity coefficient (dimensionless)
$\gamma$ = stoichiometric oxygenation factor for algae growth $(MM^{-1})$

Inspection of Eq. (8-32) reveals the evolution of water quality modeling from a simple description of mass transport to the most complex biological processes. The first three terms of the equation represent the primary physical processes of oxygen transport by fluid motion, i.e., advection, diffusion, and volume change. The next three terms—reaeration, BOD, and benthic oxygen demand—correspond to the classic Streeter–Phelps formulation for the oxygen "sag" in one-dimensional systems. Nitrogenous demands for oxidizing ammonia to nitrite and nitrite to nitrate are included next. The demand of organic detritus is tacit recognition of the conversion of soluble organics to particulate (humus) form and the contribution of biota through the processes of growth, excretion, and death to the total demand for oxygen. Respiration of living forms, typified in this example by algae, is a constant sink for oxygen exerted at the level of habitation. Oxygen may be supplied to the system by photosynthesis, by either free floating algae or aquatic vegetation attached to the bottom identified with the element. Finally, a source–sink term is included to account for local advection of dissolved oxygen to or from the element.

To complete formulation of the model, following the pattern of Eq. (8-32), requires writing similar equations for each of the independent variables indicated in Fig. 8-6. These are summarized in Table 8-2 (pages 300–301) along with the expanded form of Eq. (8-32).

## 8-4.2 Solution Technique

Solution of the equations of Table 8-2 can be accomplished by an implicit technique like that outlined above for temperature (Eqs. (8-30 to 8-37)). For a succession of elements $j-1$, $j$, and $j+1$ the mass balance equations for a constituent $C_{j-1}$, $C_j$, and $C_{j+1}$ are

$$\begin{aligned} \dot{C}_{j-1} &= \alpha_{j-1,1}C_{j-2} - \alpha_{j-1,2}C_{j-1} + \alpha_{j-1,3}C_j + \beta_{j-1} \\ \dot{C}_j &= \alpha_{j,1}C_{j-1} - \alpha_{j,2}C_j + \alpha_{j,3}C_{j+1} + \beta_j \\ \dot{C}_{j+1} &= \alpha_{j+1,1}C_j - \alpha_{j+1,2}C_{j+1} + \alpha_{j+1,3}C_{j+2} + \beta_{j+1} \end{aligned} \tag{8-33}$$

which when written in matrix form results in

$$[I]\{\dot{C}\} = [A]\{C\} + \{R\} \tag{8-34}$$

where $[I]$ is an identity matrix, $[A]$ is a tridiagonal matrix of the coefficients in Eq. (8-33) and $\{R\}$ is a vector of all known parameters and external sources of $C$.

Equation (8-34) is transformed by the linear acceleration method from which

$$\{C\} = \frac{\Delta t}{2}\{\dot{C}\} + \{B\} \tag{8-35}$$

where $\{B\}$ is a matrix of the most recently computed values of $\{C\}$ and $\{\dot{C}\}$. By substitution into Eq. (8-35) there results

$$[A^*]\{\dot{C}\} = \{R^*\} \tag{8-36}$$

in which

$$[A^*] = [I] + \frac{\Delta t}{2}[A]$$

and

$$\{R^*\} = [A]\{B\} + \{R\}$$

The computational sequence is

*1* Form $\{B\}$ from initial conditions or the most recently computed values of $\{C\}$ and $\{\dot{C}\}$
*2* Form $[A]$, $\{R\}$, $[A^*]$ and $\{R^*\}$ from known distributions of flows and boundary conditions at the end of the time step $\Delta T$
*3* Solve for $\{\dot{C}\}$
*4* Solve for $\{C\}$
*5* Repeat

When solving for multiple parameters some of which are coupled by water quality–ecologic interrelationships, as illustrated in Table 8-2, it is necessary either to adopt values from the previous time step or devise a solution sequence that calculates the most "independent" variables first so that they can then be used in succeeding computation. In LAKECO the solution for some 22 parameters begins with temperature, followed in succession by conservative substances, non-conservative substances that are uncoupled, e.g., BOD and coliforms, fish, benthic animals, zooplankton, algae, detritus, nutrients, oxygen, and $CO_2$.[38]

**Table 8-2** MASS BALANCE EQUATIONS FOR A WATER QUALITY-ECOLOGIC MODEL OF STRATIFIED IMPOUNDMENTS*

| Constituent | Symbol | Mass balance equation |
|---|---|---|

**Table 8-2**—*cont.*

| Constituent | Symbol | Mass balance equation |
|---|---|---|
| Conservative substances | $C$ | $\dot{\overline{VC}} = A + D + C\dot{V}$ |
| Biochemical oxygen | $L$ | $\dot{\overline{VL}} = A + D - L\dot{V} - K_1 LV$ |
| Detritus | DET | $\dot{\overline{(\mathrm{DET})V}} = A + D - (\mathrm{DET})\dot{V} - \underset{\text{decay}}{\beta_3(\mathrm{DET})V} - \underset{\text{sedimentation}}{as_d(\mathrm{DET})} + \underset{\text{zooplankton excreta}}{K_b\mu_z ZV\left(\frac{1}{\eta_z} - 1\right)} + \underset{\text{fish excreta}}{F_z\left(\frac{1}{\eta_f} - 1\right) + F_b\left(\frac{1}{\eta_b} - 1\right)}$ |
| Organic sediment | OS | $\dot{\overline{V(\mathrm{OS})}} = \underset{\text{decay}}{-K_s a_b(\mathrm{OS})^*} + \underset{\text{phytoplankton}}{a_b S_p P} + \underset{\text{detritus}}{a_b S_d(\mathrm{DET})V}$ |
| Carbon | CO | $\dot{\overline{V(\mathrm{CO})}} = A + D - (\mathrm{CO})\dot{V} + \underset{\text{reaeration}}{a_s K_c(\mathrm{CO}_2^* - \mathrm{CO}_2)} + \underset{\text{detritus release}}{\beta_3 c_3(\mathrm{DET})V} + \underset{\text{BOD decay}}{K_1 c_1 LV} + \underset{\text{respiration of biota}}{K_b(c_p r_p P + c_z r_z Z + c_f r_f F + c_b r_b B)V}$ |
| Ammonia nitrogen | $\mathrm{NH}_3$ | $\dot{\overline{V(\mathrm{NH}_3)}} = A + D - (\mathrm{NH}_3)\dot{V} - \underset{\text{decay}}{\beta_1(\mathrm{NH}_3)V} + \underset{\text{detritus release}}{\Psi_d n_d(\mathrm{DET})V} + \underset{\text{organic sediment release}}{\Psi_s n_s(\mathrm{OS})V}$ |
| Nitrite nitrogen | $\mathrm{NO}_2$ | $V(\mathrm{NO}_2) = A + D - (\mathrm{NO}_2)\dot{V} - \underset{\text{decay}}{\beta_2(\mathrm{NO}_2)V}$ |
| Nitrate nitrogen | $\mathrm{NO}_3$ | $\dot{\overline{V(\mathrm{NO}_3)}} = A + D - (\mathrm{NO}_3)\dot{V} + \underset{\text{nitrite oxidation}}{\beta_2(\mathrm{NO}_2)V} - \underset{\text{phytoplankton uptake}}{K_b n_p \mu_p PV}$ |
| Phosphate phosphorus | $\mathrm{PO}_4$ | $\dot{\overline{(\mathrm{PO}_4)V}} = A + D - (\mathrm{PO}_4)\dot{V} + \underset{\text{detritus release}}{\Psi_d p_d(\mathrm{DET})V} + \underset{\text{organic sediment release}}{\Psi_s p_s(\mathrm{OS})V} - \underset{\text{phytoplankton uptake}}{K_b p_p \mu_p PV}$ |

| | | |
|---|---|---|
| Coliform bacteria | CB | $\dot{\overline{V(\mathrm{CB})}} = A + D - (\mathrm{CB})\dot{V} - \underset{\text{decay}}{K_c(\mathrm{CB})V}$ |
| Algae | $P$ | $\dot{\overline{PV}} = A + D - P\dot{V} + \underset{\text{net growth}}{K_b(\mu_p - r_p)PV} - \underset{\text{sedimentation}}{as_pP} - \underset{\text{zooplankton grazing}}{K_b\mu_z\frac{ZV}{\eta}}$ |
| Zooplankton | $Z$ | $\dot{\overline{ZV}} = A + D - Z\dot{V} + \underset{\text{net growth}}{K_b(\mu_z - r_z - m_z)ZV} - \underset{\text{grazing by fish}}{\frac{F_z}{\eta_f}}$ |
| Benthic animals | $B$ | $\dot{\overline{BV}} = \underset{\text{net growth}}{K_b(\mu_b - r_b - m_b)B^*a_b} - \underset{\text{grazing by fish}}{\frac{Fb}{\eta_b}}$ |
| Nekton | $F$ | $\dot{\overline{FV}} = \underset{\text{net growth}}{K_b(\mu_f - r_f - m_f)FV} - \underset{\text{harvest}}{hFV}$ |
| Dissolved oxygen | O | $\dot{\overline{\mathrm{O}V}} = A + D - \mathrm{O}\dot{V} + \underset{\text{reaeration}}{a_sK_2(\mathrm{O}^*\text{-}\mathrm{O})} - \underset{\text{BOD}}{K_1LV} - \underset{\text{benthic demand}}{K_sa_b(\mathrm{OS})V} - \underset{\text{ammonia oxidation}}{\beta_1\alpha_1(\mathrm{NH_3})V} - \underset{\text{nitrate oxidation}}{\beta_2\alpha_2(\mathrm{NO_2})V} - \underset{\text{detritus demand}}{\beta_3\alpha_3(\mathrm{DET})V}$<br>$- \underset{\text{biota respiration}}{K_b(r_pP + r_zZ + r_fF)V} + \underset{\text{photosynthesis}}{K_b(\mu_pP)\gamma V}$ |

Terms not previously defined are as follows:

$P$ = phytoplankton $(ML^{-3})$
$Z$ = zooplankton $(ML^{-3})$
$F$ = nekton $(ML^{-3})$
$B$ = benthic animals $(ML^{-3})$
$B^*$ = benthic animals per unit of bottom area $(ML^{-2})$
$\mu_p, \mu_z, \mu_b, \mu_f$ = growth rates of phytoplankton, zooplankton, benthic animals and nekton, respectively $(T^{-1})$
$r_p, r_z, r_b, r_f$ = respiration rates of phytoplankton, zooplankton, benthic animals and nekton, respectively $(T^{-1})$
$m_z, m_b, m_f$ = mortality rates of zooplankton, benthic animals, and nekton respectively $(T^{-1})$
$s_p, s_d$ = sedimentation rate of phytoplankton and detritus $(ML^{-2}T^{-1})$
$\Psi$ = release rate of ammonia nitrogen $(T^{-1})$
$\eta_{ab}$ = digestive efficiency of predator (a) and prey (b)
$c$ = proportion of carbon
$n$ = proportion of nitrogen
$p$ = proportion of phosphate phosphorus

### 8-4.3 Alternative solution technique

Baca and Arnett have formulated a water quality model following the general approach outlined above, but which uses the finite element technique for solution.[39] The advection–diffusion equation in general form is

$$L[C] = \frac{\partial C}{\partial t} + w\frac{\partial C}{\partial z} - E_z\frac{\partial^2 C}{\partial z^2} + \lambda C - s \tag{8-37}$$

for which the boundary conditions are

$$\frac{\partial C}{\partial t}(0, t) = \frac{\partial C}{\partial t}(z_0, t) = 0 \tag{8-38}$$

and $w$ = vertical advection velocity
$E_z$ = diffusion coefficient
$\lambda$ = decay (or growth) coefficient
$s$ = source

A system of equations can be developed for the continuum of finite elements by approximating the functional form of $C$ over the element space by a linear relationship

$$C \cong \tilde{C} = a + bz \tag{8-39}$$

For adjacent elements, $j$ and $j + 1$

$$C_j = a + bz_j \tag{8-40}$$

and

$$C_{j+1} = a + bz_{j+1} \tag{8-41}$$

in which the coefficients $a$ and $b$ are defined by

$$\begin{Bmatrix} a \\ b \end{Bmatrix} = \frac{1}{\Delta z}\begin{bmatrix} z_{j+1} & -z_j \\ -1 & 1 \end{bmatrix}\begin{Bmatrix} C_j \\ C_{j+1} \end{Bmatrix} \tag{8-42}$$

By employing the Galerkin method of weighted residuals, the governing model Eq. (8-37) can be recast in integral form, such that

$$\chi = \int_R L[\mathbf{C}]W_i dz \tag{8-43}$$

where $W_i$ is an arbitrary set of weighting functions. If the approximating function $W_j$ for $\tilde{C}$ is taken to be the same as $W_j$ according to Galerkin's method then

$$\tilde{C} = \sum_{j=1}^{k} C_j W_j \tag{8-44}$$

and

$$\tilde{C}(z, t) = [W_1, W_2]\begin{Bmatrix} C_j \\ C_{j+1} \end{Bmatrix} \tag{8-45}$$

where the weighting functions are given by

$$W_1 = \frac{1}{\Delta z}(z_{j+1} - z) \tag{8-46}$$

and
$$W_2 = \frac{1}{\Delta z}(z - z_j) \tag{8-47}$$

Expanding Eq. (8-43) and integrating by parts results in

$$\chi = \int_R \left[\frac{\partial C}{\partial t} W_i + W \frac{\partial C}{\partial z} W_i - E_z \frac{\partial C}{\partial z}\frac{\partial W_i}{\partial z} + \lambda C W_i - S W_i\right] dz \tag{8-48}$$

which can be partitioned so that

$$\chi = \sum_{j=1}^{n} \chi_j^e \tag{8-49}$$

where $n$ is the number of subdomains. This may be expanded to give

$$\chi = \int_{z_1}^{z_2} [\ ]dz + \int_{z_2}^{z_3} [\ ]dz + \cdots + \int_{z_{m-1}}^{z_m} [\ ]dz \tag{8-50}$$

Individual terms in the Galerkin functional, Eq. (8-43), and the expanded form, Eq. (8-50), are approximated by

$$\frac{\partial C}{\partial t} = [W_1 W_2] \begin{Bmatrix} \dot{C}_j \\ \dot{C}_{j+1} \end{Bmatrix} \tag{8-51}$$

$$\vdots$$

$$\frac{\partial C}{\partial z} = \left[-\frac{1}{\Delta z}, \ \frac{1}{\Delta z}\right] \begin{Bmatrix} C_j \\ C_{j+1} \end{Bmatrix} \tag{8-52}$$

and
$$\frac{\partial W_j}{\partial z} = \left[-\frac{1}{\Delta z}, \ \frac{1}{\Delta z}\right] \tag{8-53}$$

Substituting these quantities into the Galerkin functional for a particular subdomain results in a particular set of integrals that can be evaluated by

$$\int_{z_j}^{z_{j+1}} W_1^\gamma W_2^\beta dz = \frac{\gamma!\beta!\Delta z}{(\gamma + \beta + 1)} \tag{8-54}$$

These are as follows

1. **Time derivative**

$$\int_{z_j}^{z_{j+1}} \begin{bmatrix} W_1 W_1 & W_2 W_1 \\ W_1 W_2 & W_2 W_2 \end{bmatrix} dz = \Delta z \begin{bmatrix} \frac{1}{3} & \frac{1}{6} \\ \frac{1}{6} & \frac{1}{3} \end{bmatrix} \begin{Bmatrix} \dot{C}_j \\ \dot{C}_{j+1} \end{Bmatrix} \tag{8-55}$$

2. **Advection**

$$\frac{1}{\Delta z} \int_{z_j}^{z_{j+1}} \begin{bmatrix} -(w_j W_1^2 + w_{j+1} W_1 W_2) & (w_j W_1^2 + w_{j+1} W_1 W_2) \\ -(w_j W_1 W_2 + w_{j+1} W_2^2) & (w_j W_1 W_2 + w_{j+1} W_2^2) \end{bmatrix} dz \begin{Bmatrix} C_j \\ C_{j+1} \end{Bmatrix}$$

$$= \begin{bmatrix} -(\frac{1}{3}w_j + \frac{1}{6}w_{j+1}) & (\frac{1}{3}w_j + \frac{1}{6}w_{j+1}) \\ -(\frac{1}{6}w_j + \frac{1}{3}w_{j+1}) & (\frac{1}{6}w_j + \frac{1}{3}w_{j+1}) \end{bmatrix} \begin{Bmatrix} C_j \\ C_{j+1} \end{Bmatrix} \tag{8-56}$$

3. **Diffusion**

$$\frac{E_z}{\Delta z^2}\int_{z_j}^{z_{j+1}}\begin{bmatrix}1 & -1\\ -1 & 1\end{bmatrix}\begin{Bmatrix}C_j\\ C_{j+1}\end{Bmatrix}dz=\frac{E_z}{\Delta z}\begin{bmatrix}1 & -1\\ -1 & 1\end{bmatrix}\begin{Bmatrix}C_j\\ C_{j+1}\end{Bmatrix} \tag{8-57}$$

4. **Decay**

$$\lambda\int_{z_j}^{z_{j+1}}\begin{bmatrix}W_1W_2 & W_2W_1\\ W_1W_2 & W_2W_2\end{bmatrix}\begin{Bmatrix}C_j\\ C_{j+1}\end{Bmatrix}dz=\lambda\Delta z\begin{bmatrix}\frac{1}{3} & \frac{1}{6}\\ \frac{1}{6} & \frac{1}{3}\end{bmatrix}\begin{Bmatrix}C_j\\ C_{j+1}\end{Bmatrix} \tag{8-58}$$

5. **Source**

$$S\int_{z_j}^{z_{j+1}}\begin{Bmatrix}W_1\\ W_2\end{Bmatrix}dz=S\Delta z\begin{Bmatrix}\frac{1}{2}\\ \frac{1}{2}\end{Bmatrix} \tag{8-59}$$

Summing and gathering terms results in a general matrix equation

$$[I]\{\dot{C}\}=[S]\{C\}+\{R\} \tag{8-60}$$

in which $[I]$ is an identity matrix, $[A]$ is the tridiagonal matrix of the coefficients of $C$ and $\{R\}$ is a vector of all known parameters and external sources of $C$. Solution of the equation for each quality constituent is accomplished sequentially according to the method outlined previously for Eq. (8-34).

The advantages of the finite element technique cited by Baca and Arnett lie in avoidance of "numerical mixing" effects, stability of solution, flexibility in length of time step, and adaptability to steep gradients. Experience in use of the method in even more complex problems, involving hydrodynamic processes, seems to confirm these attributes.[40]

### 8-4.4 Demonstration of Water Quality Simulation

The capability for simulation of water quality in stratified reservoirs is illustrated by three examples, each concerned with dissolved oxygen distribution in stratified reservoirs. Figure 8-7 shows the annual history of dissolved oxygen concentrations in the outlet from Fontana Reservoir as observed for the year 1966 and as predicted by the MIT model.[3] The curves shown illustrate the sensitivity of the model to assumed conditions of oxygen saturation in the upper layers of the reservoir, the input BOD, and the rate of BOD decay. While the model gives a reasonable account of the annual pattern of DO variation in the outlet, it appears to be quite sensitive to initial conditions and boundary conditions associated with inflow. The investigators recognize the need for "long-term" water quality data and evaluation of the DO balance in the euphotic zone. It is noted that the model does not consider photosynthetic oxygenation in the upper layers of the reservoir nor the oxygen demands imposed by detritus accretions to the hypolimnion or organic sediment on the reservoir bottom.

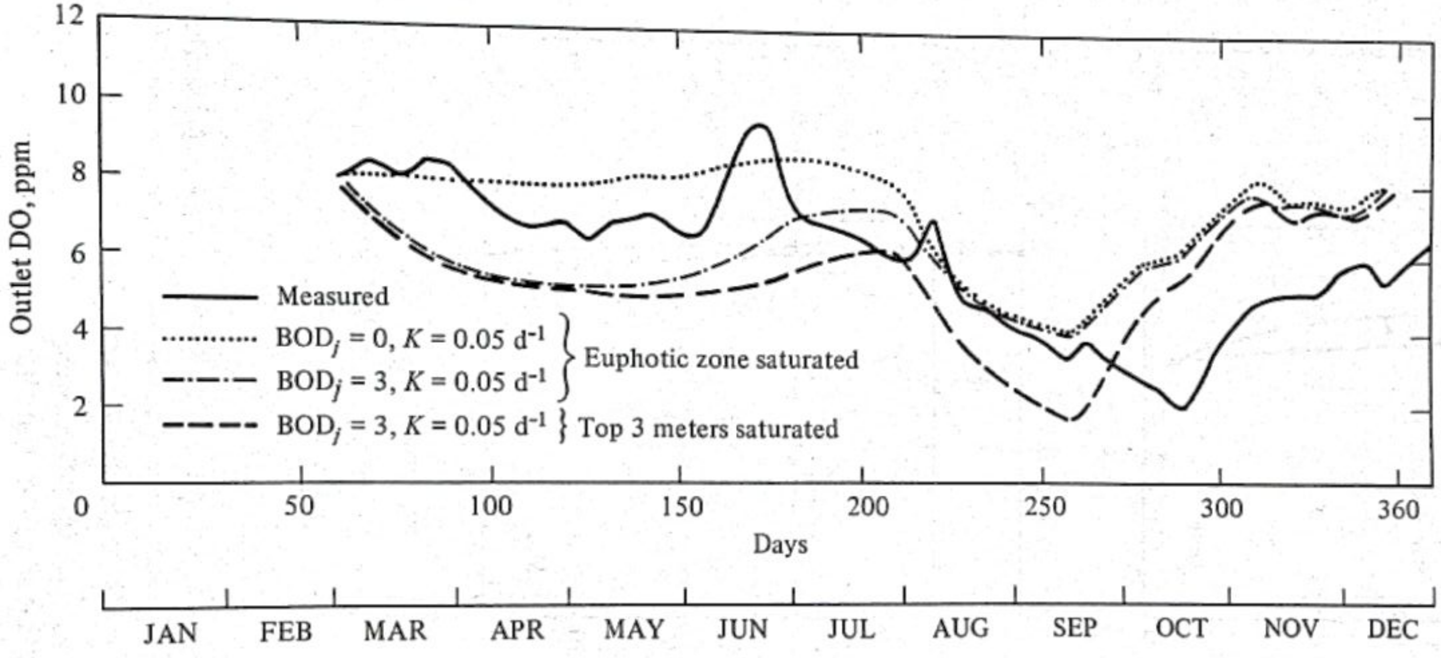

FIGURE 8-7
Measured and predicted yearly variations in dissolved oxygen, in Fontana Reservoir Outlet, 1966.

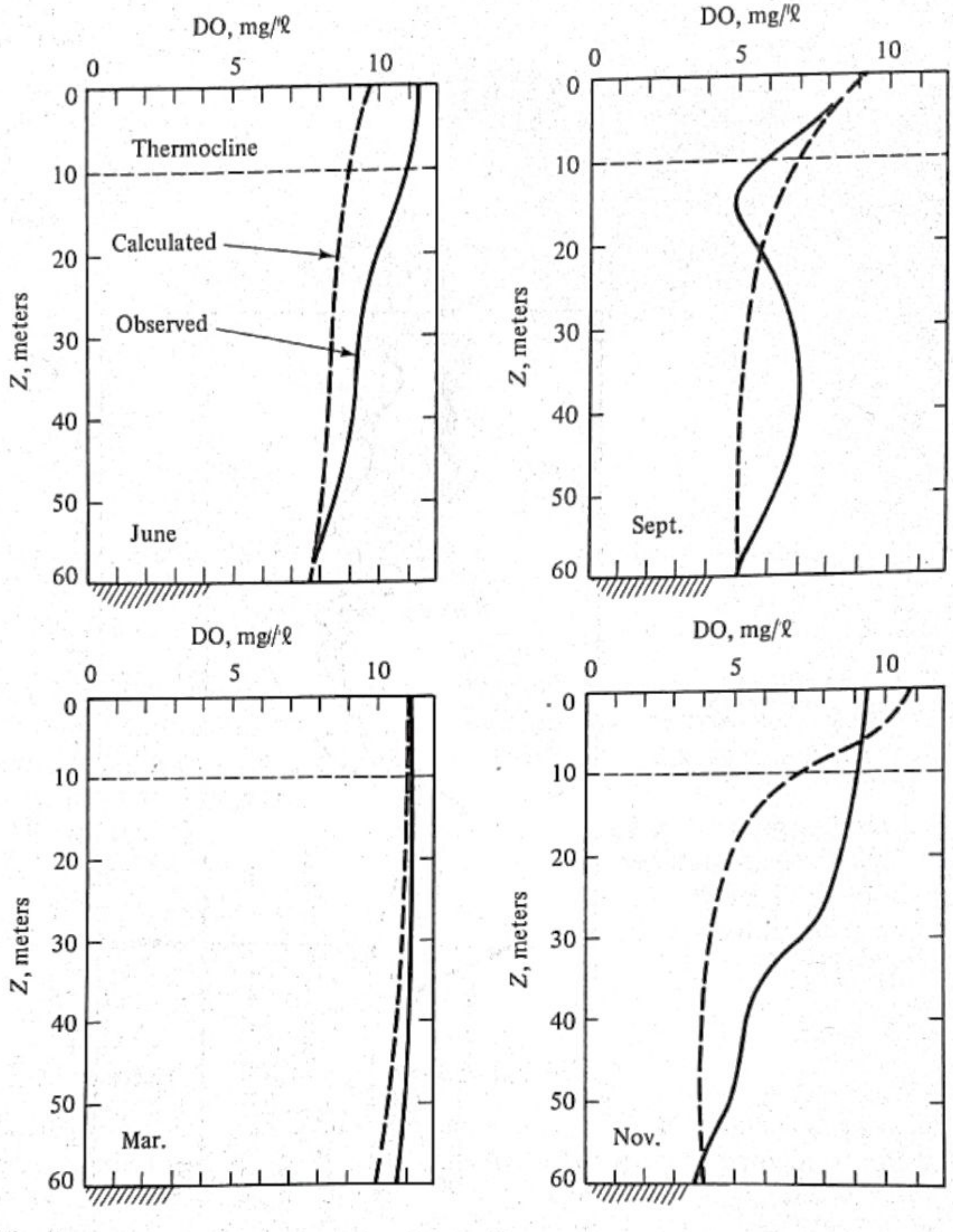

FIGURE 8-8
Simulation of dissolved oxygen in Lake Washington (After Chen and Orlob.[35])

Figure 8-8 depicts the dissolved oxygen distribution in Lake Washington as observed by Edmonson[41] and as predicted by an application of LAKECO, using average hydrologic conditions for 1962–1963. Results indicate the model's capability of following oxygen depletions in the hypolimnion during the onset of thermal stratification, but the depression in dissolved oxygen concentration in the

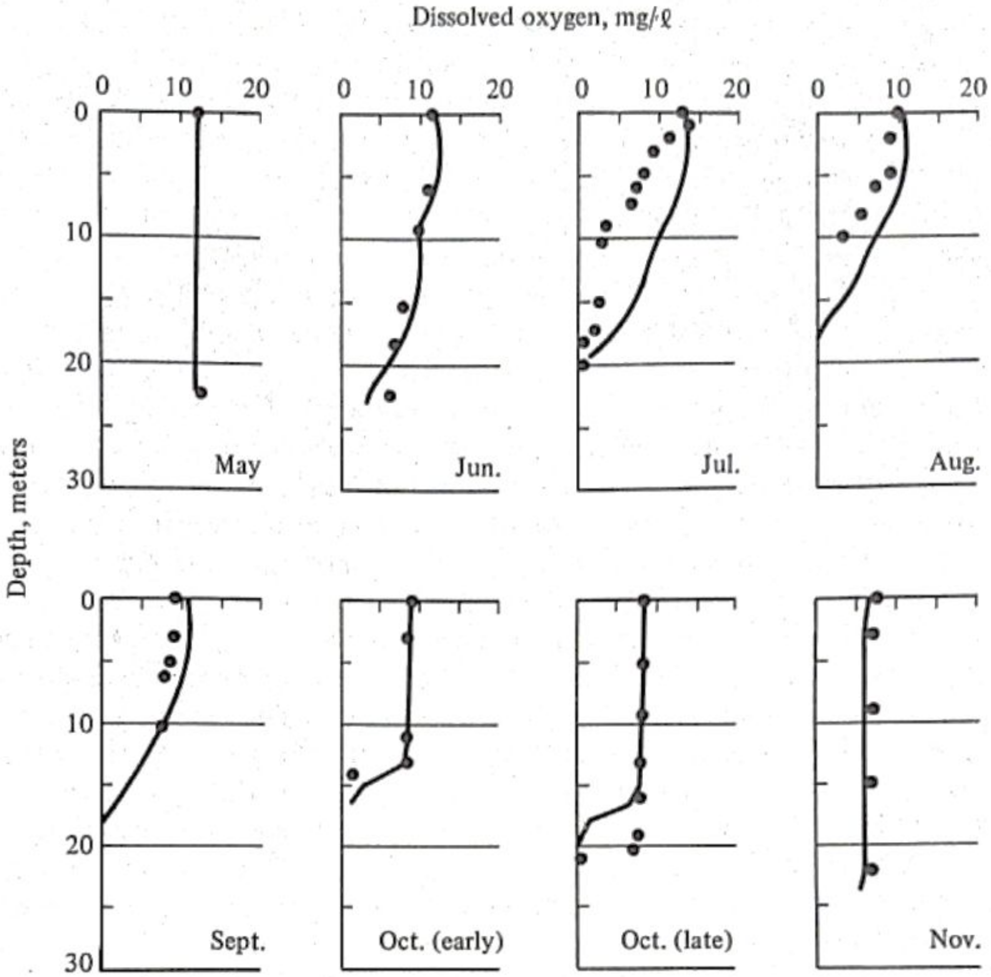

FIGURE 8-9
Simulation of dissolved oxygen in Lake Mendota using finite element model (After Baca and Arnett.[39])

region just below the thermocline (at about 10 m in September) was not well simulated. The investigators noted data deficiencies and the lack of information on algal-zooplankton population dynamics as factors limiting the use of the model. No specific attempt was made to calibrate the model.

Figure 8-9 shows results obtained in simulation of Lake Mendota with the one-dimensional finite element model of Baca and Arnett [1976]. Computed results show good agreement with observed data for dissolved oxygen. The authors report good to excellent comparisons for data on temperature, chlorophyll *a*, inorganic phosphorous, and nitrate. The model was specifically calibrated using data derived from the same sources as were used in the development of LAKECO.

## 8-5 FURTHER ADVANCES IN IMPOUNDMENT MODELING

The preceding review of mathematical modeling has been limited in scope primarily to those developments that have been focused on stratified impoundments, where the assumption of horizontal homogeneity was reasonably close to the truth. Actually, the fact that many lakes and reservoirs behave in this way, at least part of the time, is a great convenience to the modeler for which he should be grateful. It has allowed him the luxury of ignoring the complexities of the impoundment's hydrodynamic behavior in favor of solving the simpler problem.

It cannot be emphasized too strongly that the *solid* foundation for credible simulation of the prototype behavior at any level of modeling the real aquatic environment—physical, chemical, or biological—lies in representing correctly the circulatory processes that govern transport of substances identified with the fluid mass. Much of the argument that seems to rage over the merits and demerits of the advection–diffusion equation, especially the diffusional term, stems from failure—either deliberate or inadvertant—to account for fluid motion. This is especially evident in the case of one-dimensional representation of stratification in impoundments, the subject of this chapter. The simple fact that diffusion at the molecular scale cannot account for vertical transport of heat, not otherwise conveyed by simple advection, is clear indication that our characterization of heat energy, mass and momentum transfer through the horizontal plane is rudimentary at best. The next important steps in impoundment modeling, many of which have already been taken, must be addressed to modeling of circulation. A brief review of recent progress will help to set the stage for further needed advances in the state-of-the-art.

One of the more challenging problems of impoundment modeling is typified by the reservoir with a relatively large flow to volume ratio, or one that combines this characteristic with a high aspect ratio, length to width. In such impoundments the momentum and turbulence of inflow dominate the upper reaches of the reservoir, while in the deeper sections thermal stratification usually constrains the flow as it moves toward the outlets. Early attempts to model large relatively shallow reservoirs of the Lower Columbia River which are of this type, considered these impoundments as vertically mixed along the major axis.[15,16] However, in the deepest reservoir, Lake Roosevelt, significant vertical *and* longitudinal temperature gradients both were noted. Isothermal planes were inclined toward the deeper, outlet end of the impoundment. This system was simulated in a prefunctory fashion by adapting an existing one-dimensional temperature model to a series of six interconnected segments along the major axis, each of which behaved as a one-dimensional stratified reservoir. Between these segments heat transport was governed by densimetric constraints. The method was only moderately successful for the specific case because of difficulties in interfacing and lack of specific knowledge of the internal flow regime. Attempts to adapt it to other weakly stratified reservoirs [Baca, et al., 1974] pointed strongly to the need for a two-dimensional stratified flow model.

In 1970 the Corps of Engineers, Walla Walla District, confronted with a complex problem of intermingling of flows of differing densities in the backwaters of the Lower Granite Project on the Snake River, undertook the development of techniques for simulation of two-dimensional stratified flow.[42] The project was complemented by a parallel research effort sponsored by the Office of Water Resources Research (now OWRT) which produced finite element models for simulation of two-dimensional hydrodynamic and water quality behavior for both vertical and horizontal cases.[33,43] The models were successfully applied to the Lower Granite problem and to simulation of laboratory experiments of stratified flow. Subsequently, they were applied to simulation of steam power plant heat rejection to a large reservoir in the TVA system.[44]

Similar finite element models have been developed for investigation of two-dimensional unsteady circulation in shallow vertically mixed lakes and for shallow estuaries and coastal waters.[45-47] Judging from the most recent literature on impoundment modeling, FEM techniques have apparently been gaining rapidly in popularity for modeling of two-dimensional fluid systems, supplanting to an important degree the more traditional, better known finite difference and characteristic techniques.

Modeling of water quality in large, stratified water bodies like the Great Lakes appears to have followed the same pattern outlined above for one-dimensional stratified reservoirs. Water quality–ecologic models have been devised for Lake Erie and Lake Ontario.[8,48] Both models are "driven" by circulations determined exogenously. The Lake Erie model utilizes advective flows estimated by water balance methods, adding "mixing flows" in order to achieve a satisfactory balance of a conservative tracer, chlorides in this case. The Lake Ontario model utilizes simulated three-dimensional flow patterns produced by a simulation model attributed to the National Oceanographic and Atmospheric Administration (NOAA), but not documented in the literature. A similar model of Lake Ontario, using a finite difference approach, is that developed for the Canadian Centre for Inland Waters by Simons.

In summary, it appears that the state-of-the-art of modeling of large lakes and reservoirs which experience wind driven and geostrophic circulation and thermal stratification has advanced to the point where it is now limited by capability to simulate circulatory processes. Reasonably satisfactory models exist for describing the water quality–ecologic relationships in such water bodies provided one can determine the important mechanisms of transport, particularly those we tend to classify as "diffusional." A pressing need is for a fundamentally sound three-dimensional representation of stratified flow, one that reduces our dependence upon empirical characterization of vertical transport of heat, momentum, and other properties of the fluid mass. Of course, there is a continuing need also for improved description of water quality and ecologic processes and for adequate data with which to calibrate models. Most important of all, there is a need for basic knowledge of the behavioral mechanisms of the impoundment—physical, chemical, and biological—without which the capabilities and especially the *limitations* of mathematical models cannot be fully appreciated.

## ACKNOWLEDGEMENT

In preparation of this manuscript the author has drawn on an extensive body of extant literature, much of it in report form and of limited circulation. The opportunity and the resources to gather this information and digest it into this summary of the state-of-the-art of impoundment modeling was provided largely through the auspices of the Office of Water Research and Technology, to which agency the author is especially grateful.

## REFERENCES

1. TVA ENGINEERING LABORATORY, "Heat and Mass Transfer Between a Water Surface and the Atmosphere," Report no. 14, 2 app., April 1972.
2. DAKE, J. M. K., and D. R. F. HARLEMAN, "An Analytical and Experimental Investigation of Thermal Stratification in Lakes and Ponds," Report no. 99, Parsons Laboratory, MIT, 1966.
3. MARKOFSKY, M., and D. R.F. HARLEMAN, Prediction of Water Quality in Stratified Reservoirs, *J. Hydr. Div., Am. Soc. Civ. Eng.*, Paper no. 9730, pp. 729–745, May 1973.
4. CHEN, C. W., Concepts and Utilities of (an) Ecologic Model, *J. Sanit. Div., Am. Soc. Civ. Eng.*, vol. 95, no. SA5, Paper no. 7602, October 1970.
5. PARK, R. A., J. W. WILKINSON, R. C. KOHBERGER, J. A. BLOOMFIELD, and C. S. ZAHOVACK, Statistical Analysis, Data Management and Ecosystem Modeling at Lake George, New York, EDFB Memo Report 73–64, Rensselaer Polytechnic Institute, Troy, New York Department of Geology, 1973.
6. PARK, R. A., D. SCAVIA, and N. L. CLESCERI, "Cleaner, the Lake Model," Eastern Deciduous Forest Biome Contribution no. 186, IBP, 1975.
7. CHEN, C. W., and G. T. ORLOB, "Ecologic Study of Lake Koocanusa, Libby Dam," Report to Seattle Dist., Corps of Engineers, by WRE, Inc., January 1973.
8. DI TORO, D. C., D. J. O'CONNOR, R. V. THOMANN, and J. L. MANCINI, Phytoplankton–Zooplankton–Nutrient Interaction Model for Western Lake Erie, in B. C. Patten (ed.), "Systems Analysis and Simulation in Ecology," vol. III, chap. 11, pp. 423–474, Academic Press, 1975.
9. BACA, R. G., M. W. LORENZEN, R. D. MUDD, and L. V. KIMMEL, "A Generalized Water Quality Model for Eutrophic Lakes and Reservoirs," Report to EPA 211B01602, Pacific N.W. Laboratory, Battelle Memorial Institute, November 1974.
10. JØRGENSEN, S. E., A Eutrophication Model for a Lake, *J. Ecological Modeling*, vol. 2, pp. 147–165, 1976.
11. MCEWEN, G. F., A Mathematical Theory of the Vertical Distribution of Temperature and Salinity in Water Under the Action of Radiation, Conduction, Evaporation and Mixing Due to the Resultant Convection, *Bul. Scripps Inst. Oceanogr. Tech.*, vol. 2, pp. 197–306, 1929.
12. HUTCHINSON, G. E., "A Treatise on Limnology," vol. 1, John Wiley & Sons, New York, 1957.

13. ERTEL, H. E., Theorie der Thermischen Sprungschicht in Seen, *Acta. Hydrophys.*, vol. 1, pp. 151–171, 1954.
14. RAPHAEL, J. M., Prediction of Temperature in Rivers and Reservoirs, *J. Power Div., Am. Soc. Civ. Eng.*, vol. 88, PO2, pp. 157–181, July 1962.
15. RAPHAEL, J. M., "The Effect of Wanapum and Priest Rapids Dams on the Temperature of the Columbia River," Pub. Util. Dist. no. 2 of Grant Co., Wash., Ephrata, Washington, September 1961.
16. RAPHAEL, J. M., "The Effect of Wells and Rocky Reach Dams on the Temperature of the Columbia River," Pub. Util. Dist. No. 2 of Grant Co., Washington, January 1962.
17. BURT, W. V., "Heat Budget Terms for Middle Snake River Reservoirs," U.S. Fish and Wildlife Service, Ref. 58–7, December 1958.
18. BURT, W. V., "A Forecast of Temperature Conditions for the Reservoir Behind the Proposed Bruces Eddy Dam," Water Research Associates, Corvallis, Oregon, April 1960.
19. BURT, W. V., "Preliminary Study on the Predicted Water Changes of the Lower Snake River," Water Research Associates, Corvallis, Oregon, November 1963.
20. KLEIN, W. H., Calculation of Solar Radiation and the Solar Heat, *J. Meteorology*, vol. 5, no. 4, 1948.
21. MARCIANO, T. T., and G. E. HARBECK, jr., Mass Transfer Studies, in "Water Loss Investigations, Lake Hefner Studies," Technical Report, U.S. Geol. Surv. Prof., Paper 269, 1954.
22. ORLOB, G. T., "A Mathematical Model of Thermal Stratification in Deep Reservoirs," Conference of American Fisheries Soc., Portland, Oregon, September 1965.
23. ELDER, R. A., and W. O. WUNDERLICH, "Evaluation of Fontana Reservoir Field Measurement," presented at ASCE Specialty Conf. on Current Research into the Effects of Reservoirs on Water Quality, Portland, Oregon, January 1968.
24. WATER RESOURCES ENGINEERS, INC., "Prediction of Thermal Energy Distribution in Streams and Reservoirs," Report to California Department of Fish and Game, June 1967, rev. August 1968.
25. HUBER, W. C., D. R. F. HARLEMAN, and P. J. RYAN, Temperature Prediction in Stratified Reservoirs, *J. Hydr. Div., Am. Soc. Civ. Eng.*, Paper 8839, pp. 645–666, April 1972.
26. SUNDARAM, T. R., C. C. EASTERBROOK, K. R. PIECH, and G. RUDINGER, "An Investigation of the Physical Effects of Thermal Discharges into Cayuga Lake," Report VT-2616-0-2, Cornell Aeronautical Laboratory, Buffalo, N.Y., November 1969.
27. PARKER, F. L., B. A. BENEDICT, and C. TSAI, "Evaluation of Mathematical Models for Temperature Prediction in Deep Reservoirs," Report to EPA by Vanderbilt University, Ecological Research Series, EPA-660/3-75-038, June 1975.
28. ORLOB, G. T., and L. SELNA, "Prediction of Thermal Energy Distributions in Deep Reservoirs," Proceedings of the 6th Annual San. and Water Resources Engrg. Conference, Vanderbilt University, June 1967, pp. 64–77.
29. DEBLER, W. R., Stratified Flow into a Line Sink, *J. Div. of Engrg. Mech., Am. Soc. Civ. Eng.*, vol. 85, EM3, July 1958.
30. KAO, T. W., The Phenomenon of Blocking in Stratified Flow, *J. Geophysical Res.*, vol. 70, no. 4, pp. 815–822, February 1965.

31. BELLA, D. A., and W. E. DOBBINS, Difference Modeling of Stream Pollution, *J. Sanit. Eng. Div., Am. Soc. Civ. Eng.*, vol. 94, no. SA5, Paper No. 6192, pp. 995–1016, October 1968.
32. HARLEMAN, D. R. F., and K. A. HURLEY. Simulation of the Vertical Thermal Structures of Lakes under Transient Meteorological Conditions. "Dynamics of Stratification and of Stratified Flows in Large Lakes." Proc. of Workshop. Comm. on Lake Dynamics, chap. 7, pp. 79–96, International Joint Commission's Research Advisory Board, Windsor, Ontario, 1976.
33. KING, I. P., and W. R. NORTON, A Finite Element Solution for Two-Dimensional Stratified Flow, in "Finite Elements in Fluids," vol. 1, chap. 7, pp. 133–156, 1975.
34. RYAN, P. J., and D. R. F. HARLEMAN, "Prediction of the Annual Cycle of Temperature Changes in a Stratified Lake or Reservoir: Mathematical Model and Users Manual," Technical Report no. 137, Parsons Laboratory, MIT, April 1971.
35. CHEN, C. W., and G. T. ORLOB, "Ecologic Simulation for Aquatic Environments," Final Report to OWRR, WRE, Inc., December 1972a. Also "Systems Analysis and Simulation in Ecology," chap. 12, pp. 475–588, Academic Press, 1975.
36. BACA, R. G., W. W. WADDEL, C. R. COLE, A. BRANDSTETTER, and D. B. CEARLOCK, "EXPLORE-I: A River Basin Water Quality Model," Battelle Pacific Northwest Laboratory, Richland, Washington, Report to EPA 68-01-0056, August 1973.
37. ODUM, H. T., "Environment, Power and Society," Wiley Interscience, New York, 1971.
38. WATER RESOURCES ENGINEERS, INC., "Ecologic Modeling of Puget Sound and Adjacent Waters. Report no. 4. Lake Ecologic Model. User's Manual LAKECO," Report to OWRT, Washington, D.C. by WRE, Inc. September 1975.
39. BACA, R. G., and R. C. ARNETT, A Finite Element Water Quality Model for Eutrophic Lakes, Proc. Intnl. Conf. on Finite Elements in Water Resources, Princeton University, Princeton, New Jersey. (Also Battelle Pacific N.W. Laboratory JBN-SA-540), July 1976.
40. GALLAGHER, R. H., J. T. ODEN, C. TAYLOR, and O. C. ZIENKIEWICZ, "Finite Elements in Fluids," vols. 1 and 2, John Wiley & Sons, New York, 1975.
41. EDMUNDSON, W. T., "Changes in Lake Washington Following an Increase in the Nutrient Income," *Verh. Int. Verein Limnol.*, vol. 14, pp. 167–175, 1961.
42. NORTON, W. R., I. P. KING, and G. T. ORLOB, "A Finite Element Model for Lower Granite Reservoir," Report to Walla Walla District, Corps of Engineers, by WRE, Inc., March 1973.
43. KING, I. P., W. R. NORTON, and G. T. ORLOB, "A Finite Element Solution for Two-Dimensional Density Stratified Flow," Final Report to OWRR by WRE, Inc., March 1973.
44. ORLOB, G. T., I. P. KING, and W. R. NORTON, "Mathematical Simulation of Thermal Discharges from Johnsonville Steam Plant," Report to TVA, Div. of Water Control Planning by RMA, Inc., August 1975.
45. LIGGETT, J. A., Unsteady Circulation in Shallow Lakes, *J. Hydr. Div., Am. Soc. Civ. Eng.*, vol. 95, no. HY4, pp. 1273–1288, Paper 6686, July 1969.
46. GALLAGHER, R. H., Finite Element Lake Circulation and Thermal Analysis, in "Finite Elements in Fluids," chap. 6, vol. 1, pp. 116–131, John Wiley & Sons, New York, 1975.

47. TAYLOR, C., and J. M. DAVIS, Tidal Propagation and Dispersion in Estuaries, in "Finite Elements in Fluids," vol. 1, chap. 5, pp. 95–118, 1975.

48. CHEN, C. W., M. LORENZEN, and D. J. SMITH, "A Comprehensive Water Quality—Ecological Model for Lake Ontario," Report to NOAA Great Lakes Environmental Research Laboratory, Tetra Tech, Inc., October 1975.

49. NORTON, W. R., L. A. ROESNER, and G. T. ORLOB, "Mathematical Models for Prediction of Thermal Energy Changes in Impoundments," EPA Water Pollution Control Research Series 6130, EXT 12/6, 1968.

# 9

# MODEL FOR LAKE GLUMSØ, DENMARK

**Sven Erik Jørgensen**

*Langkaer Vaenge 9*
*Copenhagen, Denmark*

## 9-1 INTRODUCTION

Glumsø Lake has received mechanically–biologically treated waste water from a community having about 3,000 inhabitants. Since approximately 25 percent of the inflow to the lake (see the mass balance, Table 9-4) is waste water, the concentration of nutrient is very high—giving hypereutrophication of the lake. Different types of advanced waste water treatment have been considered as solutions to the problem. This raises four questions which will be attempted to be answered by means of investigations and a lake model:

*1* What is the present biological and chemical condition of the lake?
*2* Which limiting factor for phytoplankton growth is easiest to control?
*3* What must be required by an advanced treatment plant?
*4* Is it possible to set up a prognosis giving information about the improvement of the biological and chemical condition of the lake, which can be expected as a result of an advanced waste water treatment installation?

A map of the lake is shown in Fig. 9-1. The lake is surrounded by meadows and the landscape is flat. Two small tributaries and a bigger one flow into the lake, and a channel carries the outflow to the main river in this area—Suså River.

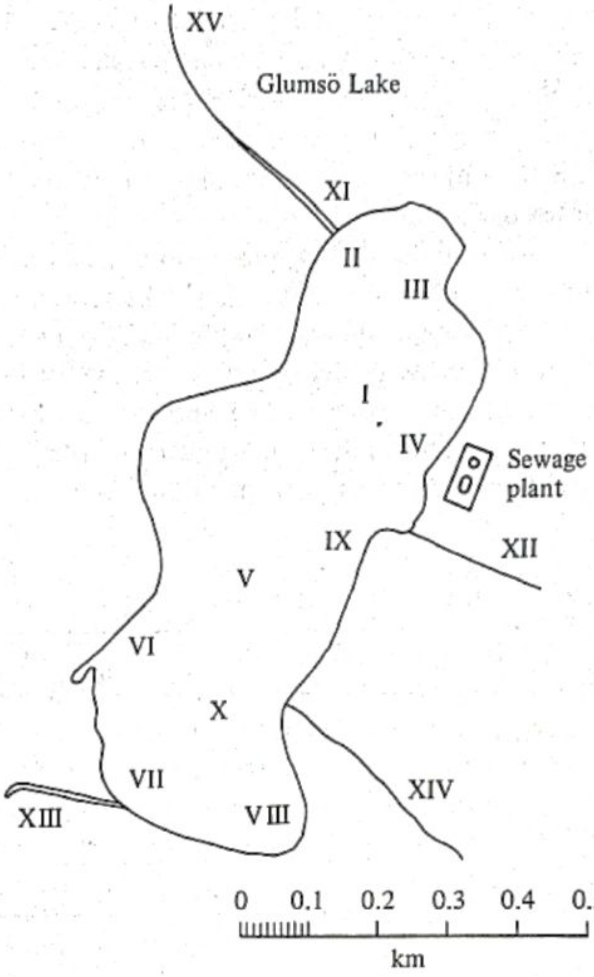

FIGURE 9-1
Map of the lake with indication of stations.

The lake is situated in a sub-glacial valley.[1] The drainage area is approximately 10.9 km—a town and an agricultural area. The lake is shallow with an average depth of about 2 m. The surface area is 266,000 $m^2$ and the volume 420,000 $m^3$. The lakes in this area have a calcite-rich sediment, which is characteristic of the moraine soil in this part of Zealand, Denmark.

## 9-2 THE BIOLOGICAL AND CHEMICAL STATE OF THE LAKE

Preliminary examinations were carried out in 1972 to determine the biological and chemical state of the lake.

The lake is surrounded by reed swamp and it contains no submerged vegetation at all, probably due to low transparency of the water and deficit of oxygen at the bottom of the lake. A total of twenty-three species of aquatic vascular plants were found. The following species of fish were found in or reported from the lake: (pike (*Esox lucius*), bream (*Abamis brama*), bleak (*Alburnus alburnus*), eel (*Anguilla anguilla*), perch (*Perca fluviatitis*), white bream (*Blicca björkna*) and roach (*Rutilus rutilus*).

Results of zoo- and phytoplankton countings are summarized in Table 9-1. It is the impression that the phytoplankton density has reached its upper limit for natural waters.

The highest phytoplankton concentration was presented in May and June with 2 × $10^9$ to 4 × $10^9$ cells per liter. Later in the summer the density seems to be stabilized at about 1.5 × $10^9$ cells per liter (see Table 9-1). During the entire period of growth phytoplankton seems to be almost a monoculture of *scenedesmus spp.* (four species). The *Scenedesmus* percentage of total algae was lowest in the spring and highest in August. In May *Scenedesmus* amounted to 52 percent and increased to 91 percent in late August.

**Table 9-1 PLANKTON IN GLUMSØ LAKE 1972**

| | Sampling date | | | | | | |
|---|---|---|---|---|---|---|---|
| **Parameter** | **May 21** | **June 13** | **July 13** | **Aug. 7** | **Aug. 23** | **Aug. 26** | **Sept. 26** |
| **Zooplankton (ind/l)** | | | | | | | |
| *Bosmina longirostris* | 0 | 453 | 344 | 1,587 | 1,728 | 142 | 552 |
| *Nanplia* | 0 | 260 | 210 | 327 | 168 | 235 | 302 |
| *Daphnia* sp. | 0 | 2 | 2 | 2 | 10 | 0 | 6 |
| *Cyclops* sp. | 4 | 120 | 14 | 24 | 28 | 30 | 12 |
| Total | 4 | 835 | 570 | 1,940 | 1,934 | 407 | 872 |
| **Phytoplankton ($10^6$ cells/ml)** | | | | | | | |
| *Scenedesmus* spp. | 1.68 | 1.36 | 0.78 | 1.08 | 0.92 | 1.10 | 1.44 |
| % *Scenedesmus* of total algae | 52 | 60 | 76 | 73 | 91 | 74 | 87 |
| Total algae | 3.80 | 2.25 | 1.01 | 1.50 | 1.01 | 1.30 | 1.66 |
| Transparency in meter | 0.15 | 0.20 | 0.20 | 0.22 | 0.22 | 0.30 | 0.23 |

As for phytoplankton, the composition of the zooplankton is very simple. One species dominated, and a total of three species were determined.[2] The density of *Bosmina longirostris* varied from early summer with approximately 500 individuals to 1,500–1,700 individuals per liter in mid August. Two other crustaceans were present—*Daphnia* and *Cyclops* (see Table 9-1).

Counting results of the bottom fauna are shown in Table 9-2 and the fauna was determined on net samples taken in the outflow of the lake (see Table 9-3). All animals found have the characteristic of showing great tolerance towards organic pollution. Further details about these investigations of the biological state of the lake can be seen in Jørgensen et al.[3] The chemical and physical state of the lake is illustrated in Fig. 9-2 ($N_{total}$ and $N_{dissolved}$, station I + X), Fig. 9-3

Table 9-2 BOTTOM FAUNA IN GLUMSØ LAKE (26 AUGUST 1972)

| Substrate | % covering of the free bottom area | Average density ind/m² | | | |
|---|---|---|---|---|---|
| | | Tubificidae | Chironomus plumosus | Other chironomidea | Total |
| Mud, central part | 70–80% | 20 | 0 | 0 | 20 |
| Mud along the shore | 15–25% | 13 | 60 | 0 | 73 |
| Reed swamps | 5% | 100 | 530 | 440 | 1,070 |

Table 9-3 ANIMALS IN NET SAMPLES TAKEN IN THE OUTFLOW OF GLUMSØ LAKE

| | |
|---|---|
| Leeches: | *Herpobdella octoculata* and *H. stagnalis* |
| Oligochaetes: | Tubificidae |
| Insects: | *Cloëon dipterum*, *Hydropsycke* sp. <br> *Corixa* sp. and *Asellus aquaticus* |
| Snails: | *Lymnea pereger* and <br> *Valvata pisciualis* |

($PO_{4,\text{total}}^{3-}$ and $PO_{4,\text{dissolved}}^{3-}$, station I + X), Fig. 9-4 (transparency and pH, station I + X), Fig. 9-5 (oxygen saturation, station I + X at noon) and Fig. 9-6 (the temperature). Figure 9-7 shows the oxygen saturation plotted to the depth at sunrise and at noon, station I + X. These observations can be summarized as follows:

*1* The nutrient concentration is very high, giving a low transparency due to hypereutrophication.

*2* pH and the oxygen concentration is high during the summer due to the high concentration of phytoplankton, while there is oxygen depletion close to the bottom—probably caused by the oxygen consumption of the detritus.

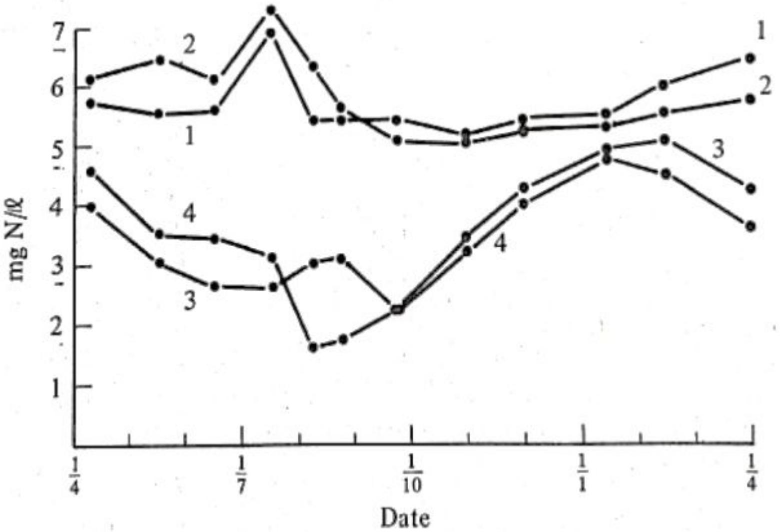

FIGURE 9-2
The seasonal variation of (1) $N_{\text{total}}$ station I, (2) $N_{\text{total}}$ station X, (3) $N_{\text{dissolved}}$ station I, (4) $N_{\text{dissolved}}$ station X.

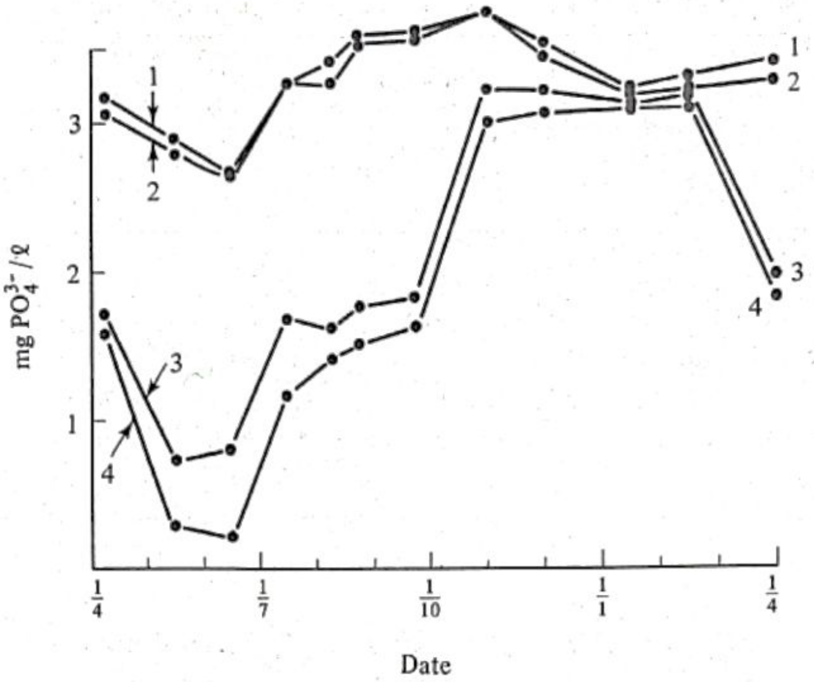

FIGURE 9-3
The seasonal variation of (1) $PO_4^{3-}{}_{total}$ station I, (2) $PO_4^{3-}{}_{total}$ station X, (3) $PO_4^{3-}{}_{dissolved}$ station I, (4) $PO_4^{3-}{}_{dissolved}$ station X.

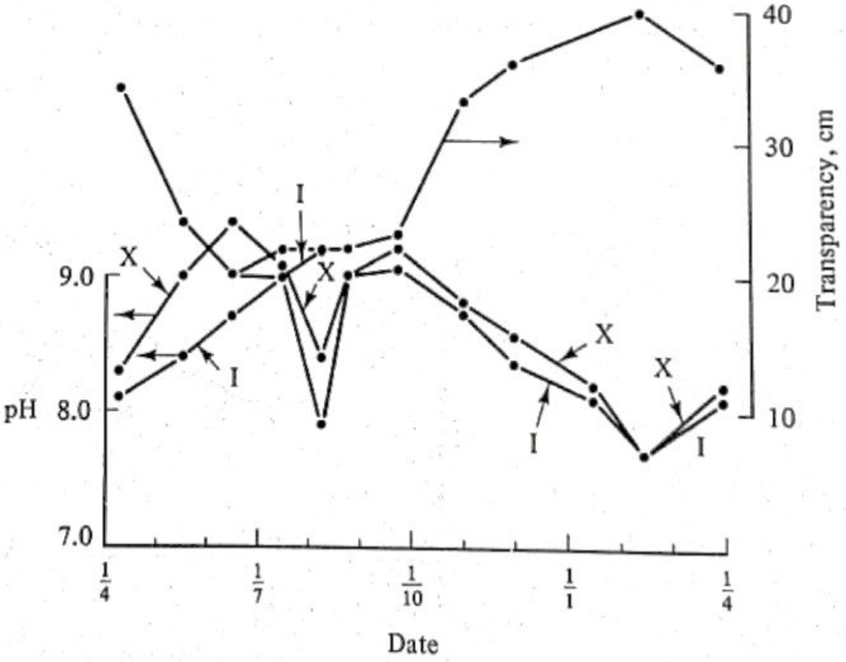

FIGURE 9-4
The seasonal variation of the transparency and pH, station I and X.

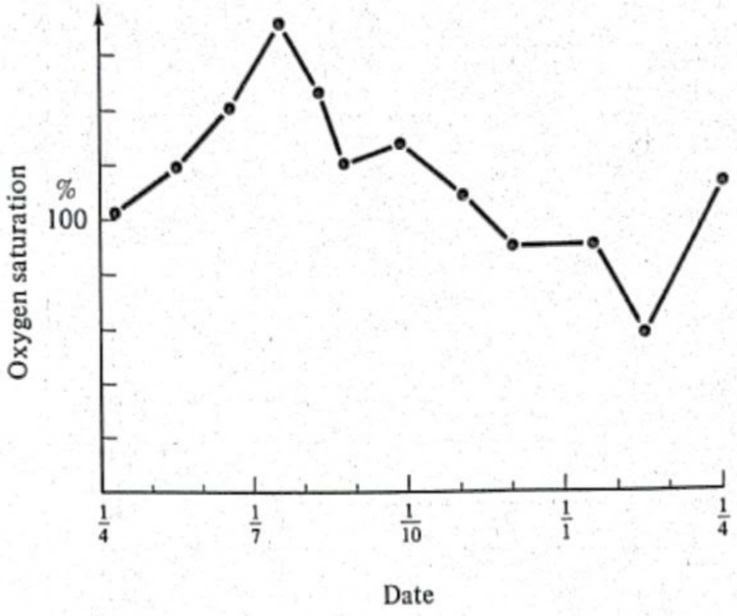

FIGURE 9-5
The seasonal variation of oxygen saturation station I and X. Depth 40 m, at noon.

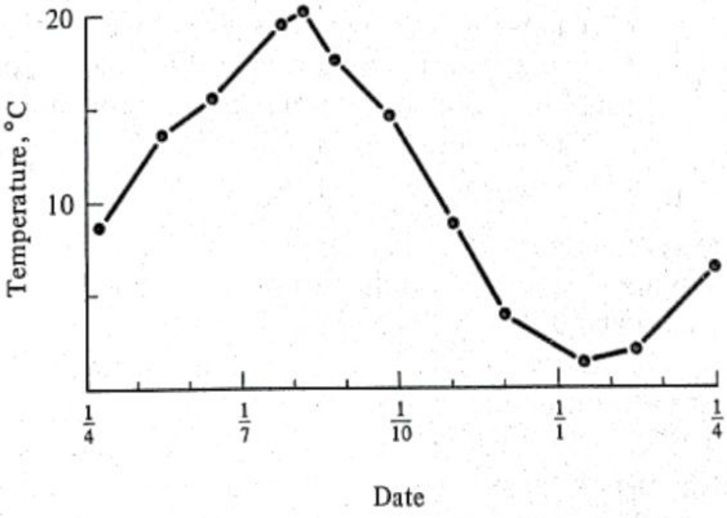

FIGURE 9-6
The seasonal variation of the temperature in 2.0 m depth.

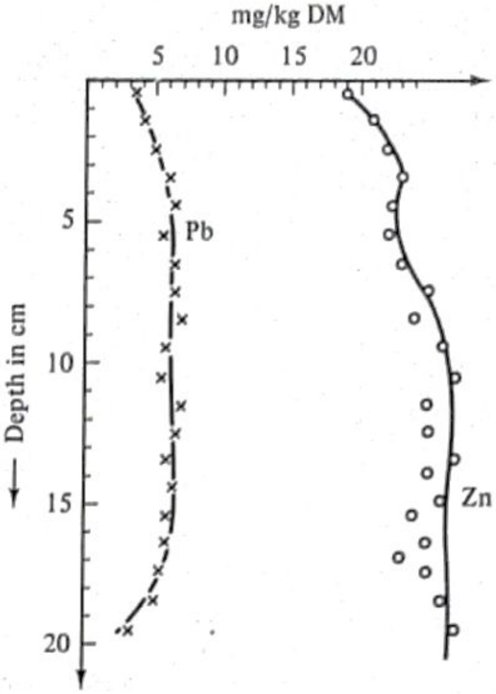

FIGURE 9-7
Metal analysis of a core from Lake Glumsø. Zinc and lead (mg/kg dry matter) are plotted against the depth.

## 9-3 MASS BALANCES

The water balance for 1972 was determined as follows:

*1* The precipitation was given by the metereological station in the town of Glumsø.
*2* The wastewater flow was given by the municipality.
*3* The tributaries were measured in accordance to DIF 1946. Twenty-four double determinations were spread throughout the year.
*4* The evaporation was calculated in accordance with the general information given.[4]

Determination of the $P_{total}$ and $N_{total}$ concentrations on water samples from the tributaries (24 × 4 samples) waste water and rain water were used to set up a mass balance for the lake (see Table 9-4).

As seen in the table, the phosphorus balance is reasonably accurate, taking into consideration that the accumulation of nutrient is not included in the mass balance. The net sedimentation rate has been determined by means of lead analysis of the sediment as a function of depth (see Fig. 9-8).

The lead concentration of the layer from 3–17 cm is approximately constant; it decreases below 17 cm and in the upper 3 cm the concentration of lead is also lower, probably because the upper 3 cm is still active and releases

**Table 9-4** MASS BALANCES

| In | m³ | mg P l$^{-1}$ | mg N l$^{-1}$ total | kg P/year | kg N/year |
|---|---|---|---|---|---|
| Precipitation | 171.500 | ~0 | 0.36 | — | 61 |
| Waste water | 264.000 | 4.8 | 23.4 | 162 | 6,190 |
| Tributaries | 530.000 | 0.21 | 6.4 | 111* | 3,340† |
| Total in | 965.500 | | 1,273 | | 9,591 |
| **Out** | | | | | |
| Evaporation | 173.000 | ~0 | 0 | — | — |
| Tributaries | 840.000 | 1 | | 1,092 | 4,620 |
| Total out | 1,013.000 | | | 1,092 | 4,620 |
| Difference | | | | 181 | 4,971 |
| Sedimentation | | | | 266 | 715 |
| Diff. – sedimentation | | | | −85 | 4,256 |

* 85 percent is due to waste water
† 15 percent is due to waste water

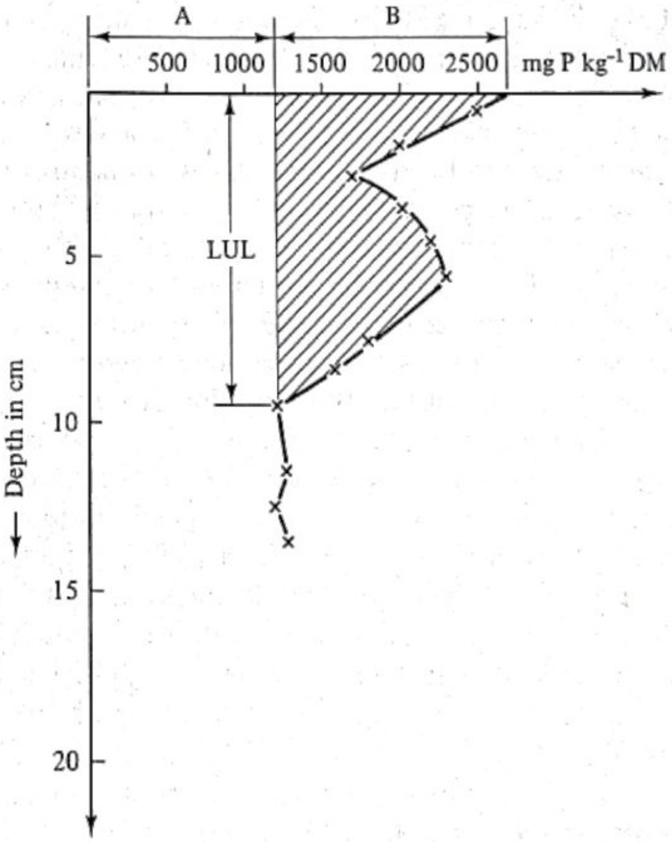

FIGURE 9-8
Analysis of core from Lake Glumsø; mg P per g dry matter is plotted against the depth. The hatched area represents exchangeable phosphorus. $F = B \cdot A^{-1}$, LUL is the unstabilized layer.

phosphorus, nitrogen compounds and organic matter, causing a futher concentration of biologically inactive compounds. Since it must be expected that the lead concentration increased about 20–24 years ago, a yearly net sedimentation of 7 mm seems reasonable. As the stabilized sediment contains about 1.2 g phosphorus per kilogram of dry matter and 12 percent of dry matter,[5] the yearly accumulation of phosphorus in the sediment can be found:

$$\frac{266{,}000 \times 7 \times 0.12 \times 1.2}{1{,}000} = 266 \text{ kg P year}^{-1}$$

The corresponding nitrogen concentration of the stablized sediment is 3 g/kg dry matter, which can only explain 715 kg of the difference found by means of the mass balance. The remaining difference of 4,256 kg can only be explained as a denitrification.

## 9-4 MODELING THE EUTROPHICATION PROCESS

From the observations referred to in Secs. 9-2 and 9-3, it is clear that Glumsø Lake is suffering from hypereutrophication, and the advanced wastewater treatment must at least include an effective removal of one nutrient. Taking into consideration that about 85 percent of the phosphorus in the tributaries is due to waste water, which could be treated in the sewage plant together with the waste water from the town, it seems easiest to control the discharge of phosphorus. Only about 15 percent of the nitrogen in the tributaries is caused by waste water, which means that only about 65 percent of the total nitrogen input is due to waste water, while more than 98 percent of the total phosphorus input is due to waste water. However, in order to be able to answer questions 2 to 4 (page 314), it is necessary to set up an ecological model describing the relation between nutrient concentrations and the eutrophication process.

The basis for all ecological models is a conceptual diagram. The model set up in this case attempts to describe all the important mass flows—from water phase to phytoplankton, from phytoplankton to zooplankton, from sediment to water phase, etc. The three main elements, carbon, nitrogen and phosphorus, are considered and the conceptual diagram for phosphorus is shown in Fig. 9-9.

An ecological model will always be a simplified description of reality. It is not possible to include all processes taking place in an ecosystem, but by focusing on the aspects that are of interest or where understanding is needed, a considerable reduction of the number of state variables may be obtained.

The mass flows of importance for the eutrophication process, which is in focus, have been selected by application of exergy calculation. When considering the flow diagram of phosphorus (Fig. 9-9), the exergy, $E$, was found as:

$$E = R \cdot T \cdot \sum a_j \left[ \mathrm{P}_j \ln \frac{\mathrm{P}_j}{\mathrm{P}^{\mathrm{eq}}} - (\mathrm{P}_j - \mathrm{P}_j^{\mathrm{eq}}) \right]$$

where $T$ = absolute temperature
$a_j$ = volume ratios
$P_j$ = the phosphorus concentration in compartment $j$ (seven compartments are considered in Fig. 9-9)
$P_j^{eq}$ = the phosphorus concentration by thermodynamic equilibrium

Jørgensen and Meyer[6] have demonstrated that the exergy is a suitable tool to include the most important mass flows in the model. Exergy calculations based on phosphorus, nitrogen, and carbon have shown that it is of importance to include:

*1* The entire chain, soluble nutrient → phytoplankton → zooplankton → fish (see Fig. 9-9).
*2* Application of a more detailed description of the exchange mud-water. The submodels published by Kamp-Nielsen,[7,8] Jørgensen et al.,[5] and Jacobsen and Jørgensen[9] are used.

These submodels are shown as Eqs. (9-14), (9-15) and (9-16), Table 9-5. In accordance to the model for phosphorus, a part of the settled phosphorus is bound to the sediment, and only $1/f$ is exchangeable. The exchangeable phosphorus, *PE*, is due to biological processes dissolved in the interstitial water, *PI*. By a diffusion process the phosphorus is transferred from the interstitial water to the lake water.

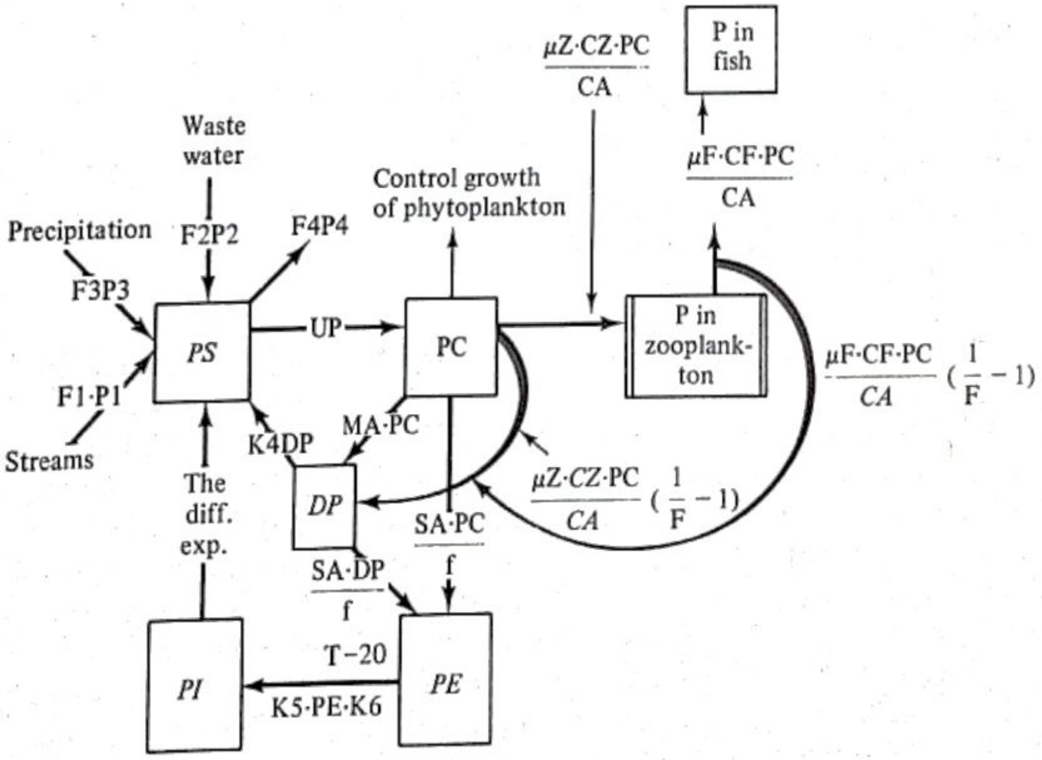

FIGURE 9-9
Principles for the model based upon phytoplankton population dynamics. Only phosphorus is included in this illustration. (Model II).

**Table 9-5 MODEL 1**

$$P4 = PS + DP + (CA + CZ)\mathrm{PP} \tag{9-1}$$

$$N4 = NS + DN + (CA + CZ)\mathrm{PN} \tag{9-2}$$

$$\mu A = \mu A_{\max} \cdot \exp\left(-2.3\left|\frac{T - 16.5}{15}\right|\right) \cdot \mathrm{Light} \cdot \frac{C}{\mathrm{KC} + C} \cdot \frac{NS}{\mathrm{KN} + NS} \cdot \frac{PS}{\mathrm{KP} + PS} \tag{9-3}$$

$$\mu Z = \mu Z_{\max} \cdot \exp\left(-2.3\left|\frac{T - 16.5}{15}\right|\right) \frac{CA - 0.5}{\mathrm{KA} + CA}, \text{ for } CA > 0.5 \tag{9-4}$$

$$RA = RA_{\max} \cdot \exp\left(-2.3\left|\frac{T - 16.5}{15}\right|\right) \tag{9-5}$$

$$RZ = RZ_{\max} \cdot \exp\left(-2.3\left|\frac{T - 16.5}{15}\right|\right) \tag{9-6}$$

$$\mu F = \mu F_{\max} \cdot \exp\left(-2.3\left|\frac{T - 16.5}{15}\right|\right) \frac{CZ}{\mathrm{KZ} + CZ} \tag{9-7}$$

$$\frac{dCA}{dt} = (\mu A - RA - \mathrm{SA} - \mathrm{MA})CA - \frac{\mu Z \cdot CZ}{\mathrm{F}} - \frac{\mathrm{F4} \cdot CA}{365 \cdot \mathrm{V}} \tag{9-8}$$

$$\frac{dCZ}{dt} = (\mu Z - RZ - \mathrm{MZ})CZ - \frac{\mu F \cdot \mathrm{CF}}{\mathrm{F}} - \frac{\mathrm{F4} \cdot CZ}{365 \cdot \mathrm{V}} \tag{9-9}$$

$$\begin{aligned}\frac{dPS}{dt} = {} & \frac{\mathrm{F1} \cdot \mathrm{P1} + \mathrm{F2} \cdot \mathrm{P2} + \mathrm{F3} \cdot \mathrm{P3}}{365 \cdot \mathrm{V}} + \frac{1.2(PI - PS) - 1.7}{1{,}000} \cdot \frac{T + 273}{280} \cdot \frac{\mathrm{S}}{\mathrm{V}} \\ & - \frac{(\mu A - RA)CA}{\mathrm{PP}} + \frac{RZ \cdot CZ}{\mathrm{PP}} - \frac{\mathrm{F4} \cdot PS}{365 \cdot \mathrm{V}} + \mathrm{K4} \cdot DP \cdot \mathrm{K6}^{(T - 20)}\end{aligned} \tag{9-10}$$

$$\begin{aligned}\frac{dDP}{dt} = {} & \frac{\mathrm{MA} \cdot CA}{\mathrm{PP}} + \frac{\mathrm{MZ} \cdot CZ}{\mathrm{PP}} - \mathrm{SA} \cdot DP - \frac{\mathrm{F4} \cdot DP}{365 \cdot V} - \mathrm{K4} \cdot DP \cdot \mathrm{K6}^{(T - 20)} \\ & + \left(\frac{1}{\mathrm{F}} - 1\right)\left(\frac{\mu Z \cdot CZ + \mu F \cdot \mathrm{CF}}{\mathrm{PP}}\right)\end{aligned} \tag{9-11}$$

---

The release of nitrogen from the sediment is described as

$$\frac{4.0\, SN + 0.08}{1{,}000\ \mathrm{LUL}} \exp(0.151 \times T)$$

where *SN* (see Table 9-7) is the nitrogen concentration in the upper layer of the sediment. As seen in Eq. (9-16), all the nitrogen in the sediment is considered exchangeable.

Equations (9-14), (9-15) and (9-16) are valid only under anaerobic conditions, while other submodels must be used when the sediment is aerobic (see Kamp-Nielsen[8]).

Two versions of the model were tested. The equations of Model 1 are shown in Table 9-5, the parameters in Table 9-6, the variables in Table 9-7 and the forcing functions in Table 9-8.

---

$$\begin{aligned}\frac{dNS}{dt} = {} & \frac{\mathrm{F1}\cdot N1 + F2\cdot \mathrm{N2} + F3\cdot \mathrm{N3}}{365\cdot \mathrm{V}} - \frac{F4\cdot NS}{365\cdot \mathrm{V}} - \frac{KD\cdot NS}{365\cdot \mathrm{V}} \\ & - \frac{(\mu A - RA)CA - RZ\cdot CZ}{\mathrm{PN}} + \mathrm{K4}\cdot DN\cdot \mathrm{K6}^{(T-20)} \\ & + \frac{4.0\cdot SN + 0.08}{1{,}000}\cdot\frac{S}{V}\cdot\exp(0.151\cdot T)\end{aligned} \tag{9-12}$$

$$\begin{aligned}\frac{dDN}{dt} = {} & \frac{\mathrm{MA}\cdot CA}{\mathrm{PN}} + \frac{\mathrm{MZ}\cdot CZ}{\mathrm{PN}} - \mathrm{K4}\cdot DN\cdot \mathrm{K6}^{(T-20)} - \frac{\mathrm{F4}\cdot DN}{365\cdot \mathrm{V}} - \mathrm{SA}\cdot DN \\ & + \left(\frac{1}{\mathrm{F}} - 1\right)\left(\frac{\mu Z\cdot CZ + \mu F\cdot \mathrm{CF}}{\mathrm{PN}}\right)\end{aligned} \tag{9-13}$$

$$\frac{dPE}{dt} = \frac{\mathrm{SA}\cdot CA\cdot \mathrm{V}\cdot 10^3}{\mathrm{f}\cdot \mathrm{PP}\cdot \mathrm{LUL}\cdot \mathrm{S}} - \mathrm{K5}\cdot PE\cdot \mathrm{K6}^{(T-20)} + \frac{\mathrm{SA}\cdot DP\cdot \mathrm{V}\cdot 10^3}{\mathrm{f}\cdot \mathrm{LUL}\cdot \mathrm{S}} \tag{9-14}$$

$$\frac{dPI}{dt} = \frac{\mathrm{K5}\cdot PE\cdot \mathrm{K6}^{T-20)}}{1 - \mathrm{DMU}} - \frac{1.2(PI - PS) - 1.7}{\mathrm{LUL}(1 - \mathrm{DMU})}\cdot\frac{T + 273}{280} \tag{9-15}$$

$$\frac{dSN}{dt} = \frac{\mathrm{SA}\cdot CA\cdot \mathrm{V}}{\mathrm{S}\cdot \mathrm{PN}\cdot \mathrm{LUL}} - \frac{4.0\cdot SN + 0.08}{1{,}000\cdot \mathrm{LUL}}\cdot\exp(0.151\cdot T) + \frac{\mathrm{SA}\cdot DN\cdot \mathrm{V}}{\mathrm{LUL}\cdot \mathrm{S}} \tag{9-16}$$

$$\left.\begin{array}{r} I_0 = f(t) \\ T = f(t) \\ NI = f(t) \end{array}\right\} \begin{array}{l} \text{forcing function based} \\ \text{upon actual measurements} \end{array} \qquad \begin{array}{r} (9\text{-}17) \\ (9\text{-}18) \\ (9\text{-}19) \end{array}$$

$$\text{Light} = \frac{\mathrm{S}}{(\alpha + \beta\cdot CA)\mathrm{V}}\cdot\ln\left(\frac{I_0 + \mathrm{KI}}{I_0\cdot\exp((-\alpha - \beta\cdot CA)(\mathrm{V}/\mathrm{S})) + \mathrm{KI}}\right) \tag{9-20}$$

---

Equations (9-3) to (9-7), give the expressions for rates of growth and respiration rates. As seen (Eqs. (9-3), (9-4), and (9-7)) the Michaelis–Menten kinetic is used. However, the rate of growth for zooplankton has a threshold concentration below which feeding is zero, which is in accordance with Steele.[12]

Equations (9-8) to (9-13) are based upon mass balances, e.g., Eq. (9-8) expresses that the change in phytoplankton concentration is equal to rate of growth – respiration – sedimentation – mortality – grazing – outflow. The denitrification (in accordance with the nitrogen balance) is included in Eq. (9-12).

The light function, Eq. (9-20), is in accordance with Schofield and Krutchkoff[13] and Scavia and Park,[14] but includes the inhibition of growth at high light intensities. As seen, the extinction coefficient of the water and the specific extinction of coefficient of phytoplankton is taken into consideration.

**Table 9-6 PARAMETERS**

| Symbol used | Definition | Value | Found by |
|---|---|---|---|
| PP | Phosphorus content in plankton | $\frac{1}{114}$ | Analysis of fraction 1—80 $\mu$ |
| PN | Nitrogen content in phytoplankton | $\frac{7}{114}$ | Analysis of fraction 1—80 $\mu$ |
| $\mu A_{\max}$ | Maximum growth rate of phytoplankton | 2.0/24 h | Calibration |
| KI | Michaelis constant for the light intensity | 400 kcal/m$^2$/24 h | Gargas[10] |
| KC | Michaelis constant for the carbon uptake | 0.5 mg/l | Chen and Orlob[11] |
| KN | Michaelis constant for the nitrogen uptake | 0.2 mg/l | Chen and Orlob[11] |
| KP | Michaelis constant for the phosphorus uptake | 0.03 mg/l | Chen and Orlob[11] |
| $RA_{\max}$ | Respiration rate of phytoplankton (maximum) | 0.6/24 h | Calibration |
| $RZ_{\max}$ | Respiration rate of zooplankton (maximum) | 0.02/24 h | Calibration |
| MA | Mortality of phytoplankton | 0.015/24 h | Calibration |
| SA | Settling rate | 0.04/24 h | Pb and Zn analysis of sediment (Jørgensen et al.)[5] |
| KA | Michaelis constant for the feeding rate of zooplankton | 0.5 mg/l | Chen and Orlob[11] |
| KZ | Michaelis constant for feeding rate of fish | 0.1 mg/l | Calibration |
| $\mu F_{\max}$ | Maximum growth rate of fish | 0.015/24 h | Calibration |
| $\mu Z_{\max}$ | Maximum growth rate of zooplankton | 0.175/24 h | Calibration |
| MZ | Mortality of zooplankton | 0.125/24 h | Calibration |
| S | Surface area of the lake | 270,000 m$^2$ | Geographic data |
| V | Volume of the lake | 420,000 m$^3$ | Geographic data |
| K4 | Biodegradation rate of detritus | 0.1/24 h | Calibration |
| F | Conversion factor phytoplankton–zooplankton biomass | 0.63 | Chen and Orlob[11] |
| f | Ratio total phosphorus/exchangeable phosphorus in sediment | $\frac{29}{12}$ | Analysis of sediment (see Jørgensen et al.)[5] |
| LUL | Upper unstabilized layer | 100 mm | Analysis of sediment (see Jørgensen et al.)[5] |
| K5 | Biodegradation rate of organic phosphorus in sediment | 0.0018/24 h | On basis of submodel (see Jørgensen et al.)[5] |
| K6 | Temperature coefficient for biodegradation | 1.02 | Chen and Orlob[11] |
| KD | Constant for denitrification rate | 0.002 | Mass balances |
| DMU | Dry matter of upper layer in sediment | 0.925 kg/kg | Analytical determination |
| $\alpha$ | Extinction coefficient of water | 0.27/m | Chen and Orlob[11] |
| $\beta$ | Specific extinction coefficient of phytoplankton | 0.18 m$^2$/g | Chen and Orlob[11] |
| CF | Concentration of fish | 0.3 mg/l | Calibration |
| F1 | Flow rate of streams going to the lake | 530,000 m$^3$/year | Measurements |
| F2 | Flow rate of waste water | 270,000 m$^3$/year | Measurements |
| F3 | Precipitation | 170,000 m$^3$/year | Measurements |

| | | | |
|---|---|---|---|
| P1 | Phosphorus in streams going to the lake | 0.019 mg/l | Measurements |
| P2 | Phosphorus in waste water | 4.5 mg/l | Measurements |
| P3 | Phosphorus in rainwater | 0.0015 mg/l | |
| F4 | Flow rate of streams going from the lake | 800,000 $m^3$/year | Measurements |
| N2 | Nitrogen in waste water | 24 mg/l | Measurements |
| N3 | Nitrogen in rainwater | 0.36 mg/l | Measurements |

Table 9-7 **VARIABLES**

| Symbol | Definition | Unit |
|---|---|---|
| *P4* | Total phosphorus in lake water | mg/l |
| *PS* | Soluble phosphorus in lake water | mg/l |
| *DP* | Detritus phosphorus in lake water | mg/l |
| *CA* | Phytoplankton concentration | mg/l |
| *CZ* | Zooplankton concentration | mg/l |
| *NS* | Soluble nitrogen in lake water | mg/l |
| $\mu A$ | Growth rate of phytoplankton | $(24\ h)^{-1}$ |
| $\mu Z$ | Growth rate of zooplankton | $(24\ h)^{-1}$ |
| *RA* | Respiration rate of phytoplankton | $(24\ h)^{-1}$ |
| *RZ* | Respiration rate of zooplankton | $(24\ h)^{-1}$ |
| $\mu F$ | Growth rate of fish | $(24\ h)^{-1}$ |
| *PI* | Phosphorus of interstitial water in sediment | mg/l |
| *PE* | Exchangeable phosphorus in upper layer of sediment | mg/l |
| *DN* | Detritus nitrogen in lake water | mg/l |
| *N4* | Total nitrogen in lake water | mg/l |
| *I* | Light intensity | kcal/$m^2$ 24 h |
| *SN* | Nitrogen in upper layer of sediment | g/l |
| *C* | Inorganic C in water, fixed value 100 mg/l is used | mg/l |

Table 9-8 **FORCING FUNCTIONS**

| Symbol | Definition | Unit | Found by |
|---|---|---|---|
| $I_0$ | Light intensity at the lake surface | kcal/$m^2$ 24 h | Measurements |
| *T* | Temperature | °C | Measurements |
| *N1* | Nitrogen in streams | mg/l | Measurements |

Model 2 uses an entirely different algae kinetic (see Table 9-9). The growth of phytoplankton is considered as a two step process:

*1 Uptake of nutrient*. The photosynthetic uptake of carbon is given in Eq. (9-23). As seen, the light function from Model 1 is applied, but the uptake rate is limited by the intracellular concentration of carbon CC as well as by the hydrogen-carbonate concentration in the lake water *C*. The respiration is deducted from the uptake. The uptake of phosphorus and nitrogen, Eqs.

(9-28) and (9-29), are limited in a similar way by the intracellular phosphorus and nitrogen and a Michaelis–Menten equation taking the concentration of soluble nutrient in the lake water into consideration.

2 *Bio-mass growth.* Equation (9-30) Table 9-9, relates the growth rate to the intracellular nutrient concentration, determined by means of Eqs. (9-40) to (9-42).

The other equations of Model 2 are similar to those of Model 1. However, in the phosphorus and nitrogen balances the zooplankton has the same composition as phytoplankton, which is a reasonably good approach.

**Table 9-9** MODEL 2

$$P4 = PS + DP + \frac{PC \cdot CZ}{CA} + PC \tag{9-21}$$

$$N4 = NS + DN + \frac{NC \cdot CZ}{CA} + NC \tag{9-22}$$

$$UC = \frac{\mathrm{S}}{(\alpha + \beta \cdot CA) \cdot \mathrm{V}} \cdot \ln\left(\frac{I_0 + \mathrm{KI}}{I_0 \cdot \exp((-\alpha - \beta \cdot CA)(\mathrm{V/S})) + \mathrm{KI}}\right) \cdot \frac{CC_{\max} \cdot CA - CC}{CC_{\max} \cdot CA - CC_{\min} \cdot CA} \cdot UC_{\max} \cdot CA \cdot \frac{C}{KC + C} - RA \tag{9-23}$$

$$\mu Z = \mu Z_{\max} \cdot \exp\left(-2.3\left|\frac{T - 16.5}{15}\right|\right) \cdot \frac{CA - 0.5}{\mathrm{KA} + CA}, \text{ for } CA > 0.5 \tag{9-24}$$

$$RA = RA_{\max} \cdot CA\left(\frac{CC}{CC_{\max} \cdot CA}\right)^{0.67} \cdot \exp\left(-2.3\left|\frac{T - 16.5}{15}\right|\right) \tag{9-25}$$

$$\mu F = \mu F_{\max} \cdot \exp\left(-2.3\left|\frac{T - 16.5}{15}\right|\right) \frac{CZ}{CZ + \mathrm{KZ}} \tag{9-26}$$

$$RZ = RZ_{\max} \cdot \exp\left(-2.3\left|\frac{T - 16.5}{15}\right|\right) \tag{9-27}$$

$$UP = UP_{\max} \cdot \frac{PC_{\max} \cdot CA - PC}{PC_{\max} \cdot CA - PC_{\min} \cdot CA} \cdot \frac{CA \cdot PS}{PS + \mathrm{KP}} \tag{9-28}$$

$$UN = UN_{\max} \cdot \frac{NC_{\max} \cdot CA - NC}{NC_{\max} \cdot CA - NC_{\min} \cdot CA} \cdot \frac{CA \cdot NS}{NS + \mathrm{KN}} \tag{9-29}$$

$$GRW = GRW_{\max} \cdot \exp\left(-2.3\left|\frac{T - 16.5}{15}\right|\right) \frac{NC - NC_{\min} \cdot CA}{NC} \cdot \frac{PC - PC_{\min} \cdot CA}{PC} \cdot \frac{CC - CC_{\min} \cdot CA}{CC} \tag{9-30}$$

$$\frac{dCA}{dt} = \frac{\mathrm{F4} \cdot CA}{365 \cdot \mathrm{V}} + (GRW \cdot 0.7 - \mathrm{MA} - \mathrm{SA})CA - \mu Z \cdot \frac{CZ}{\mathrm{F}} \tag{9-31}$$

$$\frac{dCZ}{dt} = \frac{\mathrm{F4} \cdot CZ}{365 \cdot \mathrm{V}} + (\mu \mathrm{Z} - RZ - \mathrm{MZ})CZ - \mu F \cdot \frac{\mathrm{CF}}{\mathrm{F}} \tag{9-32}$$

Model 2 involves the introduction of several new parameters (see Table 9-10), and 3 new state variables (see Table 9-11). The advantages of Model 2 compared with Model 1 can be summarized as follows:

*1* The two step kinetic used is in accordance with physiological observations, see Nyholm.[18]

*2* The respiration rate is dependent upon the carbon concentration of the cells, which is also in accordance with physiological observations (Lehman et al.[16]).

*3* The parameters $PC_{\max}$, $PC_{\min}$, $NC_{\max}$, $NC_{\min}$, $CC_{\max}$ and $CC_{\min}$ are in accordance with the actual compositions of phytoplankton.

---

$$\frac{dPS}{dt} = \frac{\mathrm{F1}\cdot\mathrm{P1} + \mathrm{F2}\cdot\mathrm{P2} + \mathrm{F3}\cdot\mathrm{P3} - \mathrm{F4}\cdot PS}{365\cdot\mathrm{V}} UP + \frac{RZ\cdot PC\cdot CZ}{CA} + \mathrm{K4}\cdot DP\cdot\mathrm{K6}^{(T-20)} + \frac{1.2(PI - PS) - 1.7}{1{,}000}\cdot\frac{T + 273}{280}\cdot\frac{\mathrm{S}}{\mathrm{V}} \tag{9-33}$$

$$\frac{dDP}{dt} = \mathrm{MA}\cdot PC + \mathrm{MZ}\cdot CZ(PC/CA) - \mathrm{K4}\cdot DP\cdot\mathrm{K6}^{(T-20)} - \frac{\mathrm{F4}\cdot DP}{365\cdot\mathrm{V}} + \left(\frac{1}{\mathrm{F}} - 1\right)\cdot\mu Z\cdot CZ(PC/CA) - SA\cdot DP + \left(\frac{1}{\mathrm{F}} - 1\right)\cdot\mu F\cdot\mathrm{CF}(PC/CA) \tag{9-34}$$

$$\frac{dNS}{dt} = \frac{\mathrm{F1}\cdot N1 + \mathrm{F2}\cdot N2 + \mathrm{F3}\cdot N3 - \mathrm{F4}\cdot NS}{365\cdot\mathrm{V}} - \frac{\mathrm{KD}\cdot NS}{365\cdot\mathrm{V}} - UN + \frac{RZ\cdot CZ\cdot NC}{CA} + \mathrm{K4}\cdot DN\cdot\mathrm{K6}^{(T-20)} + \frac{4.0\cdot SN + 0.08}{1{,}000}\cdot\frac{\mathrm{S}}{\mathrm{V}}\cdot\exp(0.151\cdot T) \tag{9-35}$$

$$\frac{dDN}{dt} = \mathrm{MA}\cdot NC + \mathrm{MZ}\cdot CZ(NC/CA) - \mathrm{K4}\cdot DN\cdot\mathrm{K6}^{(T-20)} - \frac{\mathrm{F4}\cdot DN}{365\cdot\mathrm{V}} + \left(\frac{1}{\mathrm{F}} - 1\right)\mu Z\cdot CZ(NC/CA) + \left(\frac{1}{\mathrm{F}} - 1\right)\mu F\cdot\mathrm{CF}(NC/CA) - \mathrm{SA}\cdot DN \tag{9-36}$$

$$\frac{dPE}{dt} = \frac{\mathrm{SA}(PC + DP)\mathrm{V}\cdot 10^3}{\mathrm{f}\cdot\mathrm{LUL}\cdot\mathrm{S}} - \mathrm{K5}\cdot PE\cdot\mathrm{K6}^{(T-20)} \tag{9-37}$$

$$\frac{dPI}{dt} = \frac{\mathrm{K5}\cdot PE\cdot\mathrm{K6}^{(T-20)}}{1 - \mathrm{DMU}} - \frac{1.2(PI - PS) - 1.7}{\mathrm{LUL}(1 - \mathrm{DMU})}\cdot\frac{T + 273}{280} \tag{9-38}$$

$$\frac{dSN}{dt} = \frac{\mathrm{SA}(NC + DN)}{\mathrm{LUL}}\cdot\frac{\mathrm{V}}{\mathrm{S}} - \frac{4.0\cdot SN + 0.08}{1{,}000\cdot\mathrm{LUL}}\cdot\exp(0.151\cdot T) \tag{9-39}$$

$$\frac{dPC}{dt} = UP - \mathrm{MA}\cdot PC - \mathrm{SA}\cdot PC - \mu Z\cdot\frac{CZ\cdot PC}{\mathrm{F}\cdot CA} - \frac{\mathrm{F4}\cdot PC}{365\cdot\mathrm{V}} \tag{9-40}$$

$$\frac{dNC}{dt} = UN - \mathrm{MA}\cdot NC - \mathrm{SA}\cdot NC - \mu Z\cdot\frac{CZ\cdot NC}{\mathrm{F}\cdot CA} - \frac{\mathrm{F4}\cdot NC}{365\cdot\mathrm{V}} \tag{9-41}$$

$$\frac{dCC}{dt} = UC - \mathrm{MA}\cdot CC - \mathrm{SA}\cdot CC - \mu Z\cdot\frac{CZ\cdot CC}{\mathrm{F}\cdot CA} - \frac{\mathrm{F4}\cdot CC}{365\cdot\mathrm{V}} \tag{9-42}$$

**Table 9-10 PARAMETERS**

| Symbol used | Definition | Value | Found by |
|---|---|---|---|
| $CC_{\max}$ | Maximum kg C per kg of phytoplankton biomass | 0.6 | Estimated values on basis of Stumm and Morgan,[15] Steele,[12] analysis of fractions $1-80\ \mu$, the values for single cells given by Lehmann et al.[16] related to size of the cells given by Nygaard[17] |
| $CC_{\min}$ | Minimum kg C per kg of phytoplankton biomass | 0.18 | |
| $PC_{\max}$ | Maximum kg P per kg of phytoplankton biomass | 0.03 | |
| $PC_{\min}$ | Minimum kg P per kg of phytoplankton biomass | 0.003 | |
| $NC_{\max}$ | Maximum kg N per kg of phytoplankton biomass | 0.08 | |
| $NC_{\min}$ | Minimum kg N per kg of phytoplankton biomass | 0.02 | |
| $UP_{\max}$ | Increase of kg P per kg phytoplankton biomass per 24 h | 0.0035/24 h | Calibration. The ratio $UP:UN:UC$ is in accordance with Lehmann et al. (1975) |
| $UN_{\max}$ | Increase of kg N per kg phytoplankton biomass per 24 h | 0.0096/24 h | |
| $UC_{\max}$ | Increase of kg C per kg phytoplankton biomass per 24 h | 0.45/24 h | |
| $RA_{\max}$ | Respiration of kg C per kg phytoplankton biomass per 24 h | 0.286/24 h | Lehmann et al.[16] and Nygaard[17] |
| $GRW_{\max}$ | Cell division rate per 24 h | 3/24 h | Lehmann et al.[16] |

All other parameters see Table 9-6

**Table 9-11 VARIABLES**

| Symbols | Definition | Unit |
|---|---|---|
| $PC$ | P in phytoplankton | mg/l |
| $NC$ | N in phytoplankton | mg/l |
| $CC$ | C in phytoplankton | mg/l |
| $C$ | Inorganic C in water, fixed value 100 mg/l is used | mg/l |

## 9-5 CALIBRATION AND RESULTS

Both models were calibrated to measured data of the state variables obtained 1 April 1972–15 October 1974. The calibration was carried out on the basis of a sensitivity analysis (see Table 9-12). The parameters found by the calibration of both models are given in Table 9-6. All the calibrated parameters were limited by the intervals given in the literature.

A comparison of the more important state variable, obtained with the calibrated models and the measured values are shown in Figs. 9-10 to 9-15.

The productivity is measured by means of the $C^{14}$ method (see Steemann Nielsen).[19,20] Since approximately 30 percent of phytoplankton (dry matter) is carbon (see e.g., Stumm and Morgan),[15] and the average depth is 1.8 m, the production expressed as g C $m^{-2}$/2 h is found on the basis of Model 1 as $A \times CA \times Q36 \times 1.8$ and on the basis of Model 2 as $CC \times 0.7GRW \times 1.8$.

Table 9-12 SENSITIVITY ANALYSIS

| PARAM | $S_{PHYT}$ | $S_{ZOO}$ | $S_{NS}$ | $S_{PS}$ | $\Delta t_{PHYT}$ | $\Delta t_{ZOO}$ | $\Delta t_{NS}$ | $\Delta t_{PS}$ |
|---|---|---|---|---|---|---|---|---|
| CDRMAX | 0.488 | 0.620 | −0.356 | −0.392 | −0.31 | −0.11 | −0.23 | 0.0 |
| DENIT | −0.019 | −0.010 | −0.579 | 0.013 | 0.05 | 0.0 | −0.70 | 0.0 |
| FISH | 0.008 | 0.012 | −0.011 | −0.014 | 0.0 | 0.10 | 0.0 | 0.0 |
| ICPHYT | −0.020 | −0.044 | 0.032 | 0.033 | −0.05 | −0.35 | −0.15 | 0.0 |
| ICZOO | −0.169 | −0.223 | 0.252 | 0.282 | 0.0 | −1.58 | −0.34 | 0.0 |
| KA | 0.166 | 0.275 | −0.253 | −0.288 | −0.05 | −0.35 | 0.41 | 0.0 |
| KDN10 | 0.003 | 0.010 | 0.038 | 0.001 | 0.45 | 0.0 | −0.30 | 0.0 |
| KDP10 | 0.0 | 0.001 | 0.0 | 0.006 | 0.0 | 0.0 | 0.0 | 0.0 |
| KE20 | 0.039 | 0.051 | −0.021 | 0.503 | 0.40 | 0.05 | −0.15 | 0.0 |
| KN | −0.011 | −0.032 | 0.063 | 0.019 | 0.45 | −0.05 | −0.15 | 0.0 |
| KP | −0.003 | −0.014 | 0.021 | 0.034 | 0.05 | −0.05 | −0.25 | 0.0 |
| KREL | 0.143 | 0.191 | 0.699 | −0.055 | 0.45 | 0.10 | −0.40 | 0.0 |
| KS | −0.016 | −0.021 | 0.031 | 0.031 | 0.0 | −0.15 | −0.25 | 0.0 |
| MYZMAX | −2.088 | −4.002 | 2.749 | 4.052 | −1.50 | −25.95 | −17.90 | 0.0 |
| MZ | 2.063 | 1.949 | −3.479 | −3.350 | 1.30 | 21.50 | 8.40 | 0.0 |
| PHI | 0.060 | 0.132 | −0.114 | −0.039 | −0.45 | 0.15 | −0.35 | 0.0 |
| PREDMX | 0.008 | 0.011 | −0.015 | −0.016 | 0.0 | 0.10 | −0.30 | 0.0 |
| RCMAX | −0.243 | −0.201 | 0.139 | 0.153 | 0.45 | 0.05 | −0.35 | 0.0 |
| RZMAX | 0.570 | 0.625 | −0.902 | −0.978 | 0.95 | 5.94 | 1.34 | 0.0 |
| SVD | 0.0 | 0.0 | −0.002 | 0.0 | 0.0 | 0.0 | 0.0 | 0.0 |
| SVS | −1.042 | −0.823 | 0.321 | 0.388 | −0.05 | 0.20 | 0.15 | 0.0 |
| THETA | 5.161 | −1.154 | −0.988 | −0.164 | −24.04 | −6.62 | −15.31 | 0.0 |
| UCMAX | 0.629 | 0.636 | −0.428 | −0.481 | 0.05 | 0.10 | −0.25 | 0.0 |
| UNMAX | 0.046 | 0.145 | −0.251 | −0.050 | 0.05 | −0.05 | −0.15 | 0.0 |
| UPMAX | 0.026 | 0.090 | −0.049 | −0.339 | 0.50 | 0.05 | −0.15 | 0.0 |

The phytoplankton concentration was determined in 1972–1973 by counting the number of cells, multiplied by the average biomass of one cell (taken from Nygaard).[17] In 1973–1974 the phytoplankton concentration was determined by means of the chlorophyll concentration, since chlorophyll is 1/136 of the total biomass in accordance with Patten et al.[21]

Table 9-13 gives the maximum production (g C $m^{-2}$/24 h) found by means of the models for each month, and the corresponding values measured, averaged over the 3 years from 1972–1974.

Table 9-13 MAX g C/$m^2$/24 h

| Month | Model I | Model II | Measured average |
|---|---|---|---|
| April | 13 | 2.4 | 5.0 |
| May | 3.5 | 12.0 | 11.2 |
| June | 3.0 | 5.0 | 5.0 |
| July | 3.4 | 4.8 | 3.3 |
| August* | 5.0 | 5.7 | 6.9 |
| September* | 5.0 | 3.2 | 5.0 |
| October | 0.5 | 1.6 | 2.2 |
| November | 0.5 | 0.8 | 1.5 |
| December | 0.1 | 0.4 | 1.2 |
| January | 0.1 | 0.3 | 0.4 |
| February | 0.3 | 0.4 | 1.3 |
| March | 2.5 | 2.8 | 2.7 |

* September 1st included.

The transparency $V$, found by means of the model and the relation between $V$ and max g C m$^{-3}$/24 h, published by Mathiesen,[22] was compared with the transparency measured (see Table 9-14). The total yearly production found from the model and the measured values 1973–1974 and 1974–1975 are shown in Table 9-15.

On the basis of these results, it is possible to conclude that both models give a reasonably good description of the eutrophication process. However, Model 2 must be preferred, as

*1* The maximum production and maximum phytoplankton concentration is more in accordance with the measured values for Model 1 (see Figs. 9-10 to 9-15).

*2* It gives a yearly production closer to the measured values than Model 2 (see Table 9-15).

*3* The model is in accordance with physiological observations (see above).

Table 9-14 TRANSPARENCY (M)

| Month | Model I | Model II | Measured average |
|---|---|---|---|
| April | 0.20 | 0.50 | 0.35 |
| May | 0.45 | 0.20 | 0.20 |
| June | 0.50 | 0.30 | 0.26 |
| July | 0.45 | 0.32 | 0.31 |
| August | 0.30 | 0.28 | 0.22 |
| September | 0.30 | 0.48 | 0.25 |

Table 9-15 PRODUCTION VALUES

| | | Production values g C m$^{-2}$ y$^{-1}$ |
|---|---|---|
| Model I | | 850 |
| Model II | | 1,050 |
| Measured | 1973/1974 | 1,150 |
| | 1974/1975 | 1,050 |
| | 1973/1975 | 1,100 |

## 9-6 VALIDATION

It is of great importance to validate every model against independently measured values. Therefore, another set of measurements were carried out from 15 October 1974 to 15 October 1975. No general method of validation is available, but almost the same method suggested by WMO[23] for validation of hydrological models has been applied.

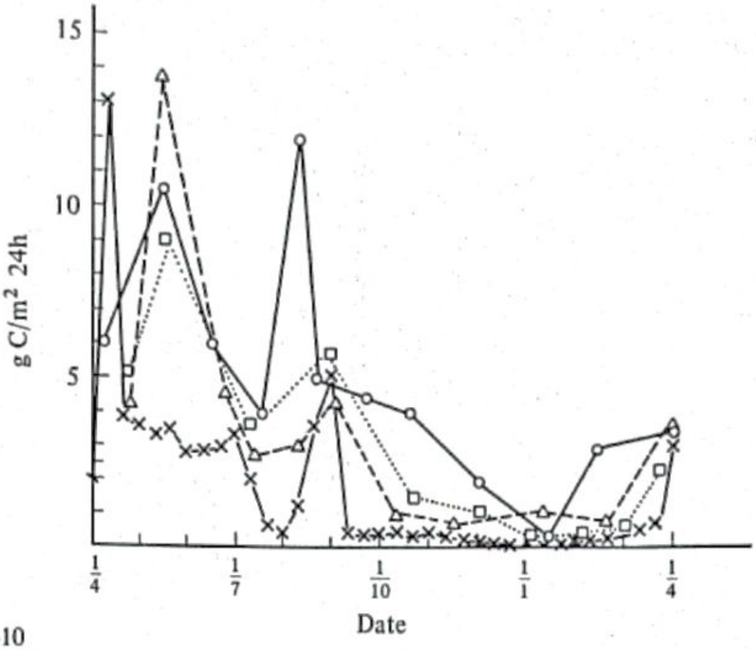

FIGURE 9-10
Production g C/m² 24 h found by means of model 1 (x) compared with the measured data ○ 1971–1973, △ 1973–1974 and □ 1974–1975.

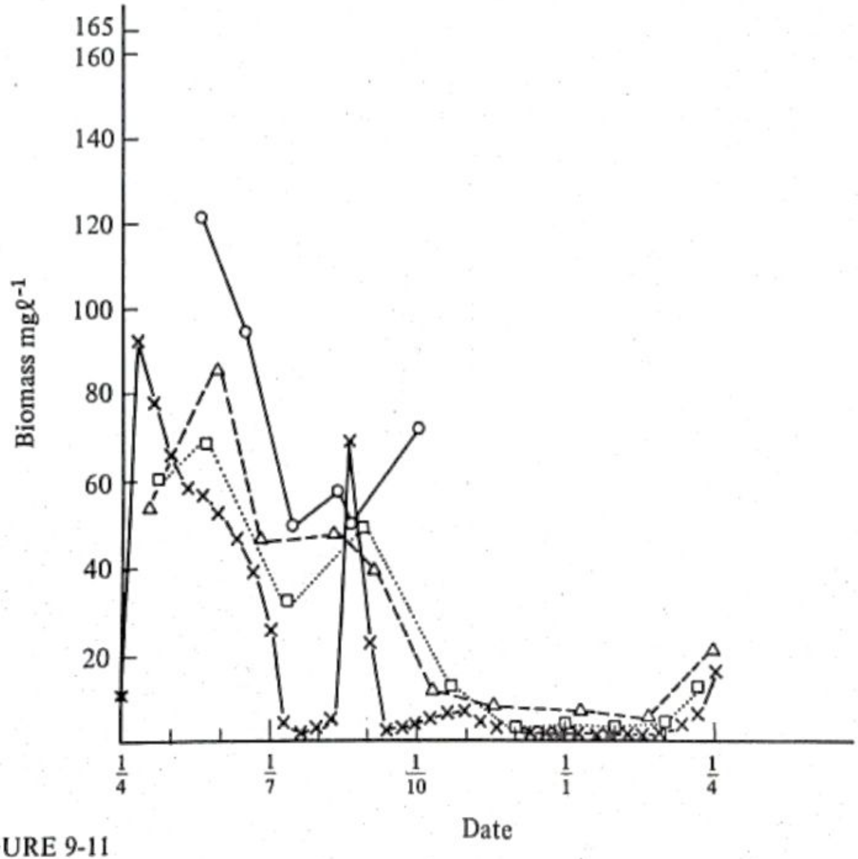

FIGURE 9-11
Biomass (phytoplankton) mg/l found by means of model 1 (x) compared with the measured data ○ 1972–1973 (counting number of cells), △ 1973–1974 (chlorophyll concentration) □ 1974–1975 (chlorophyll concentration).

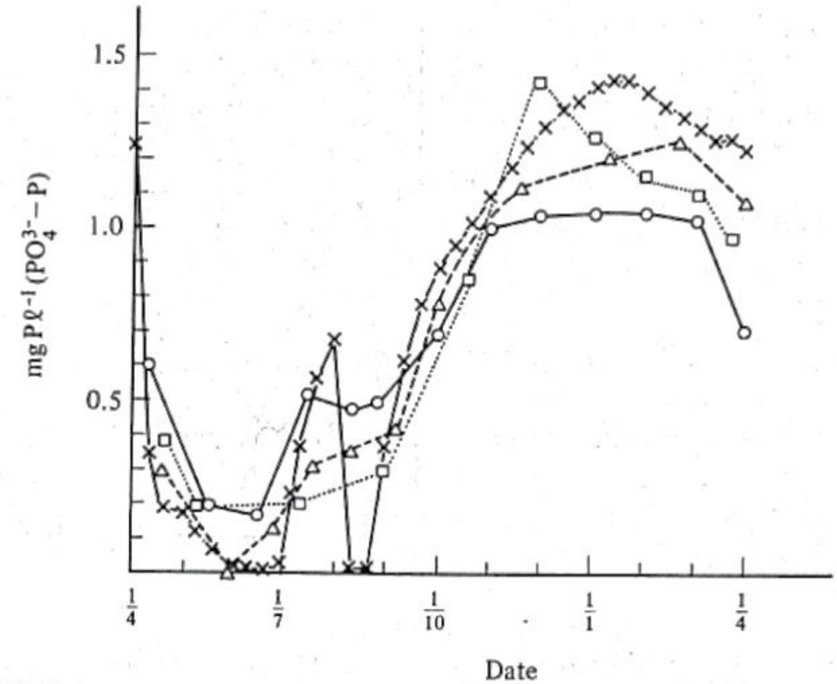

FIGURE 9-12
Soluble phosphorus mg/l found by means of model 1 (x) compared with measured data ○ 1972–1973, △ 1973–1974 and □ 1974–1975.

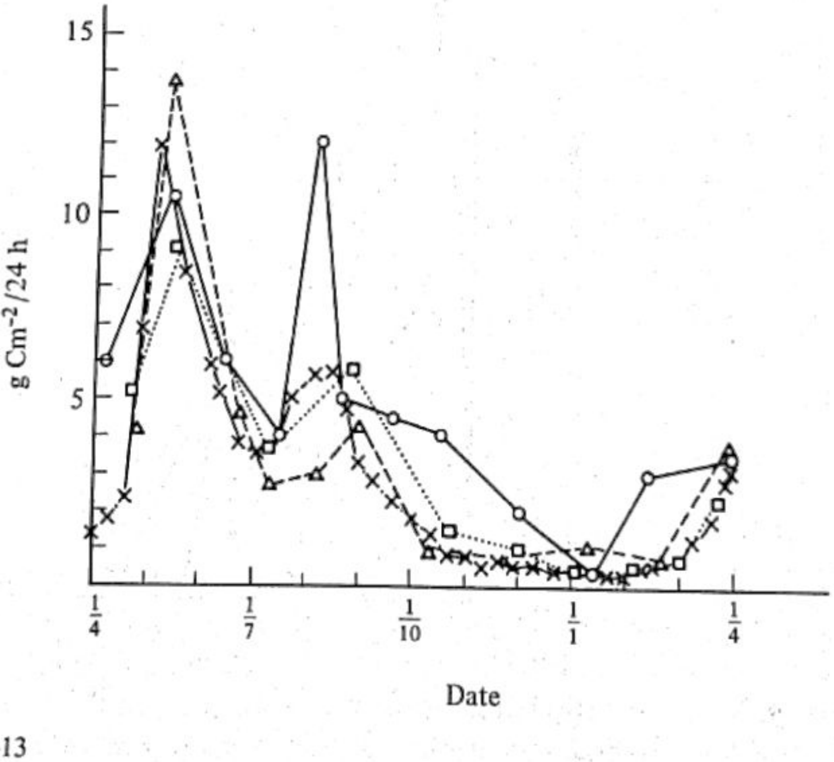

FIGURE 9-13
The production of g C/$m^2$ 24 h found by means of model 2 (x) compared with the measured data ○ 1972–1973, △ 1973–1974 and □ 1974–1975.

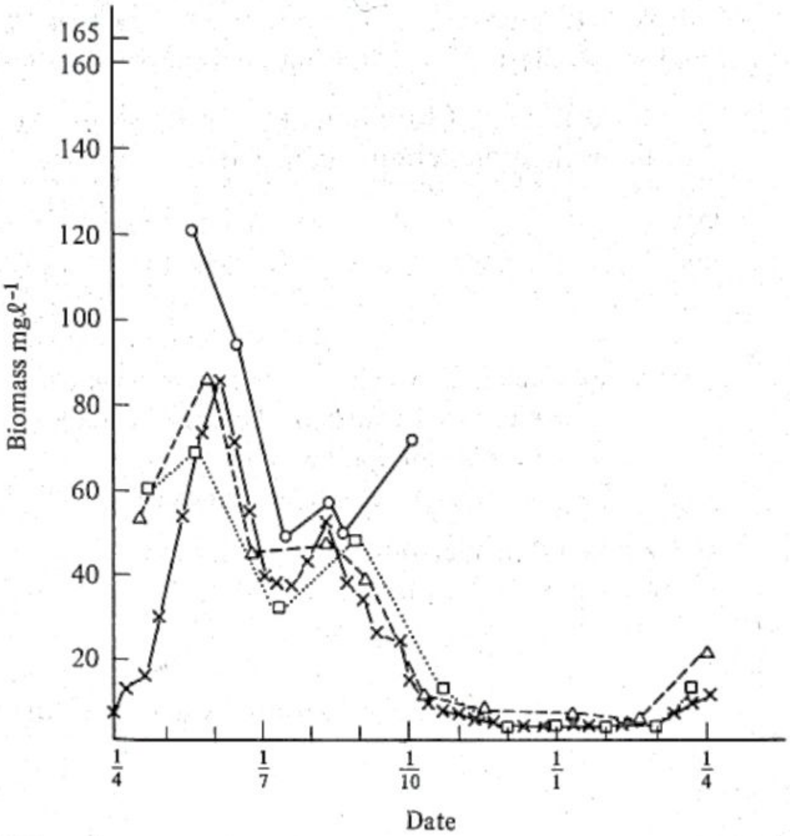

FIGURE 9-14
Biomass (phytoplankton) mg/l found by means of model 2 (x) compared with the measured data ○ 1972–1973 (counting number of cells), △ 1973–1974 (chlorophyll concentration) □ 1974–1975 (chlorophyll concentration).

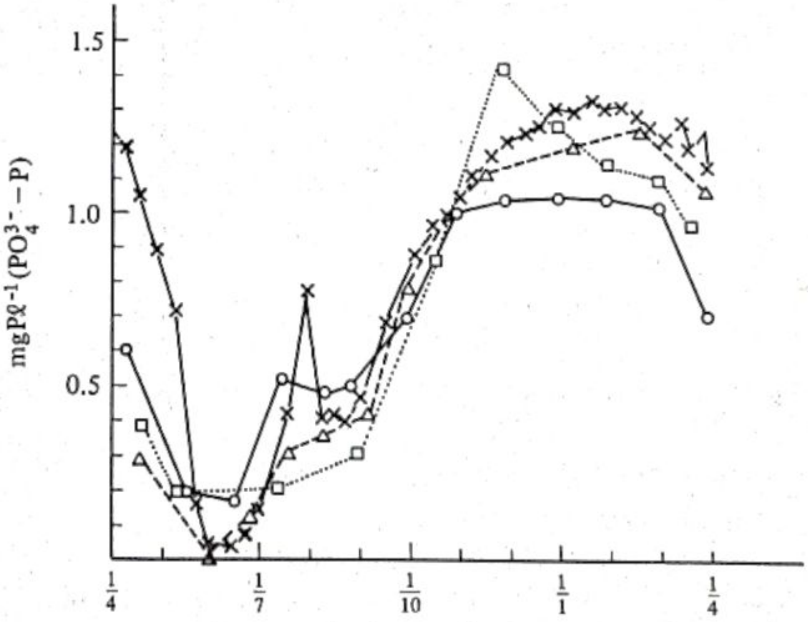

FIGURE 9-15
Soluble phosphorus mg/l found by means of model 2 (x) compared with measured data ○ 1972–1973, △ 1973–1974 and □ 1974–1975.

Table 9-16 gives the results of the validation of Model 2, which has been preferred to Model 1. The following numerical validation criteria are applied.

*1* $Y$, coefficient of variation of the residuals of errors for the state variables for the validation period, defined as

$$Y = \frac{\dfrac{[\sum (y_c - y_m)^2]^{1/2}}{n}}{\bar{y}_m}$$

where $y_c$ = calculated values of the state variables
$y_m$ = measured values of the state variables
$n$ = number of comparisons
$\bar{y}_m$ = average of measured values over the validation period

*2* $R$, the relative error of mean values:

$$R = \frac{\bar{y}_c - \bar{y}_m}{\bar{y}_m}$$

where $\bar{y}_c$ is the average of measured values over the validation period

**Table 9-16** NUMERICAL VALIDATION OF THE MODEL

| Coefficient | State variable | Value |
|---|---|---|
| $Y$ | all | 0.51 |
| $R$ | $P_{total}$ ($P4$) | 0.28 |
| $R$ | $P_{soluble}$ ($PS$) | 0.16 |
| $R$ | $N_{total}$ ($N4$) | 0.02 |
| $R$ | $N_{soluble}$ ($NS$) | 0.14 |
| $R$ | Phytopl. ($CA$) | 0.35 |
| $R$ | Zooplankton ($Z$) | 0.30 |
| $R$ | Production | 0.03 |
| $A$ | $P_{total}$ ($P4$) | 0.12 |
| $A$ | $P_{soluble}$ ($PS$) | 0.18 |
| $A$ | $N_{total}$ ($N4$) | 0.07 |
| $A$ | $N_{soluble}$ ($NS$) | 0.03 |
| $A$ | Phytopl. ($CA$) | 0.40 |
| $A$ | Zooplankton ($Z$) | 0.00 |
| $A$ | Production | 0.08 |
| TE | $P_{total}$ ($P4$) | 105 days |
| TE | $P_{soluble}$ ($PS$) | 60 days |
| TE | $N_{total}$ ($N4$) | 15 days |
| TE | $N_{soluble}$ ($NS$) | 15 days |
| TE | Phytopl. ($CA$) | 0 days*<br>120 days† |
| TE | Zooplankton($Z$) | 60 days |
| TE | Production | 0 days*<br>−30 days† |

* based upon measuring susp. matter.
† based upon chlorophyll.

*3* $A$, relative error of maximum values:

$$A = \frac{y_{c,\max} - y_{m,\max}}{y_{m,\max}}$$

where $y_{c,\max}$ = maximum value of the calculated state variable in the validation period

$y_{m,\max}$ = maximum value of the measured state variable in the validation period.

*4* TE, timing error:

$$\text{TE} = \text{Date of } y_{c,\max} - \text{date of } y_{m,\max}$$

Since no method of validation of ecological models is generally applied, it is not possible to compare this validation with other case studies, but a comparison with, for example, hydraulic models indicates that the validation is reasonably good. However, the validation can also be considered as a method to state the accuracy of the model.

## 9-7 PROGNOSIS

Prognosis for different removal efficiencies for phosphorus, nitrogen and phosphorus, and nitrogen simultaneously have been studied. It has been stated, that removal of nitrogen has only little or no effect, while removal of phosphorus has shown to give substantial reduction in the phytoplankton concentration.

The results of two case studies are summarized in Fig. (9-16) and Table 9-17:

**Case A** The treated waste water has a concentration of 0.4 mg/$l^{-1}$, corresponding to about 92 percent removal efficiency, which should be achieved by chemical precipitation.

**Case B** The treated waste water has a concentration of 0.1 mg/$l^{-1}$, corresponding to about 98 percent removal efficiency, which will require chemical precipitation in combination with, for example, ion exchange.

It has been calculated that solution A will mean increased total costs of 4 cents/$m^3$, and solution B of 7 cents/$m^3$.

As seen in Table 9-17, the two models give different results, although the difference is relatively smaller in case B than in case A. The prognosis of Model 2 has been used for decision making, since Model 2 is preferred (see above).

Table 9-17 also includes the prognosis in case the more simple first order reaction submodel for the mud–water exchange is used. As expected the improvement of the water quality is substantially less in this case, but this model has already been rejected in accordance to a previous discussion (see above).

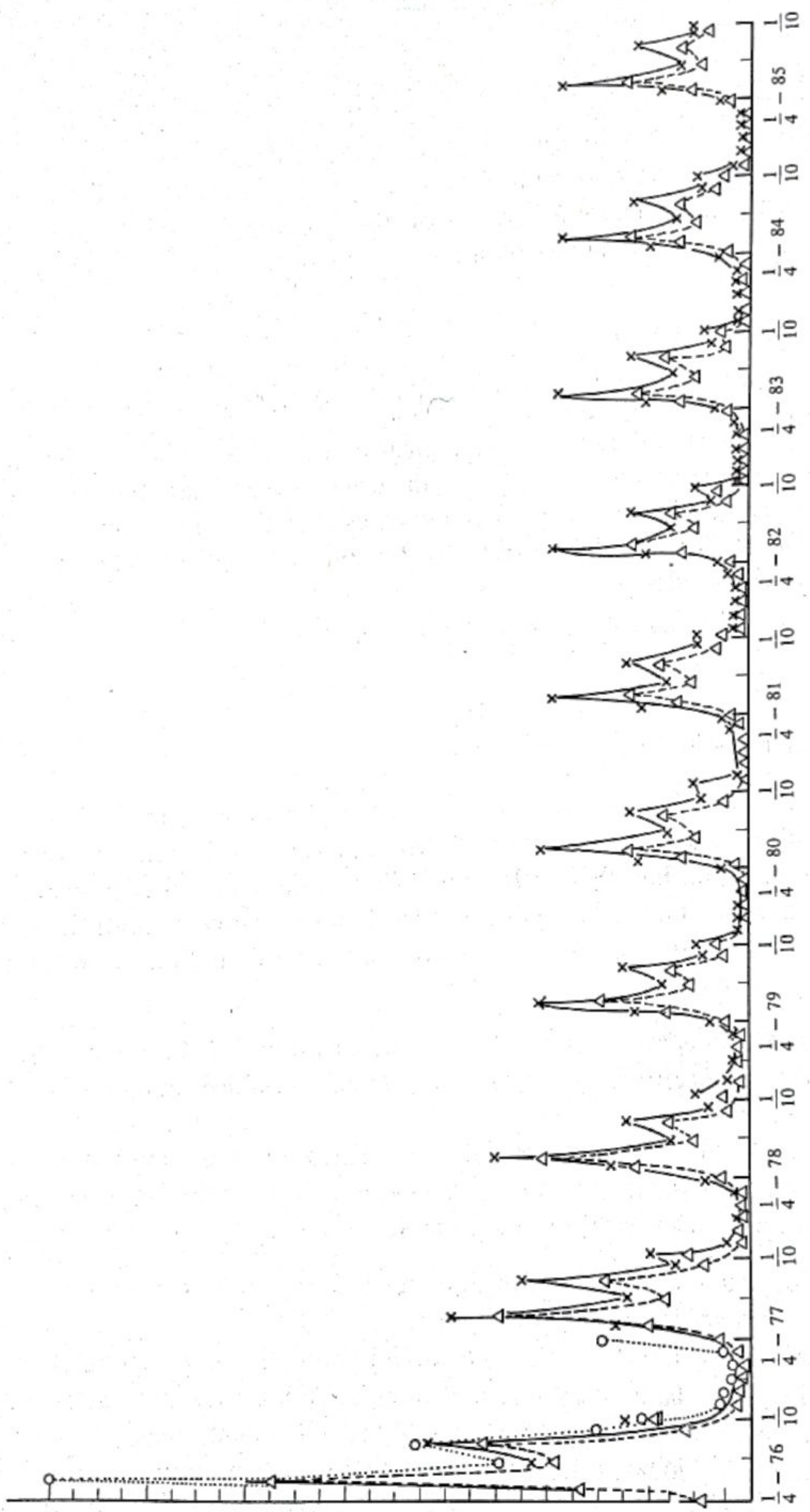

FIGURE 9-16
Productivity g C/m² 24 h in case (a) phosphorus is not removed from the waste water ○, (b) waste water with 0.4 mg P/l is discharged (x), (c) waste water 0.1 mg P/l is discharged △. All data based upon model 2.

Table 9-17 PREDICTIONS BY MEANS OF THE MODELS IN TWO CASES: CONCENTRATION OF TREATED WASTE WATER: A: 0.4 mg P/l; B: 0.1 mg P/l

| Model I: | 3rd year | | After 9th year | |
|---|---|---|---|---|
| | Case A | Case B | Case A | Case B |
| g C/m$^2$/year | 340 | 300 | 280 | 240 |
| Minimum transparency (cm) | 70 | 80 | 90 | 100 |
| Model II: | | | | |
| g C/m$^2$/year | 650 | 500 | 500 | 320 |
| Minimum transparency (cm) | 50 | 60 | 60 | 75 |
| First order reaction P-sediment water | | | | |
| g C/m$^2$/year | 850 | 800 | 610 | 480 |
| Minimum transparency (cm) | 30 | 35 | 50 | 60 |

## 9-8 DISCUSSION AND CONCLUSION

A general procedure has been suggested for modeling ecosystems:

*1* A conceptual diagram is set up.

*2* Based upon energy calculation, a limited number of state variables are selected.

*3* Calibration is carried out on the basis of sensitivity analysis.

*4* A validation, applying an independent set of measured values, is accomplished by the use of four coefficients ($Y$, $R$, $A$ and TE; the definitions are given above).

The values of these coefficients give an indication of the accuracy.

Based on this procedure, it has been possible to set up a model (called Model 2), which as shown by the validation phase describes the eutrophication processes with a reasonably good accuracy (see Table 9-16). This model has the following characteristics:

*1* The entire food chain, phytoplankton, zooplankton and fish is included.

*2* The submodel for the mud–water exchange of nutrient is considerably more detailed than the previously used first order reactions.

*3* The phytoplankton growth is described as a two-step process:

  *a* Uptake of nutrient into the cells.

  *b* Biomass growth.

*4* Denitrification is included in accordance with the mass balance.

The selected Model 2 has been used to set up prognoses for alternative treatments. It was found that an effective removal of phosphorus is the right solution to the eutrophication process. Already three years after the improved waste water treatment the transparency will be two to three times greater, depending on whether 92 percent or 98 percent efficiency of phosphorus removal is introduced. Further improvement will be recorded throughout the following years (see Table 9-17 and Fig. 9-16).

## REFERENCES

1. HANSEN, K., "The Geology and Bottom Deposits of Lake Tystrup, Zealand," DGU, Copenhagen, 1950.
2. WESENBERG-LUND, D. C., "De Danske søers og Dammes Dyriske Plankton," Munkgsgaard, Copenhagen, 1952.
3. JØRGENSEN, S. E., O. S. JACOBSEN, and I. HØI, A Prognosis for a Lake, *Vatten*, vol. 29, pp. 382–404, 1973.
4. DANMARKS NATUR., vol. 5, "Limnology," Politikens Forlag, Copenhagen, 1969.
5. JØRGENSEN, S. E., L. KAMP-NIELSEN, and O. S. JACOBSEN, A Submodel for Anaerobic Mud-Water Exchange of Phosphate, *Ecol. Modelling*, vol. 1, pp. 133–146, 1975.
6. JØRGENSEN, S. E., and H. MEYER, Ecological Buffer Capacity, *Ecol. Modelling*, vol. 3, pp. 39–62, 1977.
7. KAMP-NIELSEN, L., Mud-Water exchange of Phosphate and other Ions in Undisturbed Sediment Cores and Factors Affecting the Exchange Rate, *Arch. Hydrobiol.*, vol. 2, pp. 218–237, 1974.
8. KAMP-NIELSEN, L., A Kinetic Approach to the Aerobic Sediment–Water Exchange of Phosphorus in Lake Esrom, *Ecol. Modelling*, vol. 1, pp. 153–160, 1975.
9. JACOBSEN, O. S., and S. E. JØRGENSEN, A Submodel for Nitrogen Release from Sediments, *Ecol. Modelling*, vol. 1, pp. 147–151, 1975.
10. GARGAS, E., "A Manual for Phytoplankton Primary Production Studies in the Baltic," The Baltic Marine Biologists in Cooperation with the Danish Agency of Environmental Protection, 1975.
11. CHEN, C. W., and C. T. ORLOB, Ecologic Simulation for Aquatic Environments, in B. C. Patten (ed.), "Systems Analysis and Simulation in Ecology," vol. III, pp. 476–587, Academic Press, New York, 1975.
12. STEELE, J. H., "The Structure of the Marine Ecosystems," pp. 74–91, Blackwell Scientific, Oxford, 1974.
13. SCHOFIELD, W. R., and R. G. KRUTCHOFF, Bulletin 60 Stochastic Model for a Dynamic Ecosystem, VPI-WRRC-Bull, 60, Virginia Water Resources Research Center, Blacksburg, Va., 1974.
14. SCAVIA, D., and R. A. PARK, Documentation of Selected Constructs and Parameter Values in the Aquatic Model Cleaner, *Ecol. Modelling*, vol. 2, pp. 33–53, 1976.
15. STUMM, W., and J. J. MORGAN, "Aquatic Chemistry," Wiley Interscience, New York, 1970.
16. LEHMAN, J. T., BOTKIN, D. B., and LIKENS, G. E., The Assumptions and Rationales of a Computer Model of Phytoplankton Population Dynamics, *Limnol. Oceanogr.*, vol. 20, pp. 343–364, 1975.

17. NYGAARD, G., "Danish Phytoplankton," pp. 31–52, Gyldendal, Copenhagen, 1952.
18. NYHOLM, N., "Kinetics Studies of Phosphage Limited Algae Growth," Thesis at the Technical University of Copenhagen, Copenhagen, 1975.
19. STEEMANN NIELSEN, E., The Use of Radioactive Carbon ($C^{14}$) for Measuring Organic Production in the Sea, *I. Cons. Perm. Explor. Mer.*, vol. 18, pp. 117–140, 1952.
20. STEEMANN NIELSEN, E., On the Determination of the Activity in $C^{14}$ Ampules for Measuring Primary Production, *Limnol. Oceanogr. Suppl.*, vol. 10, pp. 249–253, 1965.
21. PATTEN, B. C., D. A. EGLOFF, and T. H. RICHARDSON, Total Ecosystem Model for a Cove in Lake Texoma, in B. C. Patten (ed.), "Systems Analysis in Ecology," vol. III, pp. 206–423, Academic Press, New York, 1975.
22. MATHIESEN, H., Environmental Changes and Biological Effects in Lakes, *Vatten*, vol. 26, pp. 149–174, 1975.
23. WMO, "Intercalibration of Hydrological Models," WMO, Geneva, 1975.

# AUTHOR INDEX

# SUBJECT INDEX